# Transport of heavy metals from mine waste of Titania

Linda Lorraine Fauske

Master Thesis in Geoscience
Geochemistry
60 credits

Department of Geoscience
Faculty of Mathematics and Natural Science

UNIVERSITY OF OSLO

September 2017

# Transport of heavy metals from mine waste of Titania

Transport of heavy metals from mine waste of Titania

http://www.duo.uio.no/

Trykk: Reprosentralen, Universitetet i Oslo

# Abstract

Mining is accompanied by vast amounts of waste. The titanium mining company Titania AS is today depositing 1.5-2.5 million tonnes tailings each year into a constructed dam at Tellenes, Rogaland county, Norway. The dam has been estimated full within 8-10 years and challenges at Tellenes today are elevated nickel concentrations in the drainage downstream the landfill and airborne material from the landfill. This study has investigated the transport of heavy metals from both land and sea mine deposits of Titania with focus on nickel, in particular. This has been achieved by measuring airborne and aqueous transported material from tailings on land. In sea, nine individual box-core liner experiments were done in a mesocosm laboratory, at NIVA's research station at Solbergstrand, by measuring fluxes from fjord bottom sediments, overlaid by a 2 cm layer of tailings from Titania. Airborne transported material from the landfill was studied by analysing two dust filters located in upper and lower Åna-Sira, 2.8 km downstream from the landfill. The dust filter closest to the mine was slightly more enriched in grains >50 μm, whereas the dust filter 300 m further away was more enriched in grains <50 μm. Both filters were dominated by grains of plagioclase with lesser grains of ilmenite, of which the ilmenite grains are highly likely originating from the mine.

The aqueous transported material on land was studied by determining heavy metals in water samples collected from rivers and creeks nearby the landfill, revealing nickel concentrations of 50 ppb at the landfill, 293 ppb below the landfill and 21 ppb in Logsvann, about 200 m downstream the landfill. The samples close to the drying plant and Titania's process water, Tellenes water, were also observed to have elevated nickel concentrations of 21-60 ppb. Oxidation of nickel sulphides in the unsaturated zone at the landfill in combination with the dissolution of nickel sulphate could be responsible for the elevated Ni concentrations in the leachate of the landfill compared to the top of the landfill. However, as $SO_4^{2-}$ decreases from the landfill to below the landfill, it is impossible to link the elevation of Ni concentration to sulphide oxidation. One of the two samples in Åna-Sira, approximate 2.8 km downstream the landfill, was also moderately affected by the mine with nickel concentrations of 30 ppb.

The tailing covered fjord sediment in the three box-core liners of Titania showed high metal fluxes of nickel and copper from the sediments to the water column with fluxes of 1381-3265 $\mu g/m^2/d$ and 15.9-24.9 $\mu g/m^2/d$, respectively, compared to control fluxes of 0.7-1.6 $\mu g/m^2/d$ and 0.9-3.6 $\mu g/m^2/d$. The significant variance within the box-core liners is most likely caused by bioturbation. Diffusive Gradients in Thin Films (DGT-probes) for future in situ environmental risk assessment was evaluated by using the correlation between DGT mean metal uptake from 0-2 cm depth and the metal fluxes from the sediments to the water column, which proved to correspond quite well, indicating it as a useful method. However, further studies should be done as there are still uncertainties related to the lower DGT-values.

# Acknowledgement

First and foremost, I would like to express my gratitude to my supervisor, Helge Hellevang, for introducing me to this study, for your enthusiasm, dedication and guidance through the year. Thanks to my co-supervisor, Morten Schaanning at NIVA, for advice, discussions and comments. For including us in the research project, NYKOS, with field work and experiments at NIVA's laboratory and research station at Solbergstrand. Thanks to my co-supervisor, Per Aagaard, for your interest and help. Special thanks to Ann Heidi Nilsen and Elise Opsal at Titania AS for your kindness, great hospitality, advice, comments and for sharing your data. I would also express my gratitude to the technical staff at the Department of Geoscience, Mufak Naoroz, Siri Simonsen, Magnus Kristoffersen, for help with the chemical analysis. Berit Løken Berg and Thanusha Naidoo and for help with SEM and XRD analysis. Beyene Haile for help with the XRD sample preparation. I would also like to thank my good friend, Hedvig Sterri, for countless hours at school, for good teamwork and support through these two years.

Finally, I would like to express my gratitude to my family and friends. My parents, for supporting me both financially and with love through my years of study. This accomplishment would not have been possible without you. To friends and family, thank you for the encouragement, love, motivation and support I have received, and also thanks to those of you who have read and corrected my text.

# Table of contents

# List of tables

# List of figures

# 1 Introduction

Minerals and metals are unquestionably necessary to maintain current living standards and to keep up with present technology. Mining has historically played a major role in the development of the human society, and the social demand for mineral resources is increasing. The world mining production was 16 863*$10^6$ tonnes in 2012, corresponding to a 79% increase since 1894 (Ramirez-Llodra et al., 2015). The Geological Survey of Norway reported in the publication Mineral Resources Norway 2014 that each person in Norway used an average of 13 tonnes mineral raw materials per year, which corresponds to a consumption of 1000 tonnes during a lifetime. Additionally, the demand for special elements is increasingly being an essential part in new environmentally friendly technology, such as windmills and hybrid cars (NGU, 2014).

Despite being a crucial part of the modern society, the mining industry is, however, accompanied by several environmental challenges. Among the challenges regarding mining, the most important one is waste management. The mining industry produces an enormous volume of waste, about 15 000 to 20 000 million tonnes annually, more than almost any other industry in the world (Lottermoser, 2007). Mining waste can contain hazardous substances and should be isolated, physically stable and chemically inert (Ramirez-Llodra et al., 2015). Unfortunately, contaminated groundwater, rivers, lakes and wind are among the negative consequences that have been related to mining. In many cases, mineral production occurs in areas that are politically unstable, with poor environmental requirements or working conditions, or where research and scientific knowledge is not a priority. Increased knowledge and focus on the environmental effects and challenges are important to contribute to stricter environmental requirements and greater prevention of the negative consequences affecting the environment and the local community.

Norway has one of the world's strictest environmental requirements when it comes to industrial activities, including the mineral industry. In the Strategy of the Mineral Industry from 2013 (NHD, 2013) the objectives are that "The Norwegian mineral industry shall be among the world's most environmentally friendly and must actively seek long-term, future oriented solutions". The objectives are not impossible to carry out, and it is certainly a step in the right direction. The European countries consume 20% of the global minerals while producing only 3%. Furthermore, NGU has stated that mineral resources in bedrock and soil in Norway have a potential value of more than NOK 2500 billion (NGU, 2014). Norway has considerable mineral resources, and an increased production of minerals and metals in Norway could contribute to the worlds need for stable access to resources (NHD, 2013) (Schwartz, 2003).

## 1.1 Mining in Norway

Mining has had a significant role in Norwegian industry and economic development since the early 1600s. With the mining industry came a new way of production and a greater degree of international growth regarding shipping and trade (Nagel, 1994). Sulphide mines were mostly mined, in particular, copper and sulphur and smaller quantities of lead, zinc, silver and gold. The Røros district is one of the largest deposits and operated at sulphides for over 300 years. Sulphide mines are very likely to oxidize and generate acid water and leaching of metals. The impact on the environment has been known since the 1700s, but water analyses were not done before the early 1970s. The activity and operation of sulphide mines gradually stopped, and the last operation closed in 1977. The Norwegian government has done remediation and monitoring in an attempt to reduce environmental contamination of the closed sulphide mines, but unfortunately, in some cases, the environmental problems will probably never disappear completely. Mining of metals mines, however, continued, and Titania AS is one of the companies still operating on metal mines today (Wolkersdorfer and Bowell, 2005).

## 1.2 Mining and processing

To extract out minerals, several methods can be used. After the excavation has been done, either by open pit mining or through undergoing tunnels, the material undergoes crushing and milling before a process called beneficiation or mineral processing. The purpose of beneficiation is to reduce the size of the material and to separate the minerals from the ore through either gravity separation, magnetic separation or flotation (Lottermoser, 2007). Very often, there is also a use of chemicals in the mineral processing. An example is the use of flocculants to separate solids from liquids or to get suspended material to aggregate by removing the surface charge of the particles (Ramirez-Llodra et al., 2015).

The waste generated by mining can be solid, liquid or gaseous. It is produced as by-products of the mining processes with no economic value. It can be divided into the overburden waste and tailings. The overburden waste is the part that needs to be removed to get to the target material and tailings are the waste remaining after the extraction of the metal through crushing, milling and separation. Tailings represent the majority of mining waste, and in cases of mining low-grade metal ores, more than 99% of the material ends up as tailings (Ramirez-Llodra et al., 2015, Lottermoser, 2007).

Tailings consist of processed chemicals and crushed rock, but the chemical and physical characteristics of the tailings vary a lot. Although it is natural to assume tailings consist of the same material as the ore, on in smaller fractions, this is not the case according to Lottermoser (2007) regarding grain size, mineralogy and chemistry. The mineral processing changes the physical and chemical characteristics of the ore, and the chemical parameters (for example pH) influences elements differently. For this reason, the content of the tailings changes continuously through processes like cementation, recrystallization, dissolution and formation of secondary minerals.

## 1.3 Disposal methods

### 1.3.1 Tailing disposal on land

Ever since the operation of mines started thousands of years ago, tailing disposal on land has been practised. The most common storage method for the mining industry worldwide is behind impoundment dams, also termed tailings dams. They can be located across a valley, on one side of a mountain or hill, on flat land or deposited in an already existing lake. The system can be open and drained by water or closed and covered by water or cap of soil. Especially minerals that becomes unstable in contact with air should be stored under water to prevent oxidation and weathering, which could further lead to acid mine drainage and transport of contaminants. Factors affecting the method of choice are climate and precipitation, properties of the tailings, (e.g. as grain sizes) chemical stability and weathering characteristics. Additionally, user conflicts and the water bodies downstream should be taken into account (Sørby et al., 2010).

The tailings themselves can be used to construct the dam if they are physically and chemically stable, preventing failure and release of contaminants. There are over 3500 tailings dams worldwide and the principle behind the constructions is comparable to water dams (Kossoff et al., 2014). They are constructed gradually over time as the impoundment fills and the embankments are raised either upstream, downstream or vertically (figure 1). With the vertical method the tailings are placed vertically on top of the earlier tailings. Raised downstream is based on new material placed on the outside of the dam, whereas dams raised upstream places the material inside the dam. The latter one is the main method which of half of all tailings dams are constructed. It requires less material, hence it is cheaper but the structure is also more exposed to erosion and thus failure (Lottermoser, 2007, Kossoff et al., 2014).

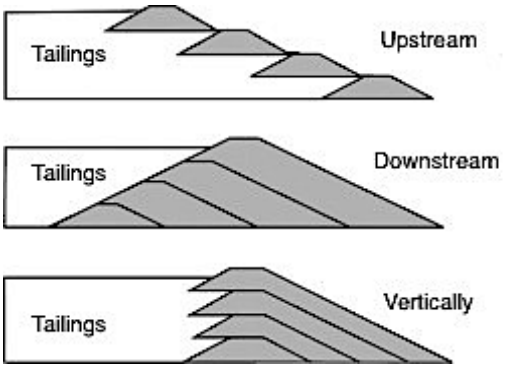

Figure 1 – Illustration of methods for constructing tailings dams, either raised upstream, downstream or vertically. Modified from (Kossoff et al., 2014).

The size of tailings dams ranges from a few hectares to thousands of hectares. The largest one in the USA is the New Carolina copper mine with a volume of $29*10^6$ $m^3$ (Kossoff et al., 2014). The largest copper mine in Europe is the Aitik mines in Sweden with an area of 11

$km^2$ (Sørby et al., 2010), and the Tellenes mine in Norway is one of the world's largest titanium mines and has a disposal area of 1.2 $km^2$ (Mellgren, 2002).

### 1.3.2 Tailing disposal in sea

In cases where the geography permits it, an alternative to constructed dams can be marine disposal. This method has been practised worldwide for over 30 years and in 2013, fourteen mines worldwide used marine disposal, where of five are located in Norway (Ocean and Consulting, 2013).

Tailings have for a long time been deposited in rivers, but in 2015, only one mine in Indonesia and three in Papua New Guinea were still dumping tailings in rivers (Ramirez-Llodra et al., 2015). Disposal in rivers can lead to several environmental problems if contaminants enter the groundwater or coastal areas, as well as visible effects such as an increase in turbidity and high sedimentation rates (Dold, 2014b). Tides and currents will contribute to an oxidizing environment in addition to erosion and migration of the deposits. Due to these problems, during the 70s and 80s, the deeper methods where developed with the aim of more stable conditions for the tailings (Ramirez-Llodra et al., 2015).

There are mainly three methods used. They are based on depth and described by Ramirez-Llodra et al. (2015) and illustrated in figure 3: coastal shallow-water disposal (CTD), submarine tailing disposal (STD) and deep-sea tailing placement (DSTP). CTD in figure 2a is deposited close to the surface in the euphotic zone where it is sufficient sunlight for the photosynthesis. STD in figure 2b is also disposed in the euphotic zone, under 100m depth but through a pipeline. This causes a gravity flow and brings the tailings even deeper below the euphotic zone with as little dispersion as possible. DSTP is deposited even deeper, below the euphotic zone through a submerged pipeline, at the edge of a drop-off and reaches the sea floor 1000 m below due to gravity flow (Ramirez-Llodra et al., 2015).

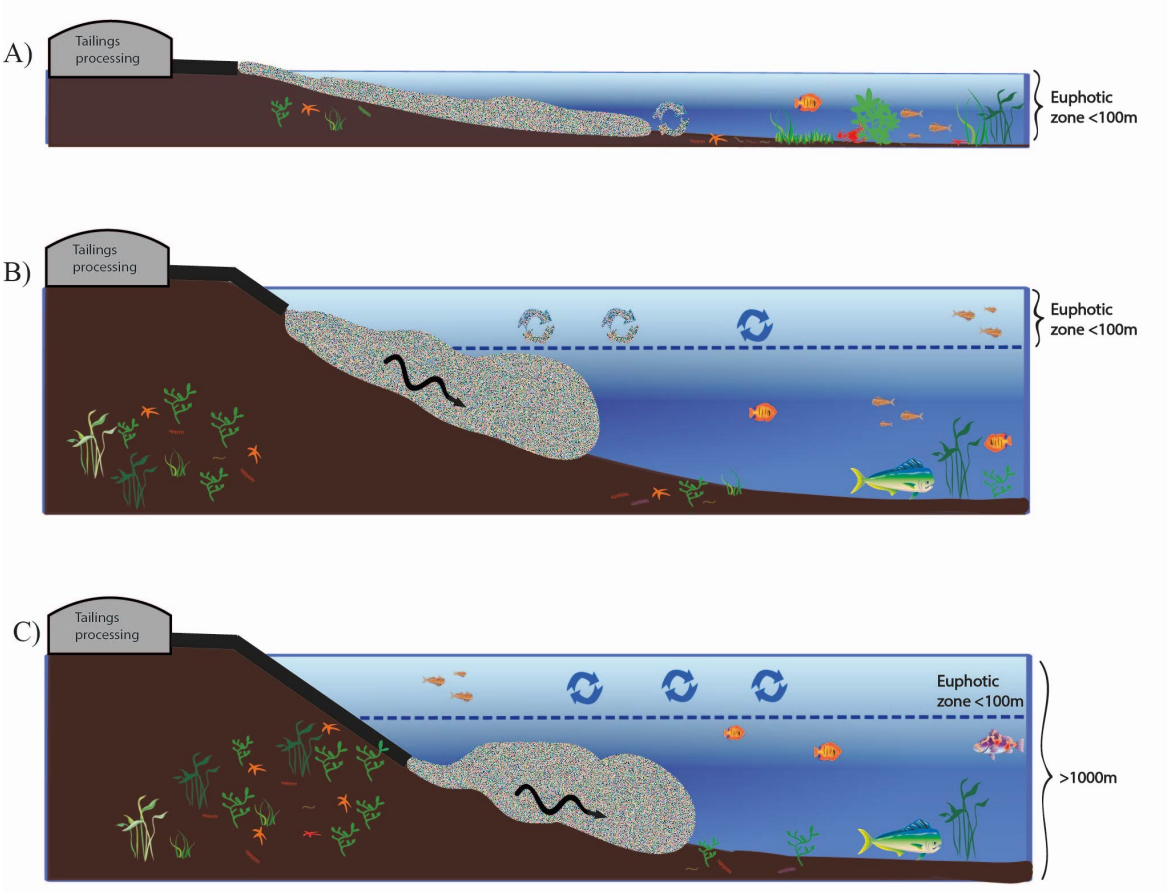

Figure 2- Different types of methods used for disposal of tailings in the sea. Illustration modified from (RAMIREZ-LLODRA ET AL., 2015).

The most important factor to consider when depositing in the sea is to add seawater in the discharge to achieve the right relationship between freshwater, seawater and tailings to obtain a higher density of the suspension of the deposits compared to the seawater, making it sink towards the bottom. Only freshwater will have the opposite effect causing spreading. The suspension should not contain air bubbles either, as this will transport the suspension up to the water surface. Among the tailings, 30% should be solid, and the chemicals used in the deposits should be easily degradable. Furthermore, the site of disposal should be geotechnical stable and carefully considered in terms of bottom topography, salinity, temperature, currents, amount of oxygen and the diversity of species and plants (Sørby et al., 2010).

In an anoxic environment in sea, minerals as sulphides can remain stable, which can prevent acid water and transport of contaminants (Lottermoser, 2007). The alkalinity of the seawater will also contribute in neutralizing the acidic water and reduce the mobility of metals. Other benefits by depositing in the sea are the economic advantage compared to on land, more stable in the sense of no construction and dam failures, less erosion, in addition to not taking up space on land (Koski and Koski, 2012). On the other hand, marine disposal is accompanied with several uncertainties, and there are still large knowledge gaps related to this practice. It can destroy the benthic bottom fauna, change the topography, the abundance of species and plants and spread contaminants. Consequently, the disposal area should be carefully considered due to migration and dispersion. Influencing factors can be grain size, settling

velocity and the stratigraphy of the water column. Other consequences of tailings in marine environments are the sedimentation rate, the frequency of discharge and sediment plumes, as well as the occurrence of unexpected incident that may occur such as turbidity, upwelling and slope failure (Ramirez-Llodra et al., 2015).

## 1.4 Aim of study

This thesis presents an investigation of both land and sea mine deposits on the occasion of a future deposit for the mining company Titania at Tellenes with emphasis on environment and sustainability. The study has been done in cooperation with the mining company Titania AS and Norwegian Institute for Water Research (NIVA) in addition to being a part of the research project "New knowledge on Sea Disposal" (NYKOS).

The main objective of the study was to investigate the transport of heavy metals, in particular nickel, from tailings in sea and on land. This aim has been achieved through a series of secondary objectives:

- Estimation of total dust emission on land in the nearby community Åna-Sira downstream of the Lundetjern landfill by analysing tailings from the landfill and two dust filters.
- Investigation of heavy metals in rivers and creeks around the landfill.
- Measurements of metal fluxes from sea tailings to the water column in box-core experiments in mesocosm laboratory at NIVAs research station at Solbergstrand, and testing of Diffusive Gradients in Thin Films (DGT-probes) as a tool by the correlation between DGT metal uptake in pore water and fluxes from sediment to the water column.

# 2 Titania

The titanium mining company Titania AS is today depositing between 1.5-2.5 million tonnes tailings each year into a constructed dam at Tellenes, Sokndal municipality. The deposit has been estimated to be full within 8-10 years. In the assessment of a new disposal site, Titania emphasizes environment and sustainability, and both land and sea disposal methods will be considered.

## 2.1 Titania AS

The mining company Titania AS is located in Hauge in Dalane, Sokndal municipality in Rogaland County, Norway (figure 3). They operate at the Tellenes mine, Europe's largest ilmenite deposit. Ilmenite is an iron titanium oxide, black in colour, which is processed to ilmenite concentrate and further to white titanium pigment used in everything from paint and paper to toothpaste and sunscreen. The production at Tellenes is owned by Kronos Worldwide and is Europe's largest and the sixth largest producers of titanium minerals in the world (NGU, 2014). In addition to ilmenite, Titania produces the by-products magnetite concentrate to the coal industry in Europe and sulphide concentrate for further extractions of nickel and cobalt (Titania, 2002).

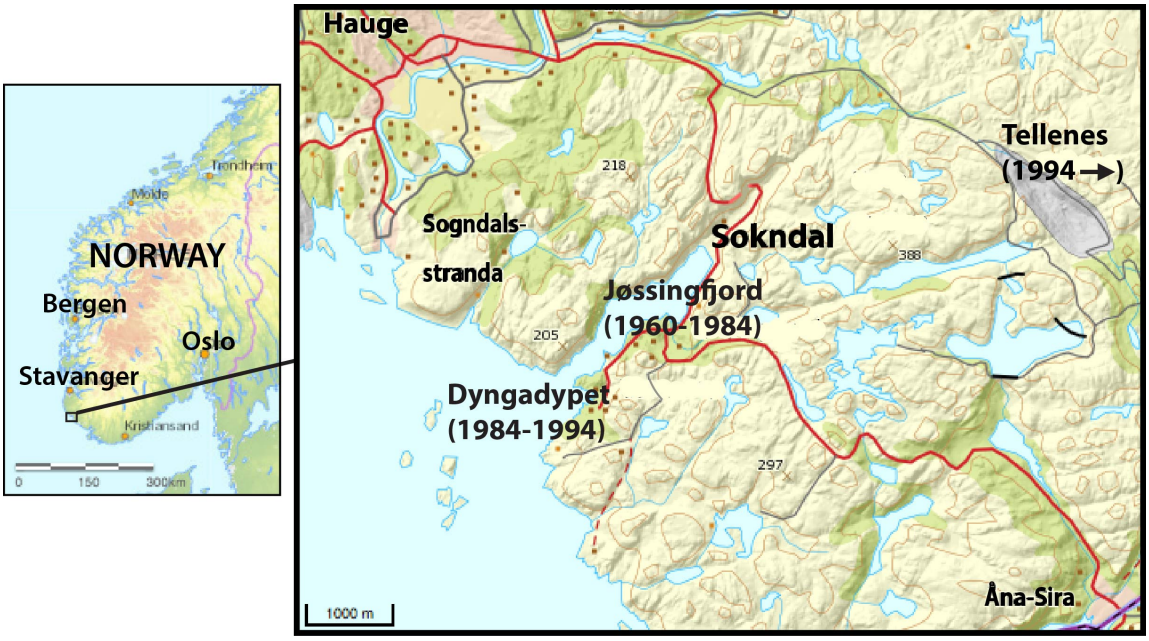


Figure 3 – Left: Map of the south of Norway modified from NVE. Right: Map of Sokndal with locations of previous disposal sites modified from NGU.

Titania has been operating with mine waste deposits for over hundred years, both marine and on land (figure 3). Since the 1960s, they have been mining the Tellenes ilmenite ore and deposited tailings in the sea at Jøssingfjord. After filling up this basin, they got permission to

move the deposits further out into the sea to Dyngadjupet (1984-1994). Since then, the fjord has not been exposed for any tailings, yet process wastewater and drainage from the open pit and the landfill, are still running out in the fjord. In addition to elevated concentrations of nickel, the leachate downstream the landfill has been proved to contain small amounts of suspended solids, organic tall oil, nitrate and ammonium according to a report by Geode Consult AS (Ettner and Sanne, 2016). However, monitoring of freshwater and marine water is performed regularly and none of the emission limits from the Norwegian Environment Agency (Miljødirektoratet) nor the concession of 4tonnes/day of suspended particles has been exceeded (Ettner and Sanne, 2016, Sørby et al., 2010).

## 2.2 Geology and the Tellenes ilmenite deposit

Ilmenite ($FeTiO_3$) is an accessory mineral in igneous, metamorphic, hydrothermal sedimentary and weathered rocks, of which the greatest economic interest is within igneous, sedimentary and weathered rocks (Force, 1991). It contains iron and titanium oxide and is the major source in the production of titanium. Titanium is the ninth most common mineral in the earth's crust and well known for its high strength and low density. Titanium as a raw material that mainly exists in rutile and ilmenite, and the major use of titanium is through processing to titanium dioxide pigment, which stands for 93% of the worlds titanium consumption. The pigment is bright white, and its main usage area is paper, plastic and paints (Korneliussen et al., 2000).

The Tellenes ilmenite deposit is the second most important ilmenite deposit in the world, after Lake Tio in Quebec, Canada. It accounts for 7% of the world's $TiO_2$ production and has a yearly production of 800 000 tonnes of ilmenite concentrate (Charlier et al., 2007). The Tellenes ilmenite is located in southwestern Norway, in the Rogaland anorthosite province, as a part of the Sveconorwegian orogeny (figure 4).

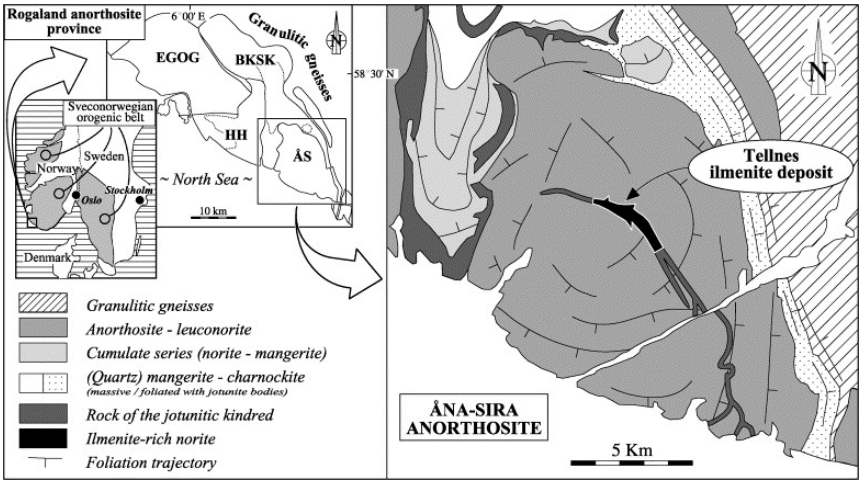

Figure 4 - Rogaland anorthosite province to the left, and Tellenes ilmenite deposit in the Åna-Sira Anorthosite to the right from (Diot et al., 2003)

The Rogaland anorthosite province consists of three large anorthosite plutons, Egersund-Ogna, Håland-Helleren and Åna-Sira, in addition to the Bjerkheim-Sokndal intrusion (Diot et

al., 2003). The plutons were formed after an event where large diapirs of plagioclase crystal mush took place and crystallized over a large pressure-temperature interval while it rose up from a deep magma chamber (Duchesne, 1999). The characteristics of all the deposits in the Egersund area are that they are igneous rocks crystallized from magmas. In a magma chamber, the iron and titanium oxides will be enriched at the bottom of the chamber due to gravity, in contrast to silicates. When silicates thereafter crystalize, the oxides can end up in the weakness zones resulting in an ilmenite deposit (Bredeli et al., 1992).

The Tellenes ilmenite deposit is a massive body of medium-grained (0.5-2mm) ilmenite-rich norite in the middle of the Åna-Sira anorthosite pluton (figure 4) and has a U-Pb age of 920±3 Ma (Charlier et al., 2007). The ore body is 2700km long and 600km wide at its widest and with an average composition in volume consisting of 53.2% plagioclase, 28.6% ilmenite, 10.2% orthopyroxene, 3.9% biotite, 0.7-2.5% magnetite and 24 accessory minerals accounting for 3.4% (Krause et al., 1985).

## 2.3 Mineralogy of tailings

The mineralogy of the tailings is dominated by plagioclase, ilmenite and hypersthene (a type of pyroxene). The typical composition of the tailings is listed in table 1 below(Myran, 2007):

Table 1 - Mineralogical composition of the tailings

| **Mineral** | **Weight percentage** |
|---|---|
| Plagioclase | 64 |
| Hypersthene | 10 |
| Biotite | 7 |
| Diverse silicates | 5 |
| Ilmenite | 13 |
| Apatite | 0.5 |
| Sulphides | 0.2 |

The type of sulphides are not specified but earlier mineralogy analysis by Hagen in 1998 detected pyrite ($FeS_2$), pyrrhotite ($Fe_{1+x}S$), marcasite ($FeS_2$), pentlandite ($(NiFe)_9S_8$) and copper iron sulphide ($CuFeS_2$) in the tailings of Titania according to a report by SARB (2014) Consulting Norge AS. All the same sulphides have been analysed in the Tellenes ore as well, pentlandite being the most important nickel mineral. In addition, rare occurrences of the cobalt nickel sulphide mineral siegenite $(Ni, Co)_3S_4$ and the nickel sulphide mineral millerite (NiS) have been detected (SARB, 2014).

## 2.4 Mining history at Tellenes

Titania AS is a mining company founded in 1902. The first attempt to benefit from the ore deposit in Sokndal-Egersund was when Moss Jernverk operated the mine (1785-1796). They mined 3000 tonnes of ore but the high titanium content made the ilmenite-bearing ore difficult to smelt and they had to give up (Krause et al., 1985). From 1864 The Norwegian Titanic Iron Ore Company Limited was established and started to ship ore from Sokndal to Hartlepool in England where it was mixed with hematite to simplify the melting process (Bredeli et al., 1992).

Neither Titania nor other small mining companies were able to melt the ore extractions until Farup and Jebsen discovered the white pigment titanium dioxide by using the sulphate process. In 1916, Titania commenced production at Storgangen mine at Sandbekk (Sæland et al., 2008). From 1936 to 1965, the coarser mine waste was dewatered and deposited on land, while finer mine waste was deposited in the Sokndalselva river which drains into the sea. Sulphide concentrations were also not separated as they are today but released with the rest of the deposits from the rest of the deposits as today. During the production at Sandbekk, more than $10*10^6$ tonnes ore was produced and represented 11-13% of the worlds $TiO_2$ production (Ibrekk et al., 1989, Krause et al., 1985).

As the demand for ore in Europe increased, an extensive magnetic exploration by aeroplanes was done and as a result, the Tellenes deposit was discovered. The quantity confirmed found was 200 million tonnes ore and the estimation up to 350 million tonnes. The production at Tellenes, 3km from Storgangen, started in 1960 and the waste disposal was deposited through a tunnel into the Jøssingfjord Sea. In 1980, as an attempt to a cheaper and more beneficial process, the gravimetric separation method was installed and no more than a few years later it took over 70% of the production, while the remaining 30% were yet flotation (Sæland et al., 2008).

The discharge into Jøssingfjord was $2.5*10^6$ tonnes annually, and as a result, according to a report done by NIVA (Norwegian Institute for Water Research) (Sørby et al., 2010), the water depth in the basin decreased from 70m to the sill depth at 20 m. In 1984 it was given permission to move the disposal site from Jøssingfjord to a basin further out, Dyngadjupet. The water depth here was 170 m and decreased to 140m after a discharge period of ten years. In 1970 a new law regarding water pollution was the start of the long debated issue about moving the disposal site on land (Bredeli et al., 1992). The spreading of particles from the deposits in Dyngadjupet proved to be greater than expected. In addition to the pressure and protests from environmental organizations, local fishermen and The Institute of Marine Research in Norway, the Government concluded in 1990, to relocate the disposal site from sea to a constructed drained dam on land from 1994 (Sørby et al., 2010).

Periodically the drainage from the constructed dam, Lundetjern, has been leaching high concentrations of nickel. In 2001, Titania had no limit of nickel concentration at the landfill and their average nickel concentration was 11.7 kg/day. In 2003, a concession limit of 6 kg

Ni/day was set by the government which was further decreased to 1.5 kg Ni/day in 2008. Despite high nickel concentration, however, acid drainage from the landfill has not been observed (SARB, 2014, Mellgren, 2002).

## 2.5 Current disposal site

The area of the Lundetjern landfill is 1.3 $km^2$. The disposal dam at the landfill is constructed as a half closed upstream dam made up of rocks and covered by a filter cloth. The constructed dam is divided in dam 1 and dam 5, respectively to the south and north, which represents the walls built up by rock fill from the open pit mine. Every three years the dam is raised by 6m. A drainage zone has been built in the dams where only water and the finest particles can pass through. Tailings are deposited through two large pipes from the ore dressing plant to dam 1 and dam 5, building up beach zones. The purpose is to reduce the water pressure against the dam. The upper part of the beach zone is unsaturated, resulting in oxidation and potential leaching of nickel (Mellgren, 2002, Nilsen, 2017).

## 2.6 Beneficiation process at Titania

The principle of the beneficiation process is to separate and concentrate the ore mineral. The manufacturing of titan dioxide pigments can be done in two different processes, the sulphate process or the chloride process. In the chloride process, titanium dioxide is produced by forming a titanium tetrachloride ($TiCl_4$) vapour. This is done by reacting natural rutile, synthetic rutile or titanium slag with chlorine gas at high temperature and then oxidizing the vapour. In the sulphate process, ilmenite (45-65% $TiO_2$) or slag (75-90%) are transformed into titanium sulphate by sulphuric acid ($H_2SO_4$) and the titanium dioxide is thereafter precipitated by hydrolysis. Titania deliver ilmenite to pigment fabrics which use the sulphate process (Middlemas et al., 2015).

By the use of the minerals own characteristics, they are separated based on density, magnetism and surface properties. After crushing and milling, a magnetic separator divides the minerals in magnetic and non-magnetic. The magnetic magnetite minerals are milled again and transported to the drying plant for further purification (figure 5, no 9). When the magnetite is separated out, the non-magnetic particles are further separated by grain sizes by hydro cyclones. The coarser particles undergo gravimetric separation based on density (figure 5, no 5). The $TiO_2$ concentration is then 43.7% and the material is subsequently transported to the drying plant for dewatering and to be cleansed for sulphides and phosphates. The finest particles from the hydro cyclone separation represent approximately 25% of the ore and are transported further to the high-intensity magnetic separation to remove all non-magnetic minerals before the froth flotation (fig5, no 6) where tall oil and sulphuric acid is used for further purification. After separation at the ore dressing plant, the ilmenite concentrate is mixed with the gravimetric concentrate and transported to the drying plant where it is added acid to reduce the phosphorous, sulphur and oil residues. In addition, nickel and copper

concentrate is separated and stored in silos (figure 5, no 10, 11, 15). At each of the steps from the grain size separation, the gravimetric separation, the high-intensity separation and the ilmenite flotation, unsuitable and unwanted grains removed. They are thereafter gathered and pumped to the ore dressing plant and subsequently to the landfill (figure5, no 2). During the processes at the ore dressing plant and the drying plant, large quantities of water are consumed. Water from Tellenes water is primarily used whereas Måkevann is used when absolutely necessary (Ettner and Sanne, 2016, Mellgren, 2002).

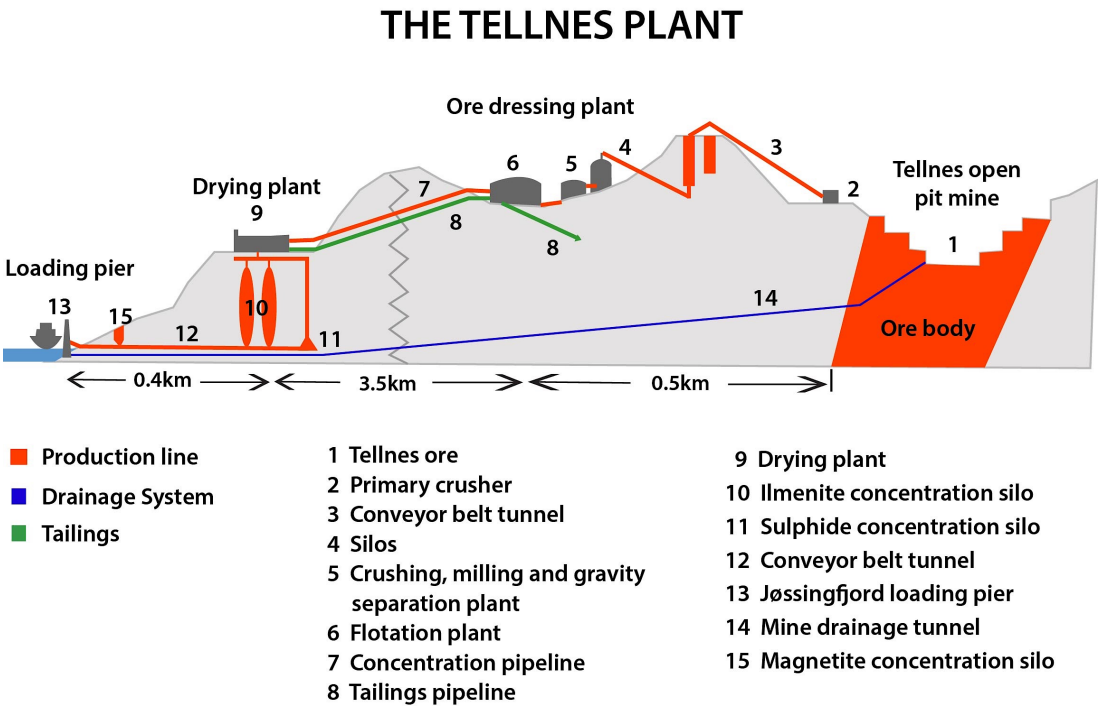


Figure 5 - The Tellenes plant. An overview of the production and processes from the ore body to the loading at the pier in Jøssingfjord. Drawing inspired by the overview of processes found in (Ettner and Sanne, 2017).

## 2.7 Process chemicals

During the blasting operation of the open pit mine, ammonium nitrate has been used and the use of explosives can result in leaching of nitrogen, nitrate and ammonium. In the froth flotation, tall oil, solvents and sulphuric acid are added to affect the surface of the minerals. The tall oil has a water repellent effect on the grains and the sulphuric acid adjusts the pH. When in contact with air bubbles the ilmenite grains cling onto the air bubbles and rises to the surface, while the remaining unwanted solids sink. Thereafter the ilmenite concentrate is transported to the drying plant. In the production processes at the drying plant, large amounts of sulphuric acid are used to solve between the ilmenite and the tall oil before it is dried and stored in silos. This results in acidic water from the drying plant. However, in mixture with water from the other processes the overall pH increases and neutralizes (Mellgren, 2002, Lottermoser, 2007, Ettner and Sanne, 2016).

## 2.8 Discharge permit and discharge points for Titania

The discharge permit for Titania has been given by the Norwegian Environment Agency dated 16. September 2016 and applies to the suspended material (SS), nitrogen, tall oil and solvents. The current discharge points are the landfill with discharge to Logsvann and the landfill, open pit, ore dressing plant and drying plant with discharge to Jøssingfjord (Ettner and Sanne, 2017). Additionally, they have a discharge limit of 1.5kg/day from the old deposits at the Sandbekk are into the Sandbekk river, but they will not be further discussed in this study. The discharge sources are illustrated in figure 6 and the discharge limits are listed in table 2 below.

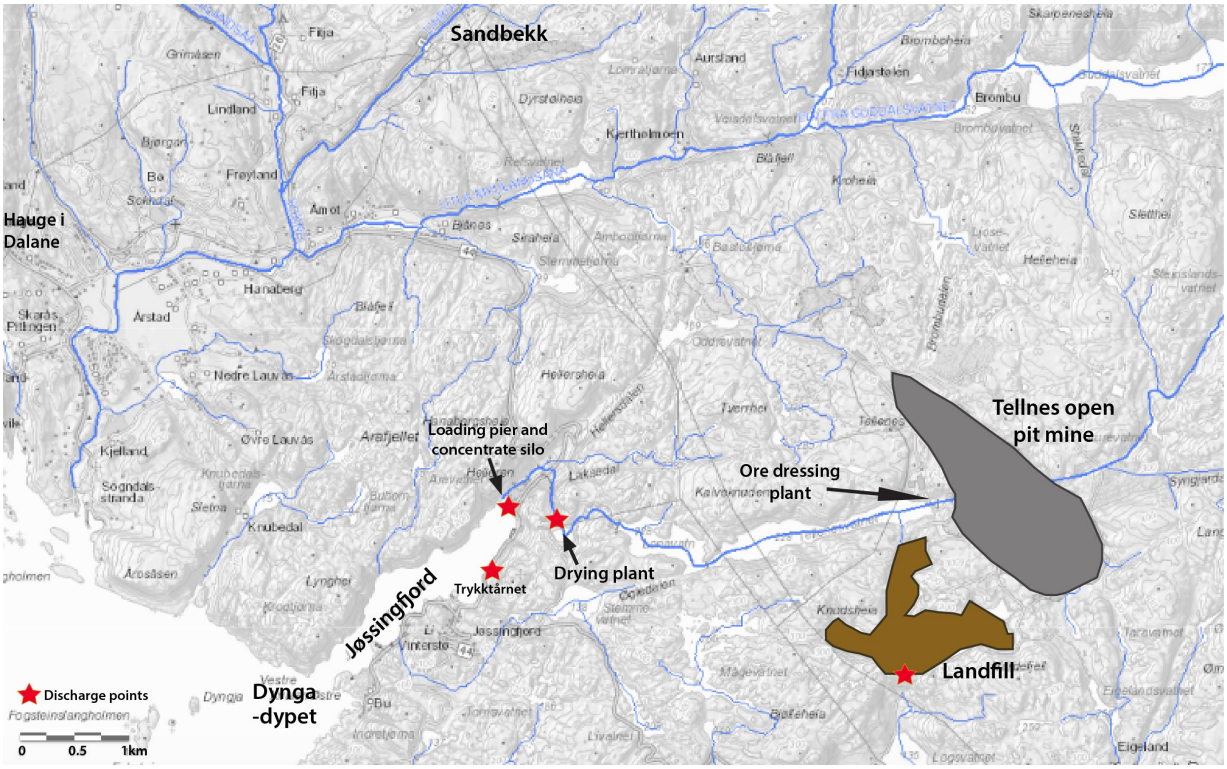


Figure 6 – Map from NVE with an overview over discharge points inspired by (Ettner and Sanne, 2017).

Table 2 - Discharge permit for the landfill, open pit, ore dressing plant and drying plant (Ettner and Sanne, 2017).

| Discharge source | Water recipient | Discharge component | Discharge limits (kg/day) |
|---|---|---|---|
| Landfill | Logsvann water course | SS<br>Ni | 150<br>1.5 |
| Landfill, open pit, ore dressing plant, drying plant | Jøssingfjord | SS<br>Ni<br>Tall oil<br>Solvent<br>Total N | 4000<br>6.0<br>50<br>2.0<br>160 |

The leachate from the landfill drains through the landfill dam with discharge to Logsvann. The concession for Ni to Logsvann is set to 1.5 kg/day and parts of the leachate from the landfill pumped in return to the top of the landfill and further pumped to Tellenes water, the process water reservoir, where it is transported through a tunnel and released in Jøssingfjord where the concession is 6 kg/day. Due to the return pump the average concentration of Ni in the leachate is 0.6 mg/l (Sweco, 2017).

## 2.9 Previous monitoring surveys

Annual monitoring surveys by identifying animals, analysis of grain size distribution and content of $TiO_2$ were carried out in the Jøssingfjord area from 1983 to 1988 to study the structure of the soft bottom communities and the effects of mine tailings after the relocation 1984 to Dyngadjupet. The discharge has been two million tonnes per year, and the tailings have contained almost inert material and non-toxic to marine life. The conclusions from the reports were that the stations with the highest content of $TiO_2$ were related to the lowest diversity of organisms. It was, however, found that it is not necessarily only the chemical characteristics of the tailings causing the largest biological effects, but rather the rate of sedimentation. The sites most disturbed by sedimentation with a sedimentation of 4-5 cm/year showed noticeably reduction and changes in diversity whereas the diversity exposed to a sedimentation rate of 1 mm/year remained unchanged. The instability is stressful and when the bottom sediments increase and become more homogenous the presence of species with their natural habitat in pore spaces will eventually disappear. The conclusion of the effect of mine tailings after the relocation was recolonization only one year after cessation and after three years an increase of species was found. The reason is probably due to the shallow water depth of 30-40 m (Olsgard and Hasle, 1993).

Monitoring in the Jøssingfjord area through recipient surveys has been done annually until 1995 when a positive development regarding the environmental condition was confirmed. However, since Jøssingfjord still receives processed waste water, drainage water and decant

water from the open pit the Climate and Pollution Agency determined new surveys in 2003 and 2007 done by DNV. They were to describe the chemical and biological changes in the bottom sediments. $TiO_2$ content has been measured to determine the degree of sedimentation whereas particles finer than sand (<63 μm) were measured to define the spreading. The survey from 2007 concluded that there is still sedimentation of tailings in Jøssingfjord. The $TiO_2$ content is unchanged and in Dyngadjupet and outer areas it is decreasing. The turbidity nearby the discharge of process water was low and not of remarkable influence regarding spreading particles. Out of the eight stations, the condition of three of them was classified as good and the rest as very good (Nøland et al., 2008). According to the water regulation in Norway, the environmental condition of all waters should be defined as "good". To be defined as "very good" the condition should be approximately in natural conditions compared to similar non-influenced water (Vannforskriften, 2015).

Upon orders from the Norwegian Climate and Pollution Agency NIVA performed in 2003 an ecotoxicological characterization of Titania run-off areas which are discharge from the landfill to Logsvann, from the intake dam with discharge to Jøssingfjord and the drainage water from the mine with discharge to Jøssingfjord presented in table 3 below (Tobiesen, 2003).

Table 3 - Nickel and pH values from discharge from the landfill, the intake dam and the mine done by NIVA in 2003.

| **Sample** | **Nickel (mg/l)** | **pH** |
|---|---|---|
| Landfill | 0.754 | 8.01 |
| Intake dam | 0.068 | 7.58 |
| Mine | 0.311 | 7.93 |

Acute toxic effects on aquatic organisms are measured by the concentration at which there is a reduction in growth rate of 50% (EC50). In the sample from the intake dam some reduction in growth rate was observed for algae (EC50=0.24 mg/l Ni) compared to EC50 values in the literature (EC=0.012-1.18 mg/l Ni) but with no effect on crayfishes. Other than that, all values were within the permissible limits set by the Climate and Pollution Agency (Tobiesen, 2003).

NIVA also did two surveys in 2015 on behalf of Titania monitoring marine soft bottom fauna in Jøssingfjord and Dyngadjupet and fresh water studies of benthic animals in Sira-Kvina. The soft bottom fauna was studied to see in what degree the fauna is influenced by the process wastewater and the drainage water from the mine, as Titania has a license to discharge 4 tonnes/day. The soft bottom fauna comprises invertebrate animals larger than 1mm and suitable for studying the effect of the mine, as they are relatively stationery. Five stations were studied and the result was "very good" at one and "good" at the rest. All of them were approved by the water regulations but the fauna appeared to have some indications of disturbance. The reason could be a combination of the current discharge and earlier discharge. Compared with the results from 2007, the amount fine particles are the same, the amount disposals in the sediments are the same and the classification of the fauna is the same and

slightly improved. Due to the positive development, the report also states that a new survey every sixth year in the future is sufficient (Trannum, 2016).

The freshwater studies were done on the bottom fauna to estimate the effect of the drainage from the landfill. Three stations were studied, but two of them turned out not to be suitable due to influence by marine water and the power station in Åna-Sira. The suitable station was a creek, Logvannsbekken, located downstream of the landfill. Even though the ecological conditions showed high diversity, the result was "moderate" possibly due to lack of certain species. However, the creek was not affected by acidification and based on the physical and chemical quality stated as "very good" (Aanes, 2016).

In accordance with the Norwegian Environments Agency, Geode Consult did a water monitoring on behalf of Titania in 2015, focusing particularly on nickel. Affected watercourses are Tellenes/Jøssingfjord and Logsvann/Siraelva. In all the water recipients, downstream of the discharge points nickel were found. Nickel is a European Union (EU) priority element when classifying chemical conditions in water recipients and one of Titania's main challenges. The nickel limit values are classified by the Norwegian Environment Agency presented in table 4. According to the National environmental quality standard (EQS) for EU condition 2 represents the annual average (AA-EQS) with the limit 4 µg/l for freshwater and 8.6 µg/l for marine water. Condition 3 represents the maximum annual concentration (MAC-EQS) with the limit 34 µg/l for both freshwater and marine water.

Table 4 - Nickel limit values in freshwater and marine water by the Norwegian Environment Agency modified from (Ettner and Sanne, 2016)

| Condition | 1<br>Very good | 2<br>Good | 3<br>Moderate | 4<br>Poor | 5<br>Very poor |
|---|---|---|---|---|---|
| Nickel freshwater | <0.5 µg/l | 0.5-4 µg/l | 4-34 µg/l | 34-67 µg/l | >67 µg/l |
| Nickel marine water | <0.5 µg/l | 0.5-8.6 µg/l | 8.6-34 µg/l | 34-67 µg/l | >67 µg/l |

The nickel in Jøssingfjord comes from discharge from the Tellenes watercourse and comprises Laksedalsbekken, where it mixes with marine water in Jøssingfjord and dilutes further out in Dyngadjupet. The drainage from the landfill results in nickel in Logsvann, Sira River and Ånafjord. Due to large water volumes in the Sira river, the condition relatively rapid changes to condition 2, resulting in a good chemical condition in the Ånafjord as shown in table 5 (Ettner and Sanne, 2016).

Table 5 - Chemical condition based on the National environmental quality standard for EU from the Tellenes watercourse and the drainage from the landfill.

| Watercourse | Water recipient | Condition |
|---|---|---|
| Tellenes | Laksedalsbekken | 5 |
| | Jøssingfjord | 4 |
| | Dyngadjupet | 3 |
| Drainage from landfill | Logsvannet | 4 |
| | Sira river | 3 |
| | Ånafjorden | 2 |

In addition to studying the effect of fresh and marine water quality effected by the mine, the Norwegian Institute for Air Research (NILU) measured the dust emission to estimate the impact on the local community in Åna-Sira. The measurements were conducted through a year from October 2006 to October 2007. According to the air quality standards, the limit of both the Pollution Control Act and the national measurement for air quality has a limit of 50 $\mu g/m^3$, whereas the recommended air quality limit is 35 $\mu g/m^3$. Birkenes measuring station in Vest-Agder has been used as background station with average values of 7 $\mu g/m^3$ (2001-2005). None of the values from Åna-Sira exceeded the limit of 50 μg/m3. The max value measured was 43.1 $\mu g/m^3$, the values from four of the months were over 35 $\mu g/m^3$ and the average value for the whole period was 11.7 $\mu g/m^3$ (Tønnesen, 2008). A report, which was done by the Norwegian University of Science and Technology, also measured the dust emission by four measuring periods of 30 days in the period 01.12-31.12.2006. The report concluded that the dust emission at both measuring points (the same location as described in section 4.3 and used in this study) was low and very low, and mineralogical part of the total sample was below 40%. Also, the dust emissions were below the air quality standards by the Pollution Control Act of 50 $\mu g/m^3$ (Myran, 2007).

# 3 Theoretical considerations

Tailings on land and in sea involve several complex geochemical processes, yet important to understand when investigating the transport of contaminants. This chapter gives an introduction and basic understanding of the most important ones. Firstly, the different transport processes and how metals become mobile. Followed by and the influence of oxidizing conditions and neutralizing effect in tailings. Finally, processes in a reduced environment in sea and the influence of bioturbation.

## 3.1 Transport

Transport moves chemicals of a fluid through the environment and understanding transport is essential when predicting the fate of chemicals. There are different transport processes. Advection is the transport of chemicals from one place to another by the movement of the bulk flow. Diffusion is spreading of chemicals due to concentration differences, whereas mechanical dispersion is spreading of solutes due to local variations in the flow of water, for instance when parts of the flow are forced to move around grains. Mechanical dispersion is dependent on the flow velocity and increases with increasing flow velocity, whereas diffusion is independent of the flow velocity (Appelo and Postma, 2005, Gulliver et al., 2012).

Flow in the saturated zone is dependent on the hydraulic gradient and the hydraulic conductivity of the material. When combining them, they are given by Darcy's law:

$$v_D = -k\frac{dh}{dx} \qquad (3.1)$$

where $v_D$ is the specific discharge/ Darcys flux (m/day), *k* is the hydraulic conductivity (m/day) and *dh/dx* is the hydraulic gradient. The pore space is not taken into account in Darcys flux and may have a significant influence of the flow. The actual velocity of water through the pores is therefore given by (Appelo and Postma, 2005):

$$v_{H_2O} = \frac{v_D}{\varepsilon_w} = -\frac{k}{\varepsilon_w} * \frac{dh}{dx} \qquad (3.2)$$

where $v_{H_2O}$ is the velocity of water (m/yr) and $\varepsilon_w$ is the water filled porosity ($m^3/m^3$).

## 3.2 Diffusion

Diffusion is mixing caused by molecular motion. As earlier mentioned it is a transport process where chemicals are spread due to concentration differences and is independent of flow velocity. The process is called molecular diffusion and is described by Fick´s law (Appelo and Postma, 2005):

$$F = -D\frac{\partial c}{\partial x} \qquad (3.3)$$

where $F$ is the flux (mol/s/m$^2$), $D$ is the diffusion coefficient (m$^2$) and $\frac{\partial c}{\partial x}$ is the concentration gradient. The minus sign indicates a negative slope as the chemicals move from high concentration to low. Thus, the diffusion develops as a result of the concentration gradient. The diffusion coefficient represents the tendency of molecules to spread a constituent mass.

The solutes in a sediment-water system has longer travel distance than in a system of only water due to the tortuosity caused by the sediment grains. This is corrected by the pore water diffusion coefficient $D_p$ by the length of the actual travel path by the solute, divided by the straight travel path:

$$D_p = \frac{D_f}{\theta^2} \qquad (3.4)$$

where $\theta$ is the tortuosity of the porous medium. This leads to an effective diffusion coefficient because only the water filled porosity contributes to the diffusive flux (Appelo and Postma, 2005):

$$D_e = \varepsilon_w D_p = \frac{\varepsilon_w D_f}{\theta^2} \qquad (3.5)$$

where $D_e$ is the effective diffusion coefficient and $\varepsilon_w$ is the water filled porosity.

Molecular diffusion is of very little importance in shallow environments where advection and dispersion dominates. The total flux of reactive elements is defined by the advective reactive dispersion equation (Loe and Aagaard, 2013):

$$\left(\frac{\partial c}{\partial t}\right)_x = -v\left(\frac{\partial c}{\partial x}\right)_t + D_L\left(\frac{\partial^2 c}{\partial x^2}\right)_t + S \qquad (3.6)$$

where $D_L$ is the longitudinal dispersion coefficient and each of the terms on the right describes advective flow, dispersion and chemical reaction/soprtion. Sorption will be further explained in the following chapter 3.3.

However, impoundments with mine tailings often contain very fine particles and typically have low permeability and not sufficient oxygen for advective or convective transport of gas-phase oxygen. With low permeability and low hydraulic gradient, the advective flow will be zero and the transport mechanism will be by diffusion only:

$$\left(\frac{\partial c}{\partial t}\right)_x = \left(\frac{D_p}{\theta^2}\right)\left(\frac{\partial^2 c}{\partial x^2}\right)_t - S \qquad (3.7)$$

The oxygen transport in sulphide-rich waste rock is therefore often dominated by diffusion, and since the process is slow, compared to advective transport, the rate of sulphide oxidation will be slowed down as well. The rate of oxygen gas diffusion in tailings is determined by the concentration gradient and the diffusion coefficient of the material of the tailings. The

diffusion coefficient on the material is dependent of the air-filled porosity and the diffusion increases with the amount of air. Mine tailings with coarser particles however and lower water table may permit advective transport of oxygen into the surface of the tailings due to the changes in atmospheric pressure(Appelo and Postma, 2005, Blowes, 1997). When it comes to marine sediments, rich in organic matter, the oxygen transport is also dominated by diffusion. However, due to consumption processes by benthic organisms, where oxygen is quickly consumed to oxidize organic matte, only a very thin surface layer of oxygen covers marine sediments. The penetration depth of oxygen in marine sediments varies from only millimetres in shallow coastal sediments to 1-2 cm in deeper oceanic sediments at depths of ca. 2000 m (Kristensen, 2000).

## 3.3 Mobilization of metals

Mobilization of heavy metals is the main problem in many mines caused by sulphide oxidation and acid mine drainage (AMD). The process of sulphide oxidation and associated AMD is described in the following chapter 3.3. The acidic water enables heavy metals to be mobile. The degree of mobility is highly dependent on mineralogy, pH, redox conditions, total organic content and various sorption processes (Bozkurt et al., 2000). The term sorption includes adsorption where chemicals sorb to a solid surface, absorption where chemicals sorb into the solid and ion exchange where chemicals within the solid and chemicals at the surface solid exchange. Sorption and ion exchange are essential processes in the fate of metals released because of the retardation influences and regulates the transport of contaminants. When contaminants are released, they are mobilized by advection and diffusion transport due to the hydraulic gradient or concentration differences, as mentioned in the previous chapter. However, the degree of mobilization is regulated by retardation. For instance, will contaminants have the velocity of water in a case with no sorption, whereas in a case with sorption, the contaminants will be retarded determined by the relationship between sorption and concentration. The retardation equation is defined as (Appelo and Postma, 2005):

$$v_c = \frac{v_{H_2O}}{1+\frac{dq}{dc}} = \frac{v_{H_2O}}{R_c} \qquad (3.8)$$

where $v_c$ is the velocity of a specific concentration, $v_{H2O}$ is the velocity of water and dq/dc is the distribution coefficient and describes the relationship between sorbed concentration (dq) and solute concentration (dc) of a chemical.

Solids with a large specific surface area have a larger reactive surface area available for sorption per unit weight of the sorbent and sorption is thus highly determined by the grain size. Grains with a diameter corresponding to the size of clay (<2 μm) have largest specific surface area and may act as an ion exchanger. Clay minerals, therefore, have a natural cation exchange capacity (CEC) related to their content of clay and organic carbon and thus varies widely among clay minerals depending on their chemical composition. Organic matter and oxides have surfaces with variable charge. Depending on pH and the composition of the

solution, their surface can have a negative or positive charge. This quality makes them important sorbents in the removal of oxyanions and heavy metals. However, the pH has a major influence, and heavy metals behave differently at varying pH as shown in figure 7a where heavy metals are sorbed to the surface of a ferrihydrite. At low pH, the sorption of heavy metals are minimal but with an increase of 2 pH units, the adsorption is close to 100% (Appelo and Postma, 2005, Smith, 1999).

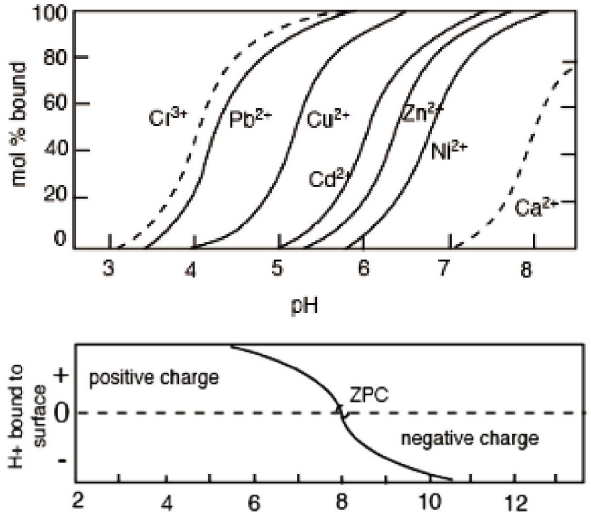


Figure 7 – Sorption of heavy metals and surface charge. A) Upper picture: Heavy metal sorption on the surface of a ferrihydrite as a function of pH. B) Lower picture: Net surface charge and point of zero charge for goethite. Modified from (Dold, 2010).

The pH at which the net surface charge is zero is called the point of zero charge (PZC) and in figure 7b, the surface charge for goethite is shown with a PZC of 8. With a decrease in pH, the mineral surface will have a net positive charge due to adsorption of protons at the surface and thus adsorb anions. In the opposite case, cations are adsorbed at the surface of net negative charge when pH increases (Dold, 2010).

## 3.4 Acid mine drainage and sulphide oxidation

Water with low pH due to oxidation of sulphide minerals is called acid mine drainage (AMD) and is regarded as one of the main pollutants of water related to mining activities (Simate and Ndlovu, 2014). High concentrations of heavy metals (Ni, Cu, Pb, Zn, Sn, Co, Cd etc.) and other toxic elements are often associated with AMD. When iron sulphides or other metal sulphides are exposed to water and oxygen, the result is acid sulphate rich drainage. It is a natural process but particularly related to mining due to the increased and more concentrated amount of sulphides in mines. The potential of AMD to occur is site specific, depending on factors as mineralogy and availability of oxygen and water (Akcil and Koldas, 2006).

Sulphides are formed under reduced conditions, either deep in the crust or in water without dissolved oxygen. When sulphide rich mine waste is exposed to oxygen, they become

chemically unstable. In the attempt of achieving equilibrium with the oxidizing environment, geochemical processes and reactions occur (Lottermoser, 2007).

Pyrite is one of the most abundant sulphides and due to its low economic value often ends up in mine waste and tailings. Besides, pyrite is one of the most efficient producers of acid and hence necessary to understand. There are mainly three steps Dold (2014a) uses to describe the oxidation of pyrite and subsequently the acidic water. First occurs the oxidation of sulphur producing ferrous iron (reaction 1), followed by oxidation of ferrous iron producing ferric iron (reaction 2) and thereafter hydrolysis and precipitation of ferric complexes and minerals (reaction 4):

$$FeS_2 + {}^{7}/_{2}O_2 + H_2O \rightarrow Fe^{2+} + SO_4^{2-} + 2H^+ \quad (1)$$

$$Fe^{2+} + {}^{1}/_{4}O_2 + H^+ \rightarrow Fe^{3+} + {}^{1}/_{2}H_2O \quad (2)$$

$$FeS_2 + 14Fe^{3+} + 8H_2O \rightarrow 15Fe^{2+} + SO_4^{2-} + 16H^+ \quad (3)$$

$$Fe^{3+} + 3H_2O \rightarrow Fe(OH)_{3(s)} + 3H^+ \quad (4)$$

$$FeS_2 + {}^{15}/_{4}O_2 + {}^{7}/_{2}H_2O \rightarrow Fe(OH)_3 + 2SO_4^{2-} + 4H^+ \quad (5)$$

The oxidation of ferrous iron to ferric iron (reaction 2) is very crucial because ferric iron can be an oxidant of pyrite (reaction 3) by microbiological activity at pH below 3. When pyrite oxidizes two scenarios may occur described by (Appelo and Postma, 2005). Scenario one, pyrite reacts with oxygen by direct reaction or by dissolution of $Fe^{2+}$+$S_2^{2-}$ followed by oxidation. Both are slow processes and results in $SO_4^{2-}$ +$Fe^{2+}$. Scenario two is oxidation of pyrite by $Fe^{3+}$ and is significantly more rapid and showed in reaction 3 above. For each mole pyrite oxidized by $Fe^{3+}$, 16 protons are produced, in comparison with only 2 protons in reaction 1.

For over 50 years, it has been known that some microorganism such as *Acidithobacillus ferrooxidans* or *Leptospirillum ferrooxidans* oxidizes $Fe^{2+}$ to $Fe^{3+}$ from the sulphides. The microbiological activity act as a catalyst and the oxidation of pyrite by ferric iron is about ten hundred times faster than by oxygen. When the ferrous and ferric rich water reaches the surface, it will fully oxidize, hydrolyse and precipitate iron hydroxide minerals as in reaction 4, unless pH is extremely low. Provided that both oxidation of pyrite, hydrolysis of $Fe^{3+}$ and precipitation of iron hydroxide occur (a sum of reaction 1, 2 and 4) the net reaction would be reaction 5, producing 4 protons. This indicates that hydrolysis of $Fe^{3+}$ (reaction 4) is the main acid producer, producing 3 out of the 4 protons in reaction 5 (Dold, 2014a). Consequently, pyrite oxidation by $Fe^{3+}$ is dominant at low pH whereas pyrite oxidation at high pH is dominated by oxygen as in scenario one because $Fe^{3+}$ has been precipitated as $Fe(OH)_3$. (Appelo and Postma, 2005, Dold, 2014a).

The rate of pyrite oxidation is therefore highly dependent on pH, type of oxidant ($Fe^{3+}$ or $O_2$) and bacterial activity. Other factors mentioned by (Akcil and Koldas, 2006) are temperature,

oxygen concentration in gas phase and water phase, exposed surface area of sulphides and occurrence of trace elements in the sulphide structure. Higher permeability in the tailings will allow a higher amount of oxygen resulting in greater chemical reaction rates. This will provide higher temperatures and permit even more oxygen through advection.

## 3.5 Neutralization

When acidic water is generated as a result of sulphide oxidation, it can be mixed with other minerals in the mine waste with a neutralizing effect. This causes acid-neutralizing reactions where H+ is consumed leading to an increase in pH. Carbonate minerals, aluminium hydroxides, ferric oxyhydroxides and aluminosilicate minerals are the minerals with highest buffering capacity (Bozkurt et al., 2000). Aluminium hydroxides and ferric oxyhydroxides are secondary minerals formed when aluminium and iron oxidizes. They are natural sorbents and due to their large surface area, they can bound mobile metals to their surface area and thus contribute as pH buffers. The precipitation of secondary minerals can also be of importance by decreasing the porosity and permeability of the mine waste and limit the supply of oxygen and water. Sulphide oxidation and neutralizing reactions results in dissolved constitutes and the most abundant of them are $SO_4$, Fe(II), Fe(III), Ca, Mg, K, Na and $HCO^{3-}$. In a reaction with mine waste water they can precipitate the minerals goethite, ferrihydrite, jarosite, goethite, ferrihydrite according to (Gulliver et al., 2012). If the mine waste is kept reduced with a neutral pH and there is sufficient buffering material the geochemical processes will remain stable (Bozkurt et al., 2000).

## 3.6 Redox

Redox reactions are reactions where electrons are transferred from one atom to another and an important process when determining the fate of pollutants. Since free electrons do not exist, every reduction is followed by oxidation. The redox condition is expressed as Eh and can in combination with pH predict the stability of dissolved species and minerals (Appelo and Postma, 2005, Dold, 2010). As soon as sediments are deposited at the seafloor they start undergoing the process of diagenesis described by (Konhauser, 2007), which is a combination of physical, chemical and biological processes. The process is driven by redox reactions and comprise compaction, changes in minerals, degradation of organic matter, generation of hydrocarbons and variations in the pore water chemistry.

At the sediment-water interface, the material is porous and oxidation is dominant whereas the environment downwards the sediments is dominated by reduction. The transition between oxic and anoxic environment is defined by amount dissolved oxygen in the pore water. During diagenesis, microbial activity plays a major role as microorganisms convert organic matter to $CO_2$ and $CH_4$. This is the beginning of a continuous sequence of reduction processes shown in figure 8, where the most energetically favourable reactions occur first. The reduction of dissolved $O_2$, $NO_3^-$, $SO_4^{2-}$, $CO_2$ and solid Mn- and Fe-oxyhydroxides determines

the pore water chemistry downwards and the result might be a quite different chemical composition with by-products such as $HCO_3^-$, $Mn^{2+}$, $Fe^{2+}$, $NH^+$, $NO_2$, $HS^-$ and $CH_4$ (Konhauser, 2007). These reduced species can thereafter result in precipitation of secondary minerals and some of they might have a significant role in the removal of mobilized metals. In anoxic environments, sulphate-reducing bacteria reduce sulphate and produces hydrogen sulphide ($H_2S$) which may consequently precipitate dissolved metals as metal sulphides. Metal sulphides have a much lower solubility than metal sulphates (Johnson and Hallberg, 2005, Kaksonen and Puhakka, 2007). Other elements can be transported by diffusion from the deeper sediments up to the sea bottom. Though transport in pore water is controlled by diffusion the rate might be considerably accelerated by bioturbation and bioirrigation where for instance worms burrow at the sea bottom and increases the diffusion of oxygen (Emerson and Hedges, 2003, Konhauser, 2007).

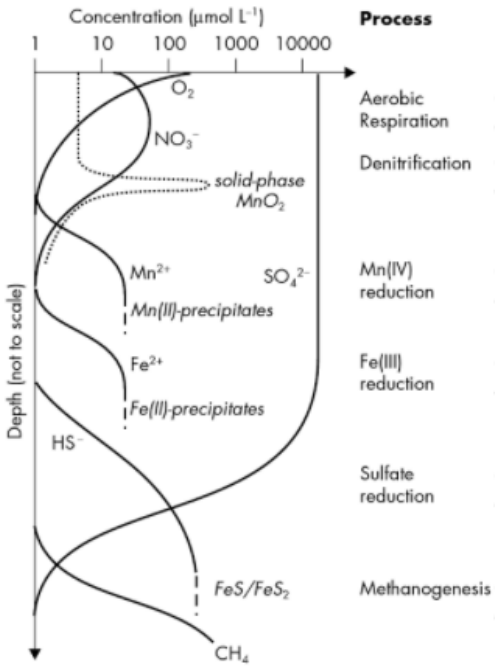


Figure 8 - Redox environment, idealized pore water, and solid phase profiles. Modified by (Konhauser, 2007), adapted from Froelich et al., 1979.

## 3.7 Bioturbation

Benthic marine animals can contribute to the sediment diagenesis at the sea floor by burrowing and feeding actions. The biological stirring of the sediments is termed bioturbation and influences especially the sediment-water interface by introducing oxygen-containing bottom water into the sediments. Tubes and burrows are pumped up with the oxic water by ventilation activities and bioirrigation (figure 9). Advection subsequently transports water through the sediments.

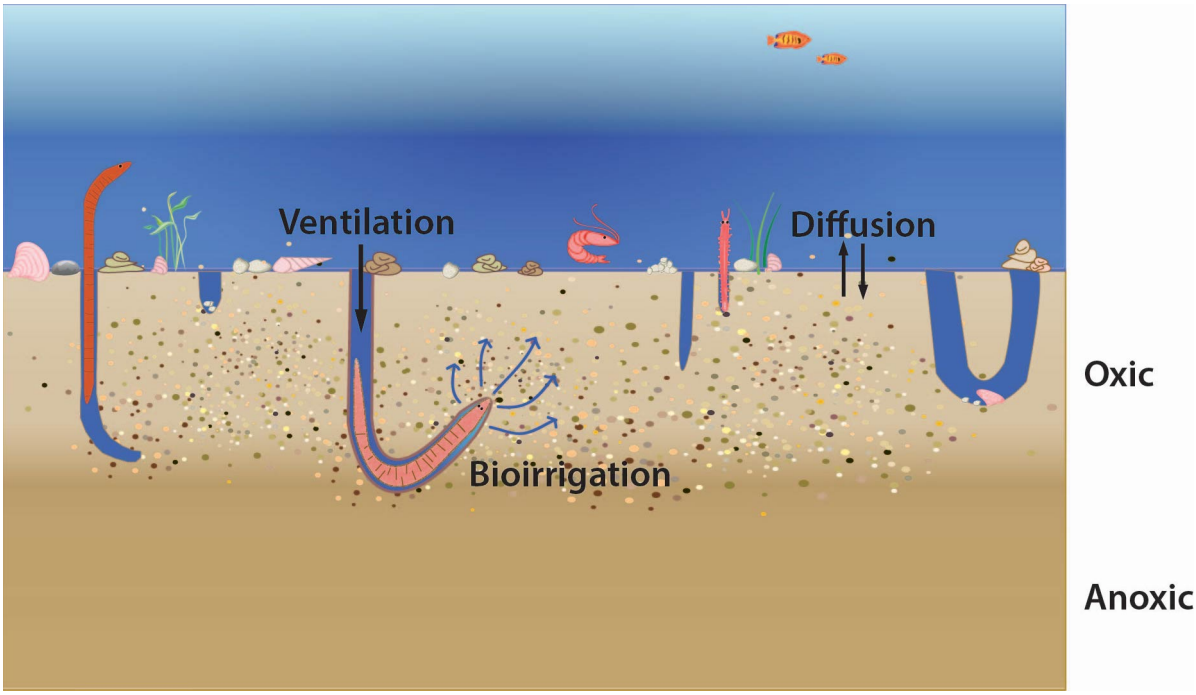


Figure 9 - Illustration of bioturbation, inspired by two figures in (Delefosse et al., 2015) and (Korre et al., 2011). Describes the processes of bioturbation, where animals flush their burrows by ventilation and bioirrigation.

Bioturbation is most intense in the upper 10cm of the sediments but can occur as deep as at 1m depth. By feeding, burrowing and constructing tubes particles are continuously relocated. Some benthic animals ingest sediments and expel undigested particles as fecal pellets or alter grains by mucus secretions to strengthen burrows, thus contributing to increase the size of sedimentary particles. With increased mass, the particles apply more pressure to the sediment surface resulting in compaction and further increased density and removal of pore water. By advection, the water is transported upward and thus also transporting reduced compounds or any possible contaminants up to the sediment water interface, in addition, to supply the sediments downward with oxygen and oxidized compounds. Thus, all fluxes are likely to be increased by the influence of bioturbation (Libes, 1992, Kristensen, 2000).

# 4 Methods/analytical techniques

This chapter gives an overview and description of methods and tools that have been used in this study in addition to the geochemical techniques and analysis.

## 4.1 X-ray diffraction (XRD)

Powder x-ray diffraction was used to identify mineral phases and amount of minerals in the tailings. The XRD uses monochromatic characteristics x-rays to determine the d-spacing in minerals as all minerals have its unique d-spacing. The x-ray analysis was performed at two samples at the Department of Geoscience at the University of Oslo, on a Bruker D8 Advance diffractometer operating at 40 mA, 40 kV and an angle of 2°-65° (2θ). Both samples were from the landfill, sample S1-S (3.01g) was dry and solid and sample S1-W (ca 1g) was liquid from the water of the landfill and centrifuged, vacuumed and dried in advance of the analysis. Preparation of sample S1-S was first crushed by hand in a mortar before 3.01 g material and 8ml ethanol was placed in a jar with bits of agate and micronized in a Glen Creston McCrone Micronizing Mill to obtain a homogeneous and ultra-fine grain size. After micronized the samples were dried at 60° overnight. Thereafter they were distributed evenly on a sample holder overlaid gently with frosted glass to obtain random orientation and to avoid relief. The software DIFFRAC.EVA was used for phase identification with PDF4 databases and software Siroquant V4 for phase quantification. The method used in Siroquant consisted of six stages described by S.Hillier (Hillier, 2000). As the XRD method is dependent on the chemical composition of the minerals that are expected to occur, it is possible that not all chemical compositions have been taken into account causing errors in the sample's weight percentages.

## 4.2 Particle size analysis with laser instrument

Particle size analysis was used to determine the particle size distribution of the tailings. The sample was taken from the top of the landfill and analysed at the Department of Geoscience at the university of Oslo with the laser instrument Beckman Coulter LS13 320. The method analyses particles in the range 0.4 μm-2000 μm. The method is based on broken light from the laser and the angle when it hits the grain surfaces providing a diffractogram with a specific pattern for each particle size. With the use of the intensity of scattered light, the number of particles in a specific interval can be presented. The particle size distribution of the tailings material was an average obtained by analysing the material in two rounds from different parts of the sample. The result was reported as a curve of cumulative distribution and a curve of differential volume (Coulter, 2009).

## 4.3 Scanning electron microscope (SEM)

Scanning electron microscope (SEM) was used to get high-resolution images from two dust filters placed about 1.5m above ground located in upper and lower Åna-Sira as illustrated in figure 10 and presented in table 6 below.

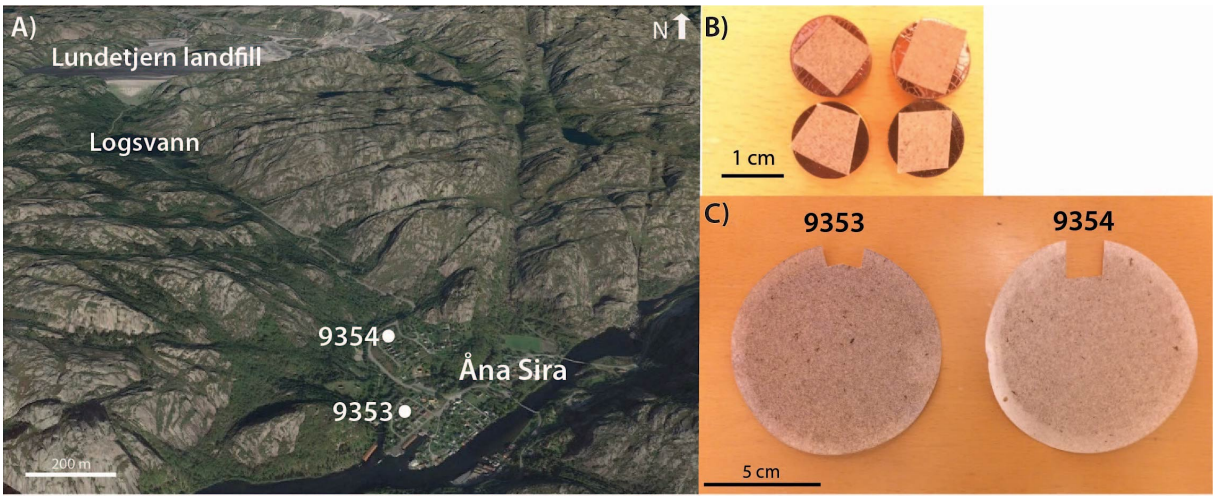


Figure 10 – A) Map of the locations of the dust filters downstream the Lundetjern landfill. They were collected by Titania from an upper part of Åna-Sira (9354) and a lower part of Åna-Sira (9353), B) cut out samples of ca 10x10 mm for SEM, C) dust filters.

Table 6 - Dust filters from upper and lower Åna-Sira analysed by SEM

| Sample | Measuring point | Location | Coating | Period |
|---|---|---|---|---|
| Sample 4a | 9354 | Upper Åna-Sira | Gold | 4/8/16-31/8/16 |
| Sample 4b | 9354 | Upper Åna-Sira | No coating | 4/8/16-31/8/16 |
| Sample 3a | 9353 | Lower Åna-Sira | Gold | 4/8/16-31/8/16 |
| Sample 3b | 9353 | Lower Åna-Sira | No coating | 4/8/16-31/8/16 |

Overall four samples were studied with a Hitachi SU5000 FE-SEM equipped with a Dual Bruker XFlash30 EDS system and HR EBSD system at the department of geoscience at the University of Oslo. The dust filters had a diameter of 9 cm (figure 10c) and samples with sizes of approximate 10x10mm were cut out for analysis (figure 10b). Two samples (3b and 4b) were coated with Carbon Coater Cressington 208C and two (3a and 4a) were coated with Gold Coater Quorum Q150R S. The images with SEM are made by a scanning an electron beam with focused electrons over the specimen and an electron detector is analysing the out coming signals and displaying it on the computer. The images taken were backscattered-electron (BSE) images being most optimal providing the chemical composition of the specimen. The backscattered electrons are determined by the atomic number. The higher atomic number and hence the density of the elements, the larger quantity of electrons of high energy resulting in higher brightness in the images. The energy dispersive spectroscopy (EDS) uses characteristics x-rays to analyse the elements of the specimen either by spot analysis or creating a distributing of elements over a larger area by element mapping (Reed, 2005).

## 4.4 Determination of grain size distribution by point counting

Manual point counting was a method used to get an overall impression of the grain size distribution of two dust filters, sample 3a and sample 4a. The method was based on pictures taken with SEM. At each sample four different spots where randomly chosen and three different zooms weere applied for each spot (x100, x500 and x1000) illustrated in figure 11.

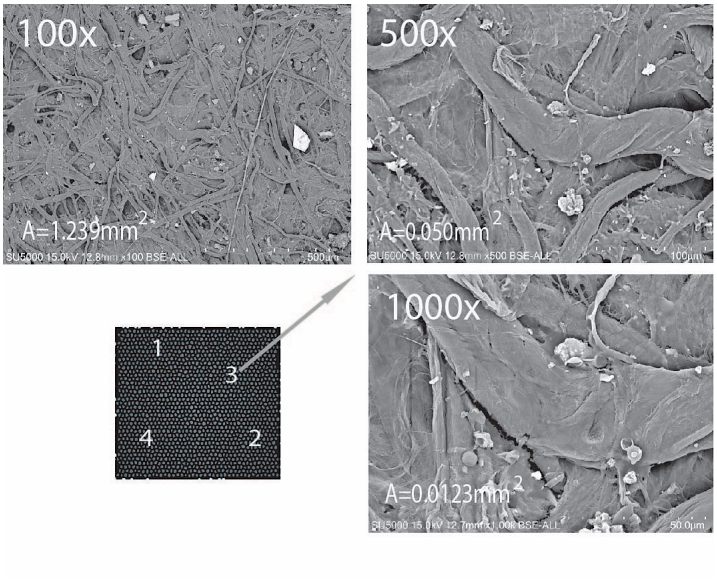


Figure 11 - Illustration of the filter down in left corner with four randomly chosen spots for analysis and three different zooms for each spot.

Each picture was overlaid grids of different sizes making it easier to count and after that the particles where evaluated from a subjective point of view and divided into four groups <10 µm, 10-50 µm, 50-100 µm, >100 µm. In total 24 pictures were taken and counted (Appendix A, table 17 and 18). An exception was the grains smaller than 10 µm in the x100 zoom which was not counted as they were too small and difficult to evaluate the size of and would nevertheless be counted more precise in the other zooms. The x100 zoom obviously gives a better overview of the largest grains whereas the x1000 zoom will be more accurate for the smallest grains.

After counting, an average of the all the x100 zooms, the x500 zooms and the x1000 zooms where calculated to get one average number for each particle group representing each zoom. Then it was calculated how many of the different picture-zooms that would fit the whole sample by assuming the total area of the sample was 10 mm*10 mm=100 $mm^2$. The area of each picture were calculated as illustrated in figure 12, using the scale on the picture. For instance, would 81 pictures with 100x zoom fit in the whole sample, 2000 pictures with x500 zoom and 8130 pictures with x1000 zoom (Appendix A, figure 47 for all zooms). At last each particle group were multiplied with pictures to get an overall grain size distribution.

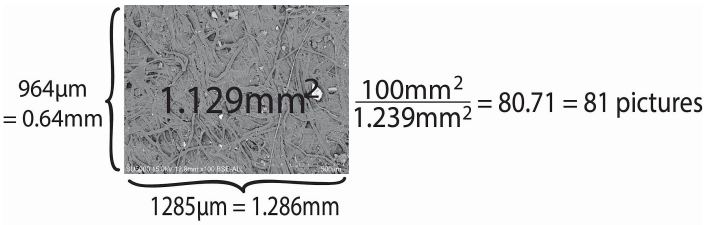


Figure 12 - Illustration of a 100x zoom picture how the area of the sample was calculated

## 4.5 Water samples and preparation

Water sampling was done both in freshwater on land and in seawater from box core liners at NIVA's research station at Solbergstrand. The water samples at Solbergstrand was done with DGT probes and subsequently lab work and ICP-MS. The field work done in advance of the water samples from the liners at Solbergstrand are described in chapter 4.8 whereas the DGT method and lab preparation is more detailed described in chapter 4.9.

The sampling on land was done the 23$^{th}$ of November 2016 at nine different localities at Tellenes around the landfill, both in situ pH measuring by pH-meter and laboratory analysis by ICP-MS and Ion Chromatography. Map with locations of the water samples can be seen in figure 6. After collection, they were kept cold until chemical analysis. Sample 1 consisted of wet sediments and water. It was dark coloured and taken directly from the top of the landfill. In advance of the laboratory analysis, sample 1 was centrifuged to separate sediments from water. The sediments in sample 1 were furthered vacuumed and prepared for XRD. The rest of the samples were without sediments, clear in colour and taken from freshwater bodies, streams and creeks. All water samples were filtered before ion chromatography, whereas filtered and acidified with two drops of $HNO_3$ in prior to the ICP-MS analysis.

A second campaign was performed the 20$^{th}$ of April 2017 where an extra round of water sampling was done for sample 3-9. The pH was measured with pH test paper strips to get a rough knowledge of pH for comparison with the previous samples before analysed by ICP-MS.

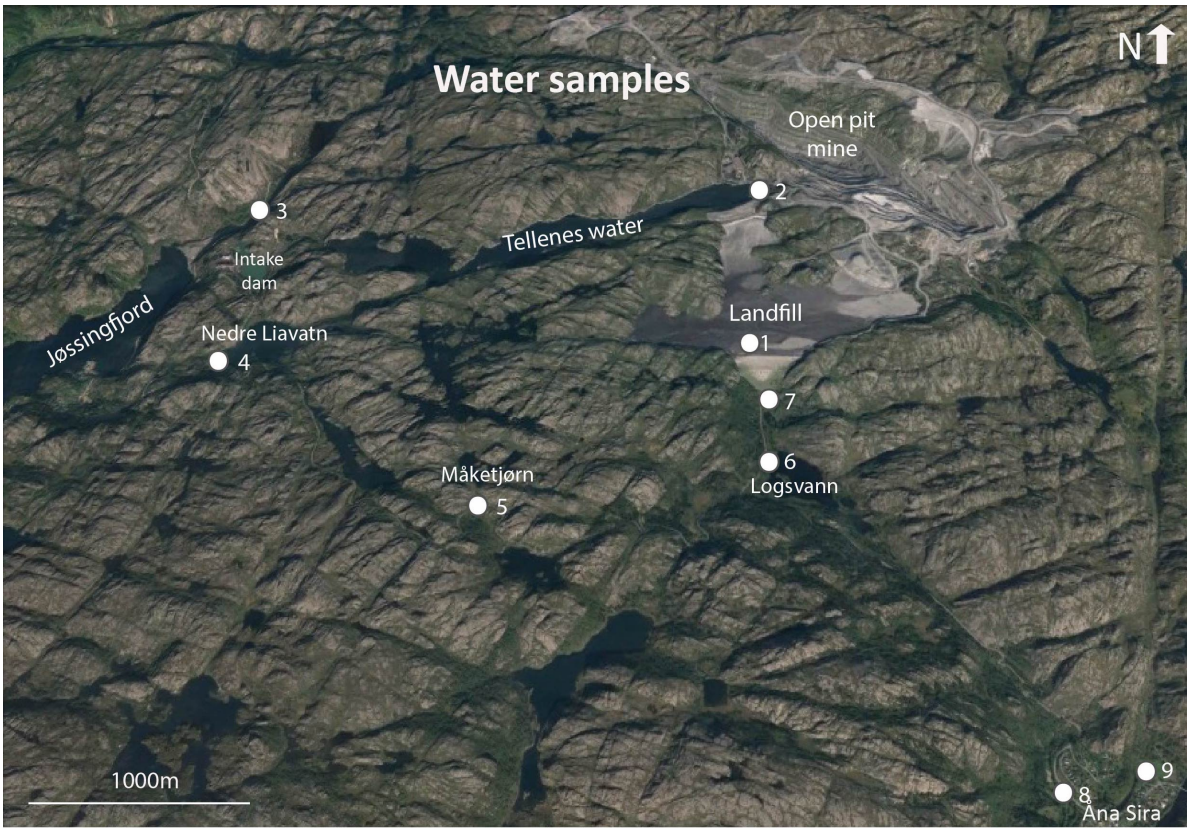


Figure 13 - Map of locations of the water sampling around the landfill at Tellenes

After water analysis the concentrations found in the water samples were compared with rainwater concentrations by Norwegian Institute for Air Research (Aas et al., 2009), guidelines for drinking-water quality set by WHO (2017), maximum annual concentration by environmental quality standards in freshwater (MAC-EQS) by EU and acute toxic effect values set by Norwegian Environment Agency (Miljødirektoratet, 2016).

## 4.6 Quadropole inductively coupled plasma mass spectrometer (Q-ICPMS)

Ionic Coupled Plasma Mass Spectrometry (ICP-MS) was used to determine heavy metals in water samples, shown in figure 13 above. A total of 16 samples and the heavy metals Cr, Co, Ni, Cu, Zn, Cd and Pb were analysed from the freshwater around the landfill with a Bruker Aurora Elite quadropole inductively coupled plasma source mass spectrometer at the department of geoscience at the University of Oslo. The samples were kept cold, filtered and added two drops of $HNO_3$ in prior to the analysis. A total of 81 samples and the elements Fe, Mn, Cd, Ni, Cu, Zn and Co were analysed from the DGT probes deployed in the liners at Solbergstrand. They were deployed in sediments in seawater for 24 hours but none of them contained saltwater. The detailed lab work in advance of the analysis is described under the DGT method in chapter 4.9. The mass spectrometry can be used for qualitative, quantitative and semi quantitative analysis and can have detection limits down to parts per trillion for

some elements. The Q-ICPMS is build up by an ion source, a quadropole mass analyser and a detection system and uses plasma to generate positively charged ions. The sample is introduced to the ion source as aerosol droplets and is dried, vaporized, atomized and ionized by high-temperature argon plasma (Thomas, 2008). Hereafter the samples are compared with standard samples for calibration and calculated into concentrations. For the samples in this thesis, the detection limits were under 0.04 ppb and by recommendation from the technician at UiO values below detection limits have been marked or not used. To demonstrate how easy a sample may be contaminated, a test with the Q-ICPMS was done with water in contact with a finger for one second, revealing a concentration of 118 ppb of Zn.

## 4.7 Ion exchange chromatography

Ion exchange chromatography was used to analyse the cations and anions F, Cl, SO4, Br, NO3, PO4, Na, K, Mg and Ca in the water samples. Nine samples from around the landfill from field trip 1 were analysed at a Dionex ICS-2000 at the department of geoscience at the University of Oslo. Cations and anions are analysed separately due to their different charge affinity. For instance, the anions will be separated based on their affinity to the anion exchange resin. The technique is based on exchange equilibria between ions in solution and ions of the same charge on the surface of a solid with fixed exchange sites. The ions are transported through a column with an eluent, acid for anion exchangers while base for cation exchangers for separation. Thereafter the eluent is neutralized and a conductivity detector counts the amount of cations or anions (Hagedorn, 2007, Skoog et al., 2007).

## 4.8 Box-core experiments in mesocosm laboratory

Field work and experiments at NIVA's research station at Solbergstrand were done at the sea tailings. Box-core sampling with the tool KC Denmark box corer (figure 14B) was carried out in Oslofjorden outside of Drøbak with the boat FF Trygve Braarud, UiO, 16/3-17 at approximate 175 m depth. To reduce erosion at the sediment surface, as much water as possible was removed from above the sediments on deck. In total 11 box core liners (0.1 $m^2$), where collected, three of which for Titania (T), three for an anonymous mine (N), three for control (K) and two extra not used (3 and 9). Thereafter they were transported and placed at NIVA's research station Solbergstrand in a mesocosm laboratory (figure 12E) to create an experimental environment similar to the natural condition in the fjord with dim light and supplied with a water flow of 2 ml/min with water from Olsofjorden at 60 m depth (Schaanning et al., 2008). The boxes are called "liners" and are specially made by NIVA for taking up undisturbed sea floor. The day after 17/3-17, the tailings were distributed over the sediments in the liners from a plastic box (figure 12D). The tailings from Titania where partly frozen and reheated before a 4 kg of wet tailings with a density of 2 $g/cm^3$ were mixed into the overlying water in each box and allowed to settle on the sediments in an even layer with a thickness of approximately 2 cm.

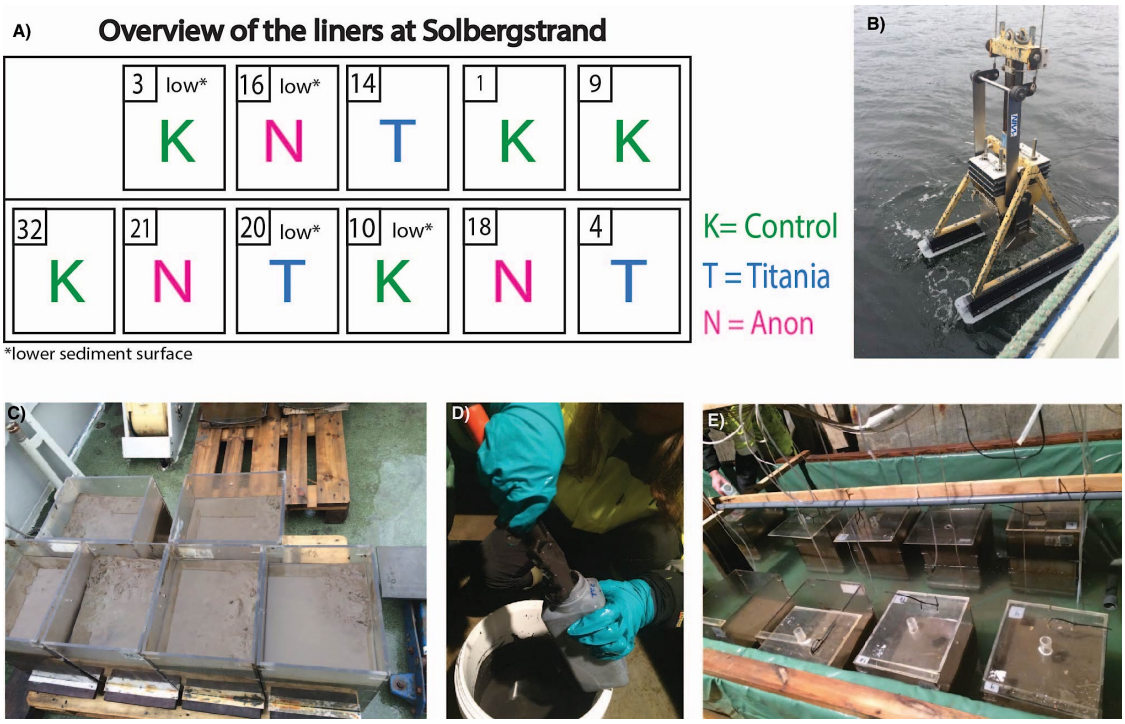


Figure 14 – A) Overview of the liners at Solbergstrand, B) box corer C) liners on deck D) pouring tailings in a plastic box for easier distribution over the sediments in the liners, E) liners in mesocosm laboratory at Solbergstrand.

Fluxes of Pb, Cd, Cu, Co, Ni and Zn across the sediment-water interface was measured the 20/4, 24/4 and 26/4 by technicians at Solbergstrand and calculated by the formula:

$$F = ((C_{in} - C_{out}) * Q)/A \qquad (4.1)$$

where F is flux across sediment-water interface ($\mu g m^{-2} h^{-1}$), $C_{in}$ in the concentration in the supply-water ($\mu g L^{-1}$), $C_{out}$ is the concentration in the water out of each of the liners ($\mu g L^{-1}$), Q is the flow rate through each liner ($L h^{-1}$) and A is the area of the liner (0.1 $m^2$). More detailed description of the set-up and the flux measurements are to be found in these two articles by Schaanning and Trannum (Trannum et al., 2010, Schaanning et al., 2008). All flux values used in this study is an average of the three values.

## 4.9 Diffusive Gradients in Thin films

Diffusive gradients in thin films have been used to measure the metal uptake in the pore water of the sediments at Solbergstrand. They are measured in fluxes of $ng/cm^2$ per 24h in pore water and can not measure metal fluxes out of the sediments nor be compared to polluting concentration limits. However, they have been used to compare non-contaminated sediments (control liners) and contaminated sediments (Titania liners) since DGT-probes have been deployed at both. Besides, the proportionality between the DGT uptake and fluxes from sediment to water column has been tested, as they are expected to be proportional. If the correlation is good, the regression line may be used to calculate fluxes out of sediments.

Although this has not been done in this thesis, it may be used for future in situ measurements.

The DGT probe is a technique developed by Hao Zhang and William Davison in 1994 and comprises a membrane filter, a diffusive gel layer and a resin layer as illustrated in figure 15 below, and gives in situ concentration or uptake of the accumulated ions during the time of deployment.

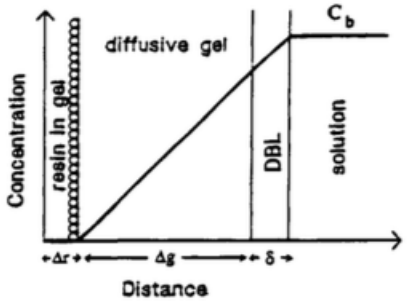


Figure 15 - - Representation of the layers through the DGT in contact an aqueous solution. The metal ions diffuse from the bulk solution through a diffusive boundary layer (DBL) and a diffusive gel before it reaches the ion exchange resin of Chelex gel. The diffusion rate is assumed to be the same in the bulk solution and the gel (Zhang and Davison, 1995).

The technique is based on diffusion through the membrane filter (DBL) and the diffusive gel layer and subsequent accumulation onto the resin gel, as in this case consist of Chelex-100 gel (Zhang and Davison, 1995). The device used in this thesis is a LSPM Loaded DGT device for metals (A) in sediment (cations) with 0.8 mm APA diffusive gel, polyethersulphone filter membrane and Chelex binding layer. After deployment of the DGT-probes in the sediments for 24 hours the membrane filter and the diffusive gel were removed whereas the Chelex was cut in intervals of 0-5 mm, 5-10 mm, 10-15 mm, 15-20 mm, 20-30 mm, 30-50 mm, 50-70 mm and 70-90 mm as illustrated in figure 16. Thereafter each of the gel pieces was placed in sample tubes and covered with 1ml $HNO_3$ for at least 24 hours for the metals to be extracted. The gel was then removed and the fluid left was poured over in new sample tubes and filled up with deionized to a total volume of 10ml before analysis with QICP-MS.

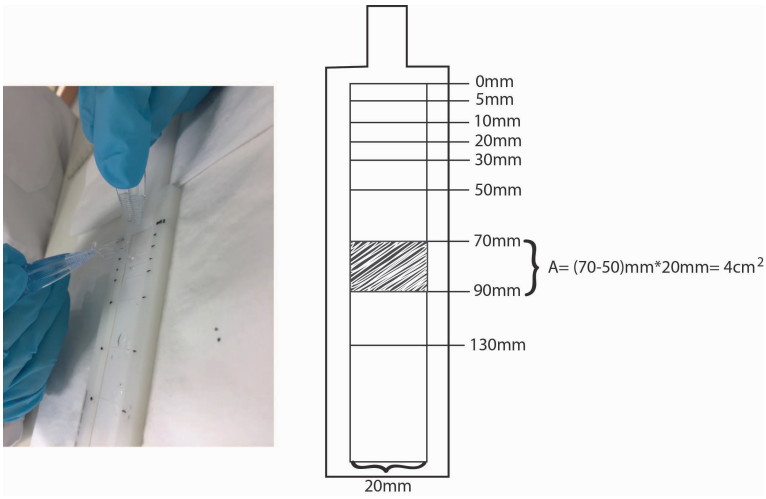


Figure 16 – Photograph of a DGT probe to the left and an illustration of the probe to the right with an example of

how the uptake area was calculated.

The concentrations from QICP-MS were then to be calculated from mass concentration in the extract to uptake in pore water (in ng/cm$^2$) by the formula:

$$DGT\ metal\ uptake = C * V/A \qquad (4.2)$$

where C is the concentration in the extract measured by QICP-MS (in μg/L), V is the volume of the extract (L), and A is the uptake interval area (cm$^2$). The volume of the extract was 0.01L and the area was calculated by using the width of the probe and multiplying it by the depth interval as illustrated in figure 16.

## 4.10 Electrode measurements

Electrode measurements were performed with a device consisting of a reference electrode and sensors for pH, the redox potential and $S^{2-}$- ions. Platinum electrodes were used for measuring the redox potential and Ag | $Ag_2S$ electrodes for measuring sulphide ions. More detailed information about the method is described in Norwegian Standard 9410:2007 and related article (Schaanning and Hansen, 2005, Anon, 2007). In advance of the measurement, the pH meter was calibrated with pH 4 and pH 7 and the surface water in the liners was removed. The device was placed above the sediments and moved vertically downwards. The measurements were taken at 1cm intervals as soon the values stabilized and down to a sediment depth at 7.5 cm (figure 17). This was performed at 11 liners (see overview illustration in chapter 4.8). The sulphide content proved to be insignificantly low and therefore excluded from the results. Calculations for Eh were done by adding the half-cell potential of the reference electrode. The half-cell potential has been tested on the electrodes in a redox buffer solution, resulting in a potential of 185 mV, which gives an Eh by the formula:

$$Eh = Eh' + 185mV \qquad (4.3)$$

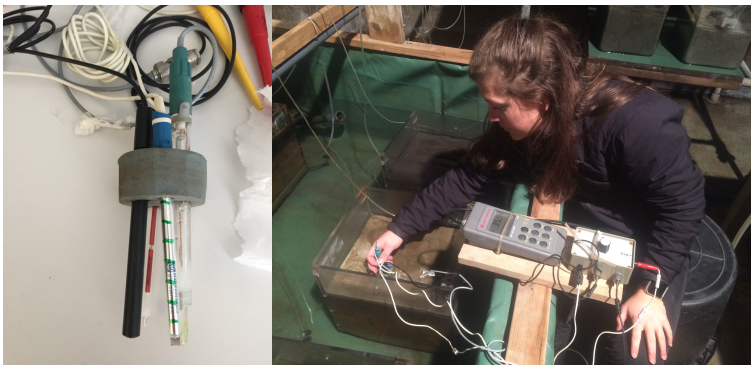

Figure 17 – Electrode measurement device. Reference electrode in red at the back to the left, pH meter in the back to the right, a black electrode in front to measure the content of sulphides and electrode in front to the right for measuring the redox potential where each green mark shows intervals of 1cm.

# 5 Results

## 5.1 Tailing disposal on land at Tellenes

### 5.1.1 Tailings material in landfill

Two analysis has been done on the tailings material in the landfill, named sample 1-sediment, consisting of sediments, and sample 1- slurry, consisting of finer particles in a slurry from the water phase in the landfill. The analysis of the mineralogical phases of the tailings was performed at both samples and obtained by XRD. The particle size distribution was performed at sample 1-sediment by laser instrument Beckman Coulter. In addition, particle size distribution was performed at two dust filters by point counting in SEM with results described in chapter 5.1.2. A cumulative distribution curve and a differential volume curve obtained by laser instrument of sample 1-sediment are presented in figure 18 below. The differential volume curve shows a non-uniform distribution of particle sizes with a mean of 225 μm and a positive skewness (1.114). The cumulative curve shows a wide distribution of particles with approximately 75% of the measured material in the range between 60-400 μm, corresponding to a particle size ranging from very fine sand to medium sand by the sediment size class terminology of Udden-Wentworth (Terry and Goff, 2014). The median was calculated to be 188μm representing a particle size of fine sand (125-250 μm).

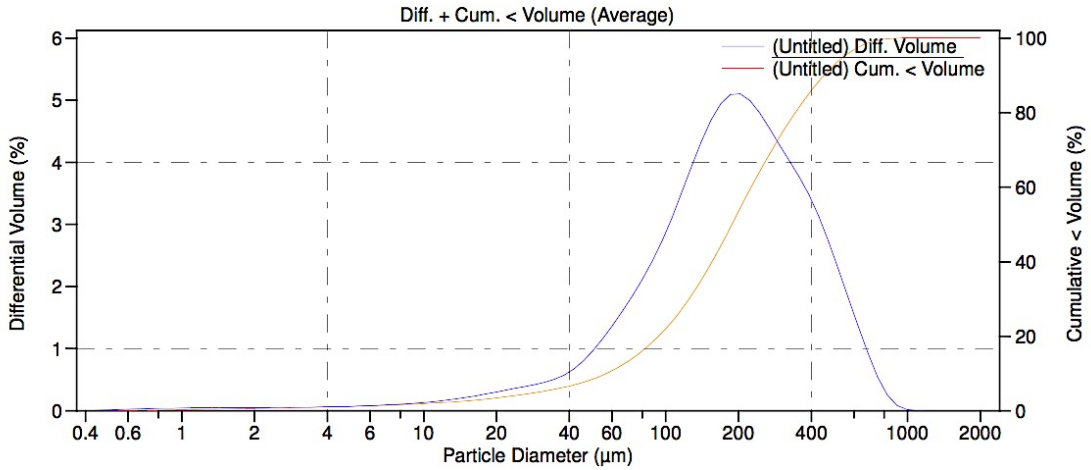


Figure 18 – Particle size distribution of sample 1 from the landfill by the particle size analyser.

XRD analyses were done on both sample 1-sediment and sample 1-slurry. The results are presented in figure 19 and 20 below. Sample 1-slurry was obtained by centrifuging the water sample 1.1 (water samples are described in chapter 5.1.3) and subsequently vacuuming and drying the material in an oven at 60 degrees until dry.

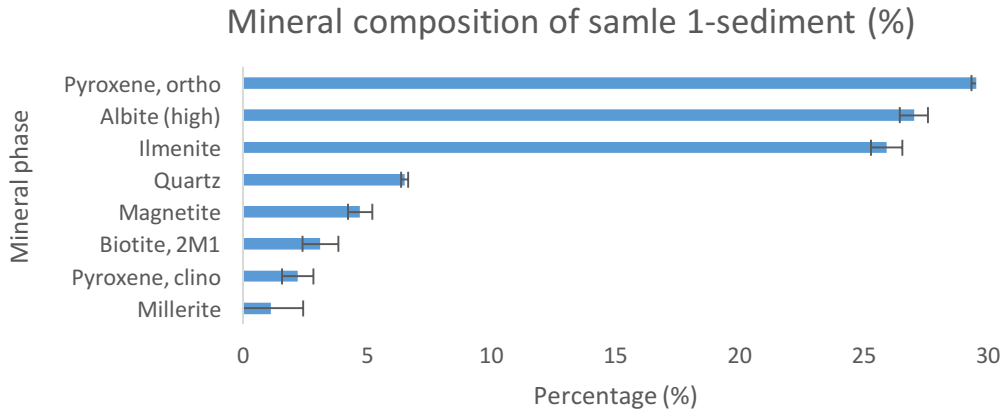


Figure 19- Results from XRD of solid sample from the top of the landfill

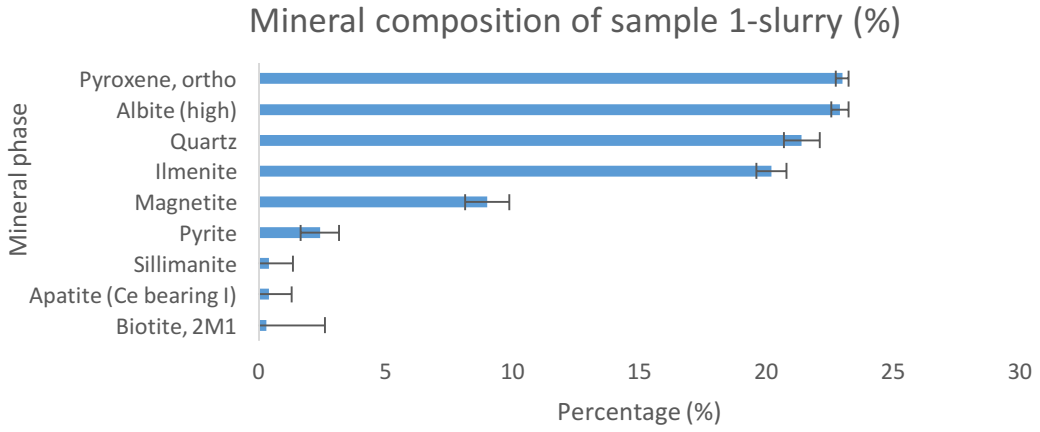


Figure 20 - Results from XRD of vacuumed material centrifuged from water sample from the top of the landfill

The results from the XRD analysis for the two samples came out with different mineralogical phases. However, both samples were enriched in orthopyroxene, albite and ilmenite. Sample 1-sediment was dominated by orthopyroxene (29%), albite (27%) and ilmenite (25.9%) with minor amounts of quartz (6.5%), magnetite (4.7%), biotite (3.1%), clinopyroxene (2.2%) and millerite (1.1%). The error of fit was 1.32 for millerite and less than 1 for the rest of the minerals. For sample 1-slurry, orthopyroxene (23%), albite (22.9%), quartz (21.4%), ilmenite (20.2%) dominated with minor amounts of magnetite (9%), pyrite (2.4%) and very small amounts of silimanite (0.4%), apatite (0.4%) and biotite (0.3%). The error of fit was highest for biotite with 2.3 and less than 1 for the rest of them.

### 5.1.2 Windblown/airborne material

The windblown material was obtained from two dust filters, sample 3a and 4a. The material was analysed by SEM with the element mapping function whereas the particle size distribution was obtained by manual point counting.

The pictures taken with SEM were used to determine the grain sizes of the grains in the two dust filters by point counting. Two randomly chosen pictures from the dust filters are shown below (figure 21). Both samples were poorly sorted with grain size diameters from less than 10 μm to over 100 μm. Most of the grains were subangular with some sharp edges and corners, and few were rounded.

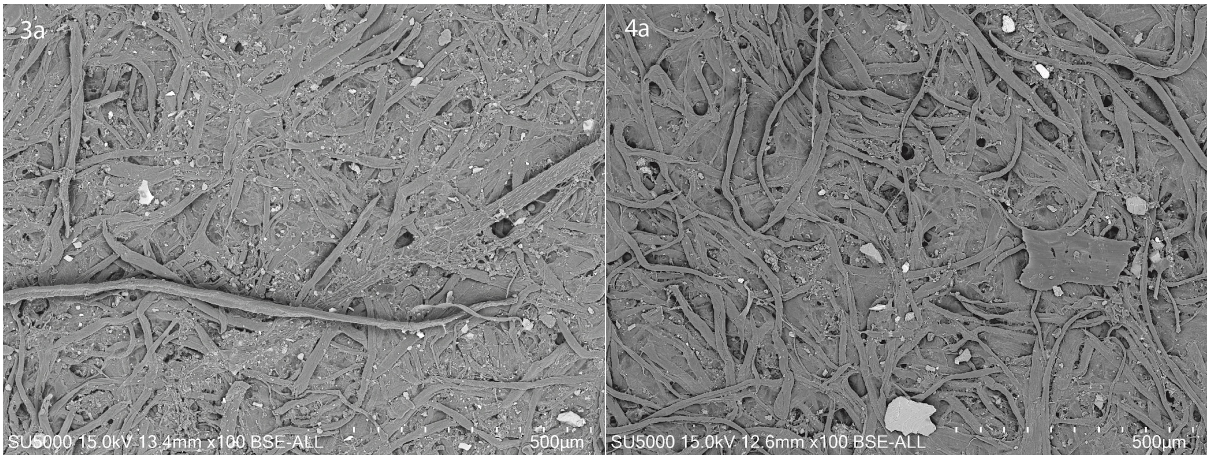

Figure 21 – Pictures of sample 3a (left) and 4a (right), both taken with zoom x100 with SEM.

Both the dust filters, sample 3a and 4a (figure 22), were enriched in particles with a diameter smaller than 10 μm, corresponding to a diameter of fine silt (Terry and Goff, 2014). The quantity of particles also decreases with increasing diameter size for both samples, as shown in the graph below (figure 22). Sample 3a is from the lower part of Åna-Sira and consist of more particles under 50 μm than sample 4a, corresponding coarse silt and finer. In contrast, sample 4a, located in the upper part of Åna-Sira and closer to the mine, consists of more particles larger than 50 μm corresponding to coarse silt to very fine sand.

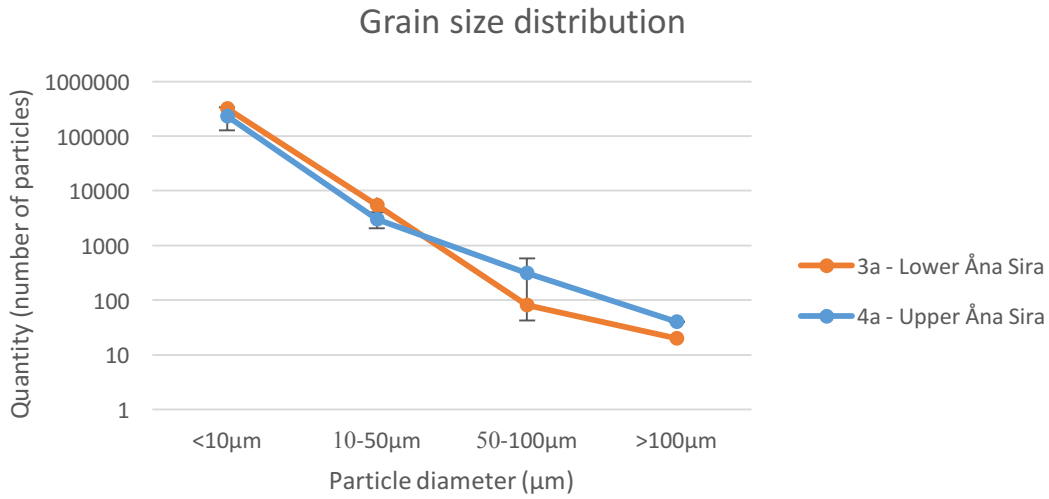


Figure 22 - Grain size distribution from dust filters obtained by point counting.

To do a rough estimate of the mineral content of the dust filters point analysis at eight pictures were performed with energy dispersive x-ray spectrometry (EDS) on SEM, three of which with a zoom of x50, whereas six with zoom x500. At each of the pictures 3-10 points, a total of 61 points were analysed. The analysed grains were randomly chosen, but a focus on the heaviest grains may have occurred. Notice that the percentage of the elements is not representative for the whole sample, but only for the grains chosen. An average of the elements resulted in a highest percentage of oxygen (24.2-43.5%), iron (9.9-30.3%), titanium (2.7-36.4%), silicon (5.4-23.3%) and calcium (0.7-12.4%), with smaller amounts of aluminium (1.9-8.4%) and magnesium (1.6-7.7%). In addition, some very small percentages of sodium (0.6-3.6%), potassium (1.6-6.4%) and copper (0.9-1.9%). The high percentage of iron and titanium are possible due to ilmenite grains. However, iron was also found in combination with oxygen, and in combination with magnesium, silica and aluminium, possible indicating magnetite ($Fe_3O_4$) and pyroxene ((Mg, Fe) $SiO_3$). Iron and titanium were also often observed with 1-2% of copper as well. Calcium and sodium were often in combination with silicon and aluminium, which could indicate plagioclase ((Na, Ca) $Al_{1-2}Si_3O_8$). A grain likely to be biotite were also observed (K $(Mg, Fe)_3O_{10}$ $(Fe, OH)_2$), and a grain likely to be pentlandite ($(NiFe)_9S_8$).

A few elemental maps were also performed, but a percentage of the elements were not stated. However, a clear trend of grains with the combination Si, Al and Ca/Mg and the combination of Fe and Ti was observed. These observations could indicate the mineral plagioclase ((Na, Ca) $Al_{1-2}Si_3O_8$) whereas the combination of Ti and Fe could indicate ilmenite ($FeTiO_3$). The results of two of the elemental maps, one from sample 3a and one from 4a, both with a zoom of x500, are pictured below (figure 23 and 24). In figure 23 from sample 3a all the grains were under 50µm and most of the grains were sub angular and some subrounded. The sample was dominated by grains with the combination Al and Si, likely to be plagioclase, with fewer grains of ilmenite with Fe and Ti. In addition, one very visible grain up in the left corner with the elements phosphorus (P) and calcium (Ca) was observed, likely to be an apatite grain.

In figure 24 from sample 4a, three grains stood out from the others with a diameter over 50μm whereas the rest of the grains were significantly smaller. The biggest of them was possible a plagioclase consisting of Si and Al and Ca, while the two other big grains were likely ilmenite. The shape of the big grains was angular with sharp edges while most of the smaller grains were subrounded. One grain in the middle of the picture differed from the others with its long, thin and sharp shape. Almost all the smaller grains were likely to be a combination of Al and Si.

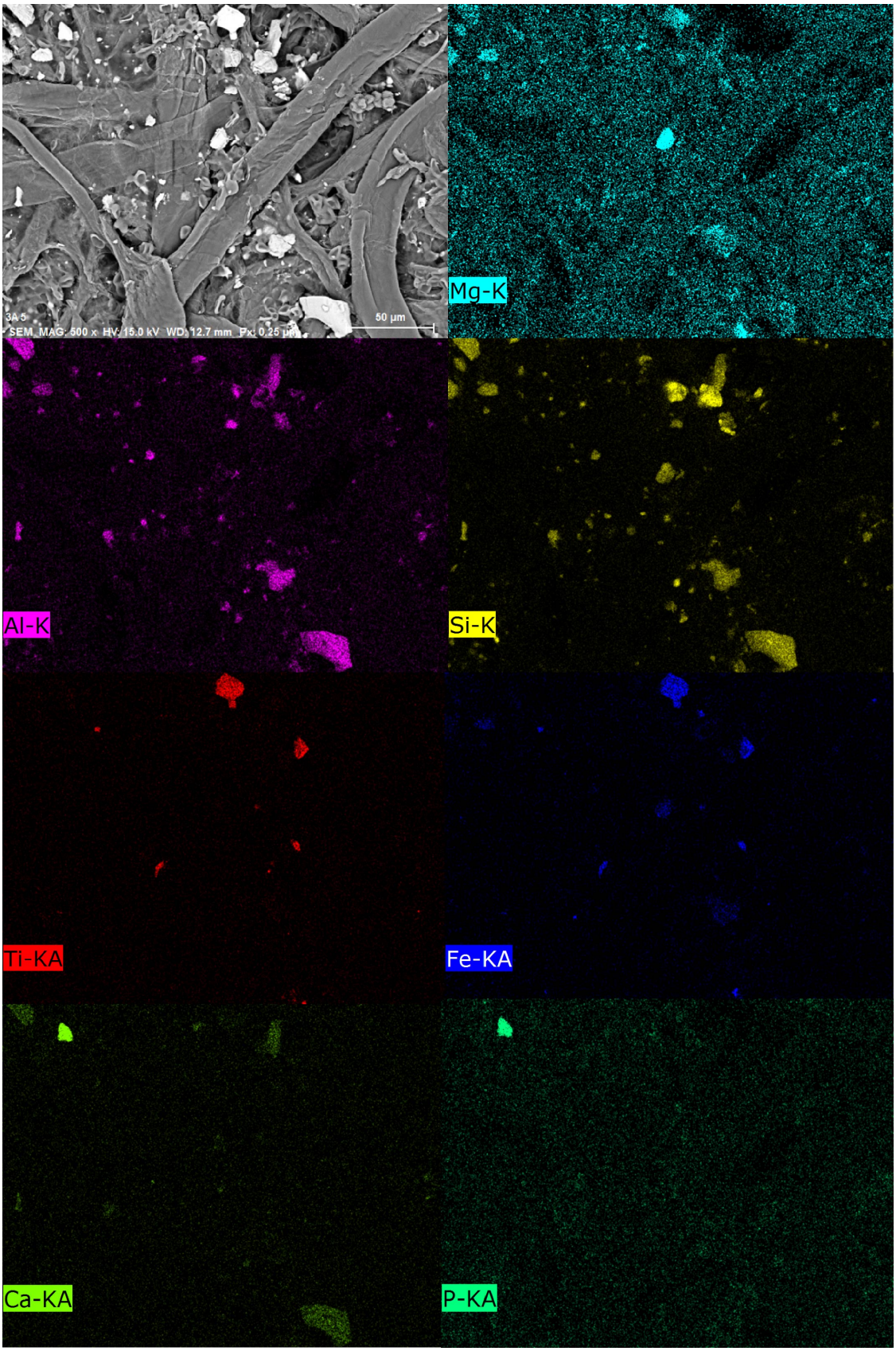


Figure 23 - Sample 3a from lower Åna-Sira. Picture taken with SEM with a zoom of x500 to the left and six smaller pictures from the elemental map with the elements Al, Si, Ti, Fe, Ca and P to the right.

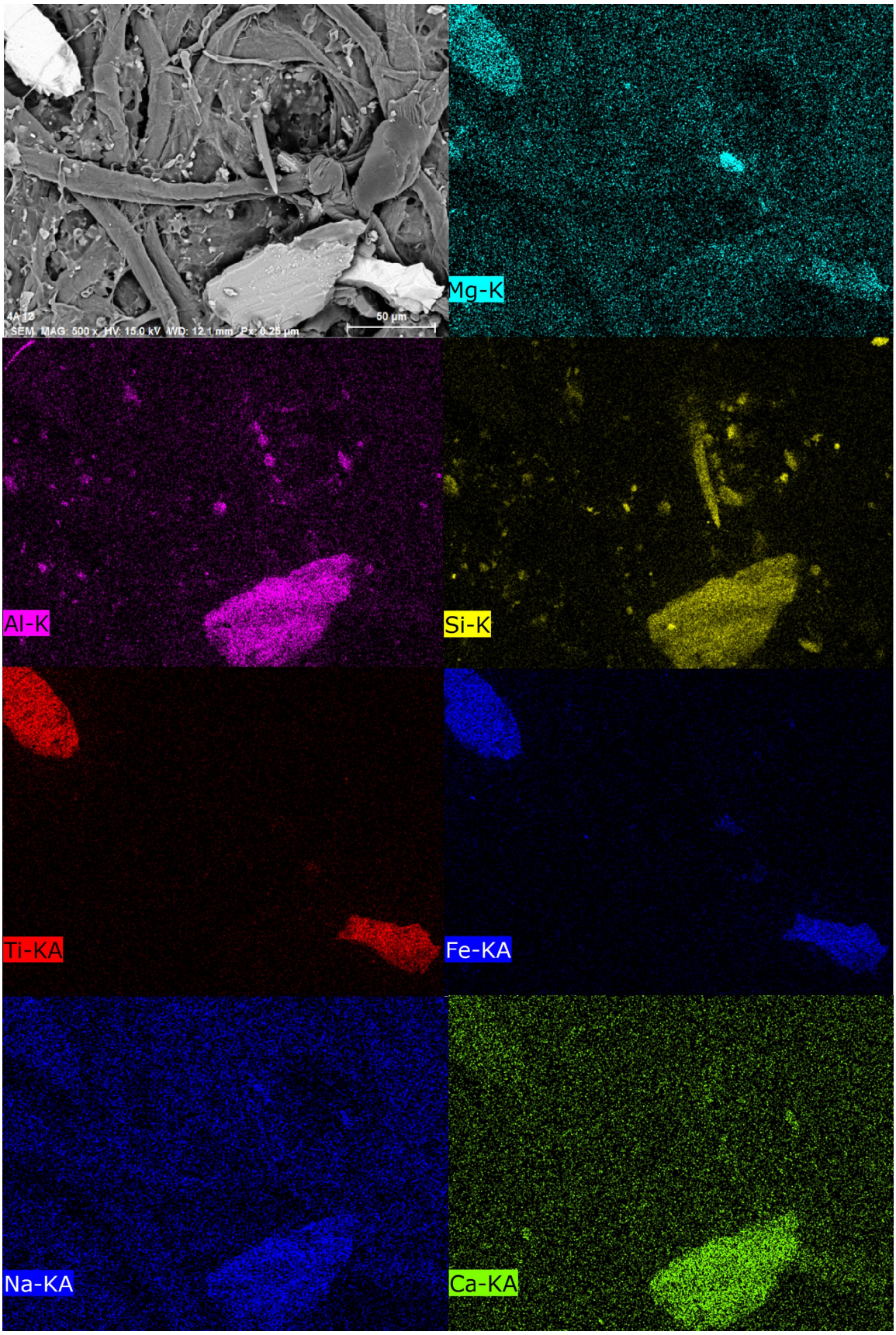


Figure 24- Sample 4a from upper Åna-Sira. Picture taken with SEM with a zoom of x500 to the left and six smaller pictures from the elemental map with the elements Al, Si, Ti, Fe, Ca and Mg to the right.

### 5.1.3 Total dust emissions on land

Total dust emissions have been calculated based on one of the dust filters in upper Åna-Sira (sample 4a) applied for approximate a month (28 days) in august 2016. The particles have been assumed spherical with a density of 2700 g/cm$^2$, slightly higher than plagioclase of 2620 g/ cm$^2$ (Spalla et al., 2010), due to the presence of ilmenite. The flux was calculated to be 0.0878 kg/m$^2$/year (see Appendix A, table 21). An arbitrary area of 1 km$^2$ would correspond to a flux of 87800 kg/year. If assuming that all particles originate from tailings of Titania, 0.03% would be Ni (Mellgren, 2002) corresponding to a Ni flux of 26.3 kg/year. It is not taken into account that the number of particles varies with height above ground level. The flux applies to all particles counted in the dust filters, and it must be mentioned that the amount nickel is only a tiny percentage of this flux.

### 5.1.4 Aqueous transported material

Water samples were collected by two field campaigns done November 2016 and April 2017. An overview of the samples is shown in the method chapter 4.5 (figure 13). Samples were numbered accordingly, X.Y, with X being the sampling locality and Y being campaign 1 or 2. Sample 1.1 was located directly on the top of the landfill as illustrated in figure 25. All trace elements and major ions have been described. However, since Zn concentrations from campaign 1 and campaign 2 turned out to be significantly different, Zn has been chosen to be included in the tables yet not described. Contamination during sample preparation is suspected as an explanation for the high concentrations of Zn in campaign 1.

Nickel has been emphasized considering nickel as one of Titania's main challenges. The legend of nickel concentrations in ppb in the left upper corner is the environmental quality standards set by the Norwegian Environment Agency (Miljødirektoratet, 2016), where yellow denotes the maximum annual concentration EQS-MAC for Ni. Further comparisons to the standards are treated with more details later, under discussion chapter 6.1.2.

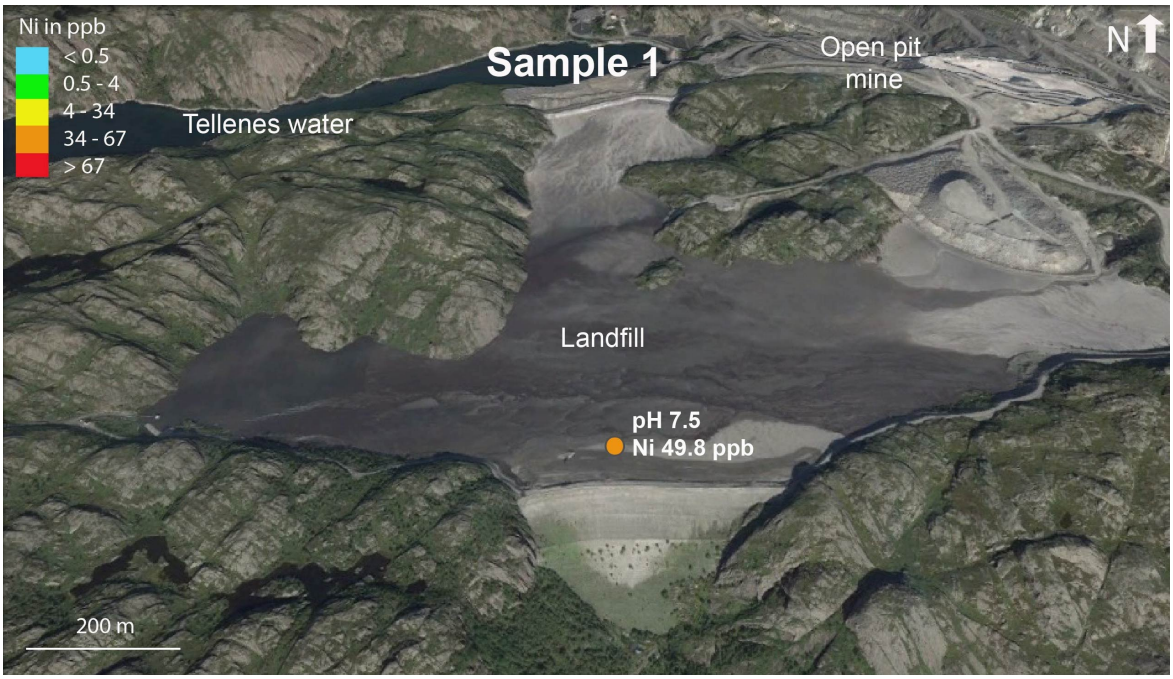


Figure 25 - Location of sample 1 on top of the landfill with a pH of 7.5 and a nickel concentration of 49.8 ppb

Since sample 1.1 was taken directly from the water phase in the landfill, it can be assumed that it represents the tailings in content. Therefore, it can be suitable for comparison of the other samples in addition to the mineral reactions from the landfill to samples downstream the landfill.

The pH of sample 1.1 was measured to be 7.5 and the nickel concentration 49.8 ppb, exceeding the maximum annual concentration of freshwater by the Norwegian Environment Agency given by EU. The results of trace elements and major ions of sample 1 is presented in table 7 below.

Table 7 – Results of trace elements, major ions in and pH in water sample 1. Rain water concentrations by (Aas et al., 2009), guidelines for drinking-water quality set by (WHO, 2017), maximum annual concentration by environmental quality standards in freshwater (MAC-EQS) and acute toxic effect values set by (Miljødirektoratet, 2016). N.a: not analysed.

| | Unit | Sample 1 | Rain water Birkenes obs. | Drinking-water (WHO) | MAC- EQS freshwater | Acute toxic effect |
|---|---|---|---|---|---|---|
| **pH** | | 7.50 | 4.77 | | | |
| **Trace elements** | | | | | | |
| Cr | ppb | 0.0211 | 0.12 | 50.0 | 3.4 | > 3.4 |
| Co | ppb | 0.589 | 0.01 | | | |
| Ni | ppb | 49.8 | 0.13 | 70.0 | 34 | > 67.0 |
| Cu | ppb | 0.516 | 0.39 | 2000 | 7.8 | > 15.6 |
| Zn | ppb | 29.6 | 2.9 | 100 | 11 | > 60 |
| Cd | ppb | 0.0046 | 0.025 | 3 | 1.15 | >15 |
| Pb | ppb | 0.0202 | 0.78 | 10.0 | 14 | > 57 |
| **Major ions** | | | | | | |
| F | ppm | 1.06 | | 1.5 | | |
| Cl | ppm | 10.3 | 2.59 | 250 | | |
| SO4 | ppm | 234 | 0.26 | 250 | | |
| Br | ppm | n.a. | | 0.01 | | |
| NO3 | ppm | 1.67 | 0.35 | 50.0 | | |
| PO4 | ppm | 1.62 | | | | |
| Na | ppm | 15.5 | 1.59 | 200 | | |
| K | ppm | 6.44 | 0.08 | | | |
| Mg | ppm | 26.80 | 0.20 | | | |
| Ca | ppm | 106 | 0.13 | | | |

The Ni concentration of 49.8 ppb was the highest of the trace elements in sample 1.1. The SO4 concentration of 234 ppm and PO4 concentration of 1.62 ppm were higher than in all the other water samples. None of the values were above the guidelines for drinking water by WHO.

Sample 2.1 was located at the end of the Tellenes water, north of the landfill and below the open pit mine. The pH was measured to be 7.26, and the nickel concentration was 30.9 ppb, within freshwater condition 3, which is moderate and below MAC-EQS (figure 26). Other trace elements and major ions are presented in table 8 below.

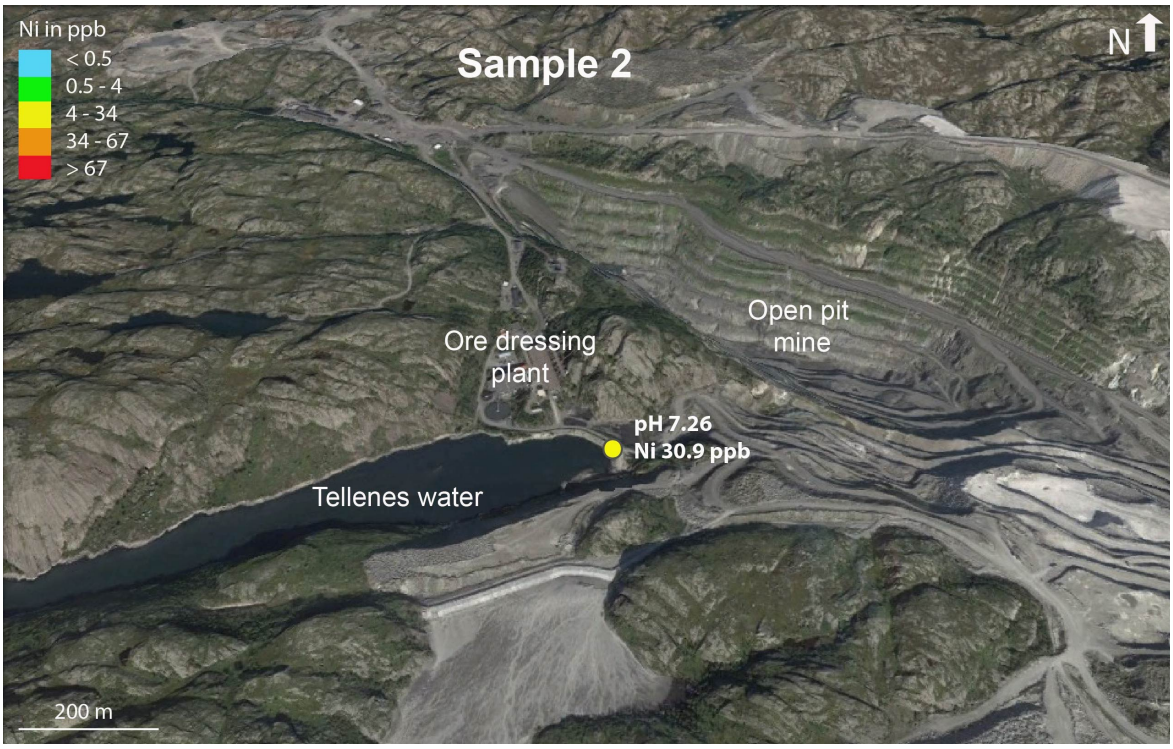


Figure 26 - Location of sample 2 in the end of the Tellenes water, below the open pit mine and north of the landfill.

Table 8 - Results of trace elements, major ions in and pH in water sample 2. Rain water concentrations by (Aas et al., 2009), guidelines for drinking-water quality set by ((WHO), 2017), maximum annual concentration by environmental quality standards in freshwater (MAC-EQS) and acute toxic effect values set by (Miljødirektoratet, 2016). N.a: not analysed.

| | Unit | Sample 2 | Rain water Birkenes obs. | Drinking- water (WHO) | MAC-EQS freshwater | Acute toxic effect |
|---|---|---|---|---|---|---|
| **pH** | | 7.26 | 4.77 | | | |
| **Trace elements** | | | | | | |
| Cr | ppb | 0.05 | 0.12 | 50.0 | 3.4 | > 3.4 |
| Co | ppb | 2.41 | 0.01 | | | |
| Ni | ppb | 30.9 | 0.13 | 70.0 | 34 | > 67.0 |
| Cu | ppb | 1.90 | 0.39 | 2000 | 7.8 | > 15.6 |
| Zn | ppb | 191 | 2.9 | 100 | 11 | > 60 |
| Cd | ppb | 0.03 | 0.025 | 3 | 1.15 | >15 |
| Pb | ppb | 0.05 | 0.78 | 10.0 | 14 | > 57 |
| **Major ions** | | | | | | |
| F | ppm | 0.08 | | 1.5 | | |
| Cl | ppm | 10.2 | 2.59 | 250 | | |
| SO4 | ppm | 43.3 | 0.26 | 250 | | |
| Br | ppm | n.a. | | 0.01 | | |
| NO3 | ppm | 3.57 | 0.35 | 50.0 | | |
| PO4 | ppm | n.a. | | | | |
| Na | ppm | 9.88 | 1.59 | 200 | | |
| K | ppm | 3.49 | 0.08 | | | |
| Mg | ppm | 2.93 | 0.20 | | | |
| Ca | ppm | 15.0 | 0.13 | | | |

In sample 2, the Ni concentration was the highest of the trace elements and SO4 (43.3 ppm) the highest of the major ions. Both Co (2.41 ppb) and Cu (1.9 ppb) were slightly increased compared to sample 1. However, all elements are below all standards and limits used as comparison in this study.

Sample 3 in figure 27 was located in the innermost part of Jøssingfjord, in a creek called Lonebekken, which drains from the intake dam and is approximate 2.8km west of the landfill. The pH was measured to be 6.5 at campaign 1 and 5.5 at campaign 2 and the Ni concentrations to be 59.5 ppb and 23.2 ppb, within freshwater condition 4 and 3. The results of trace elements and major ions are presented below (table 9).

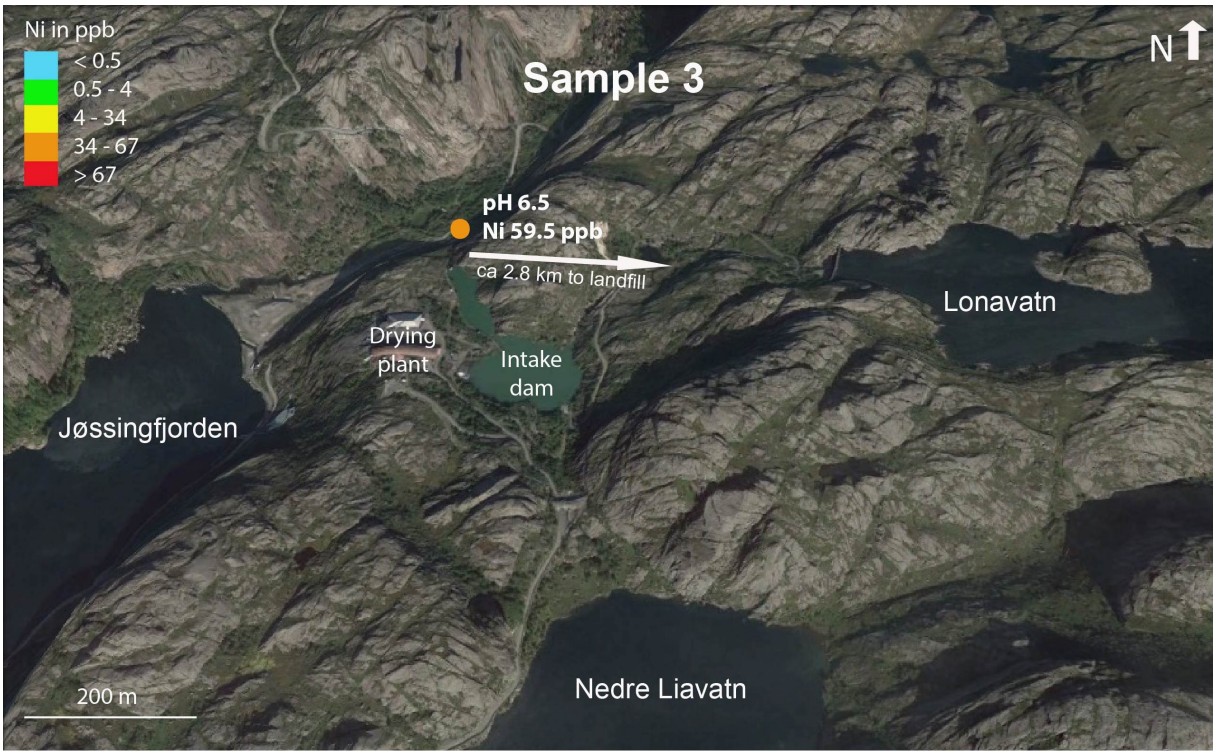


Figure 27 - Location of sample 3 and results of pH and Ni concentrations.

Table 9 - Results of pH, trace elements and major ions from water analysis of sample 3. N.a: not analysed, n.d: not detected.

| | Unit | Sample 3.1 | Sample 3.2 | Rain water Birkenes obs. | Drinking-water (WHO) | MAC- EQS freshwater | Acute toxic effect |
|---|---|---|---|---|---|---|---|
| **pH** | | 6.50 | 5.5 | 4.77 | | | |
| **Trace elements** | | | | | | | |
| Cr | ppb | 0.84 | 0.790 | 0.12 | 50.0 | 3.4 | > 3.4 |
| Co | ppb | 2.81 | 0.092 | 0.01 | | | |
| Ni | ppb | 59.4 | 23.2 | 0.13 | 70.0 | 34 | > 67.0 |
| Cu | ppb | 2.77 | 1.100 | 0.39 | 2000 | 7.8 | > 15.6 |
| Zn | ppb | 240 | 0.663 | 2.9 | 100 | 11 | > 60 |
| Cd | ppb | 0.0221 | n.d. | 0.025 | 3 | 1.15 | >15 |
| Pb | ppb | 0.0591 | n.d. | 0.78 | 10.0 | 14 | > 57 |
| **Major ions** | | | | | | | |
| F | ppm | 0.218 | | | 1.5 | | |
| Cl | ppm | 11.6 | | 2.59 | 250 | | |
| SO4 | ppm | 89.9 | | 0.26 | 250 | | |
| Br | ppm | n.a. | | | 0.01 | | |
| NO3 | ppm | 1.56 | | 0.35 | 50.0 | | |
| PO4 | ppm | 0.449 | | | | | |
| Na | ppm | 10.4 | | 1.59 | 200 | | |
| K | ppm | 4.03 | | 0.08 | | | |
| Mg | ppm | 6.95 | | 0.20 | | | |
| Ca | ppm | 28.4 | | 0.13 | | | |

Ni concentrations in sample 3.1 exceeds the MAC-EQS limit for freshwater, however, campaign 2 measured almost half the concentration. SO4 was observed to be 89.92 ppm.

Sample 4 was located in the lower part of Nedre Liavatn, west of Jøssingfjord and approximately 2.5 km west of the landfill as illustrated in figure 28. The pH was measured to be 5.54 and 5, and the Ni concentrations were both within condition 2 corresponding to good conditions. Results of other trace elements and major ions is presented in table 10. All concentration in sample 4.1 were observed to be below all standards and limits used as comparison in this study.

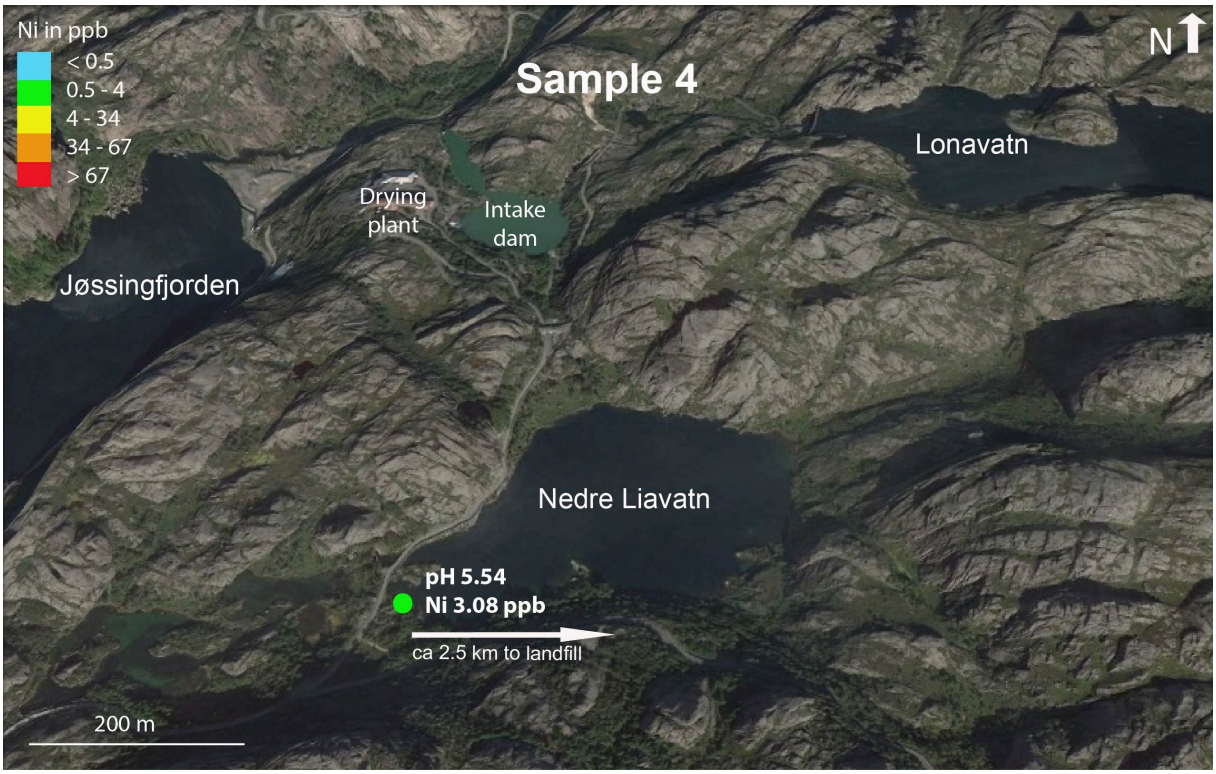


Figure 28 - Sample 4 located 2.5 km west of the landfill with results of Ni and pH.

Table 10 -Results of pH, trace elements and major ions from water analysis of sample 4.

| | Unit | Sample 4.1 | Sample 4.2 | Rain water Birkenes obs. | Drinking-water (WHO) | MAC- EQS freshwater | Acute toxic effect |
|---|---|---|---|---|---|---|---|
| **pH** | | 5.54 | 5 | 4.77 | | | |
| **Trace elements** | | | | | | | |
| Cr | ppb | 0.04 | 0.0358 | 0.12 | 50.0 | 3.4 | > 3.4 |
| Co | ppb | 1.03 | 0.254 | 0.01 | | | |
| Ni | ppb | 3.08 | 1.31 | 0.13 | 70.0 | 34 | > 67.0 |
| Cu | ppb | 0.671 | 0.328 | 0.39 | 2000 | 7.8 | > 15.6 |
| Zn | ppb | 151 | 2.06 | 2.9 | 100 | 11 | > 60 |
| Cd | ppb | 0.0817 | 0.0375 | 0.025 | 3 | 1.15 | >15 |
| Pb | ppb | 0.499 | 0.252 | 0.78 | 10.0 | 14 | > 57 |
| **Major ions** | | | | | | | |
| F | ppm | 0.050 | | | 1.5 | | |
| Cl | ppm | 13.02 | | 2.59 | 250 | | |
| SO4 | ppm | 2.82 | | 0.26 | 250 | | |
| Br | ppm | 0.46 | | | 0.01 | | |
| NO3 | ppm | 1.18 | | 0.35 | 50.0 | | |
| PO4 | ppm | 0.253 | | | | | |
| Na | ppm | 6.29 | | 1.59 | 200 | | |
| K | ppm | 1.32 | | 0.08 | | | |
| Mg | ppm | 0.801 | | 0.20 | | | |
| Ca | ppm | 0.723 | | 0.13 | | | |

Location of sample 5 was south of Måketjern and southwest of the landfill as shown in figure 29 together with Ni concentration of 1.22 ppb and 1.31 ppb (sample 5.2) and pH 5.64 and 5. The Ni concentrations were characterized as good, within condition 2. Results from water analysis are presented in table 11. All values in sample 5 were in good conditions and well under the limits used as comparison in this study.

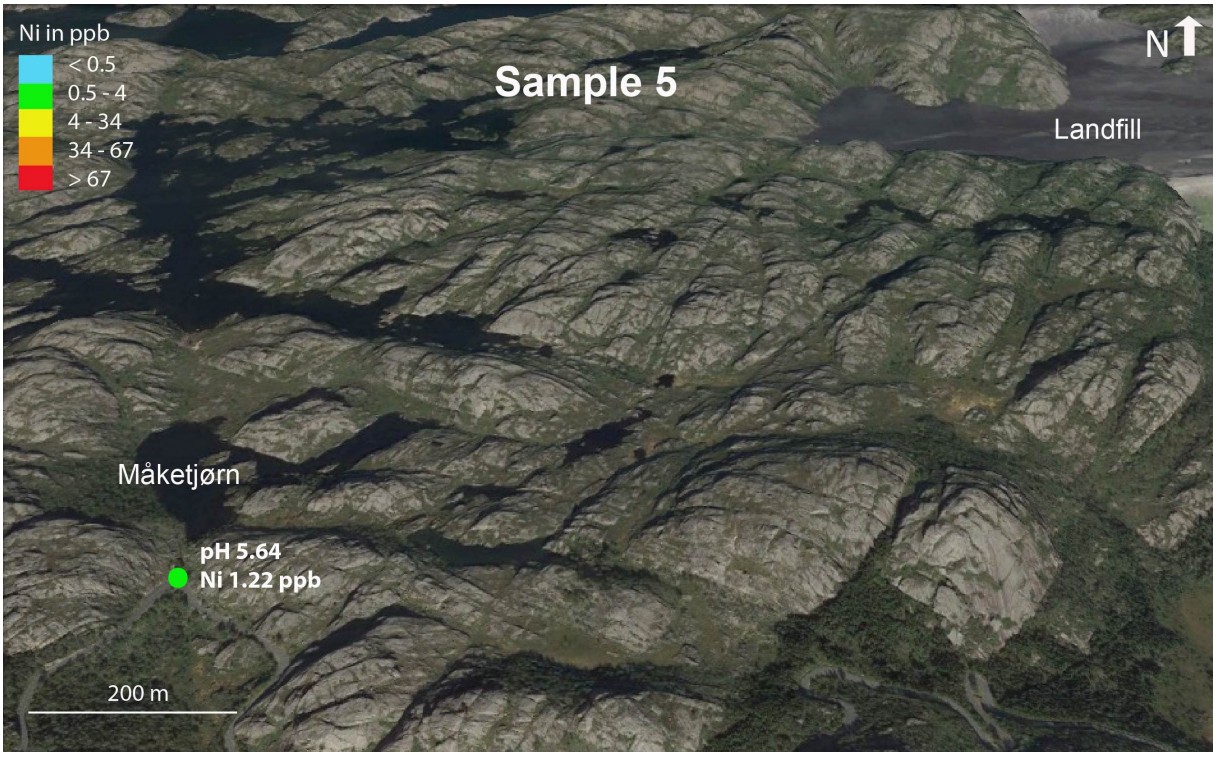


Figure 29 - Location of sample 5 southwest of the landfill and results of pH and Ni.

Table 11 - Presentation of results of water analysis of sample 5. N.a: not analysed.

| | Unit | Sample 5.1 | Sample 5.2 | Rain water from Birkenes obs. | Drinking-water (WHO) | MAC- EQS freshwater | Acute toxic effect |
|---|---|---|---|---|---|---|---|
| **pH** | | 5.64 | 5 | 4.77 | | | |
| **Trace elements** | | | | | | | |
| Cr | ppb | 0.06 | 0.0573 | 0.12 | 50.0 | 3.4 | > 3.4 |
| Co | ppb | 0.590 | 0.253 | 0.01 | | | |
| Ni | ppb | 1.22 | 1.31 | 0.13 | 70.0 | 34 | > 67.0 |
| Cu | ppb | 0.556 | 0.483 | 0.39 | 2000 | 7.8 | > 15.6 |
| Zn | ppb | 115 | 4.12 | 2.9 | 100 | 11 | > 60 |
| Cd | ppb | 0.081 | 0.0657 | 0.025 | 3 | 1.15 | >15 |
| Pb | ppb | 0.720 | 0.671 | 0.78 | 10.0 | 14 | > 57 |
| **Major ions** | | | | | | | |
| F | ppm | 0.0557 | | | 1.5 | | |
| Cl | ppm | 9.59 | | 2.59 | 250 | | |
| SO4 | ppm | 1.88 | | 0.26 | 250 | | |
| Br | ppm | 0.457 | | | 0.01 | | |
| NO3 | ppm | 1.18 | | 0.35 | 50.0 | | |
| PO4 | ppm | n.a. | | | | | |
| Na | ppm | 4.78 | | 1.59 | 200 | | |
| K | ppm | 1.38 | | 0.08 | | | |
| Mg | ppm | 0.566 | | 0.20 | | | |
| Ca | ppm | 0.474 | | 0.13 | | | |

Sample 6 was taken in Logsvann downstream the landfill. The pH was measured to be 6.35 and 5.5 (sample 6.2). The Ni concentration was observed to be 20.8 ppb in sample 6.1 and 27.9 for sample 6.2, both within moderate condition 3 and under MAC-EQS, see figure 30 and table 12. The results of other trace elements and major ions are presented in below. Both sample 6.1 and 6.2 had all concentrations below guidelines for drinking water by WHO.

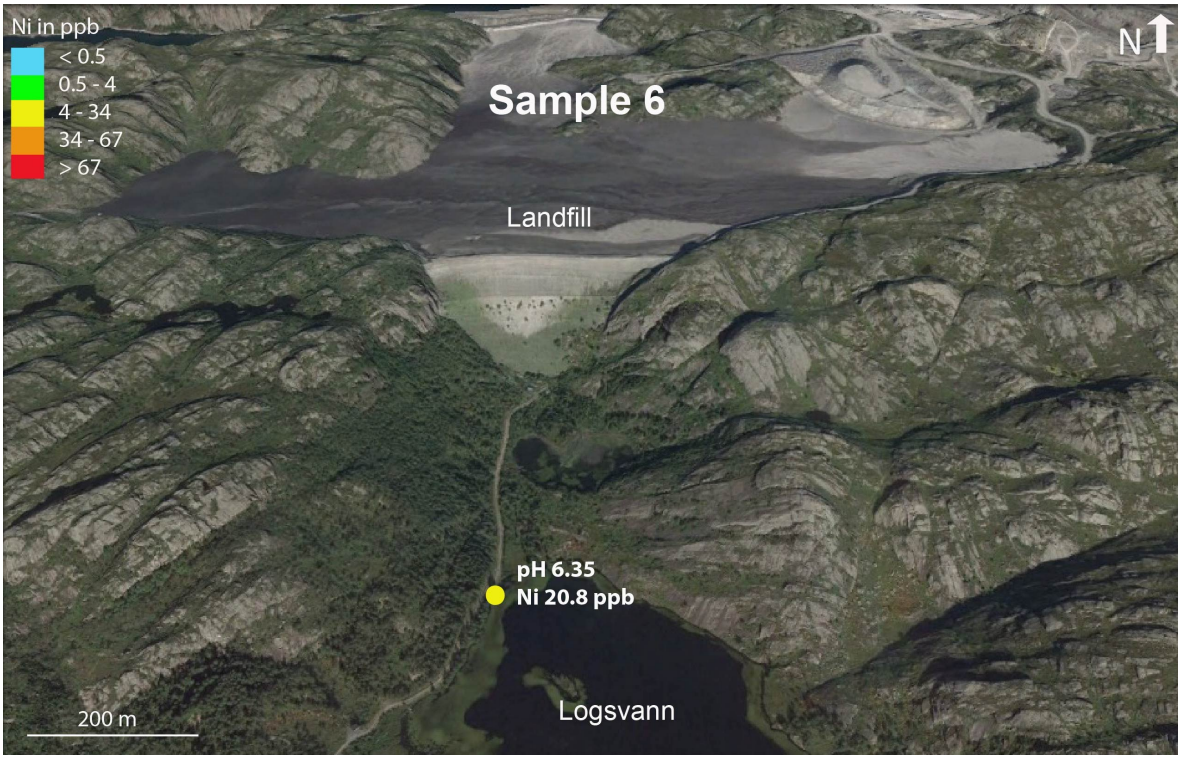


Figure 30 - Location of sample 6, downstream of the landfill in the Logsvann.

Table 12 - Results of trace elements and major ions from water analysis of sample 6. N.a: not analysed, n.d: not detected.

| | Unit | Sample 6.1 | Sample 6.2 | Rain water Birkenes obs. | Drinking-water (WHO) | MAC- EQS freshwater | Acute toxic effect |
|---|---|---|---|---|---|---|---|
| **pH** | | 6.35 | 5.5 | 4.77 | | | |
| **Trace elements** | | | | | | | |
| Cr | ppb | 0.052 | 0.112 | 0.12 | 50.0 | 3.4 | > 3.4 |
| Co | ppb | 0.592 | 0.081 | 0.01 | | | |
| Ni | ppb | 20.8 | 27.9 | 0.13 | 70.0 | 34 | > 67.0 |
| Cu | ppb | 0.397 | 0.590 | 0.39 | 2000 | 7.8 | > 15.6 |
| Zn | ppb | 53.4 | 5.63 | 2.9 | 100 | 11 | > 60 |
| Cd | ppb | 0.0250 | n.d. | 0.025 | 3 | 1.15 | >15 |
| Pb | ppb | 0.0633 | n.d. | 0.78 | 10.0 | 14 | > 57 |
| **Major ions** | | | | | | | |
| F | ppm | 0.0942 | | | 1.5 | | |
| Cl | ppm | 13.2 | | 2.59 | 250 | | |
| SO4 | ppm | 24.4 | | 0.26 | 250 | | |
| Br | ppm | n.a. | | | 0.01 | | |
| NO3 | ppm | 1.090 | | 0.35 | 50.0 | | |
| PO4 | ppm | n.a. | | | | | |
| Na | ppm | 7.76 | | 1.59 | 200 | | |
| K | ppm | 1.11 | | 0.08 | | | |
| Mg | ppm | 2.98 | | 0.20 | | | |
| Ca | ppm | 9.50 | | 0.13 | | | |

The location of sample 7 below the landfill as illustrated in figure 31. Sample 7.1 was measured to have a pH of 7.5 whereas sample 7.2 was measured to have a pH of 7. Results from trace elements and major ions are presented in table 13.

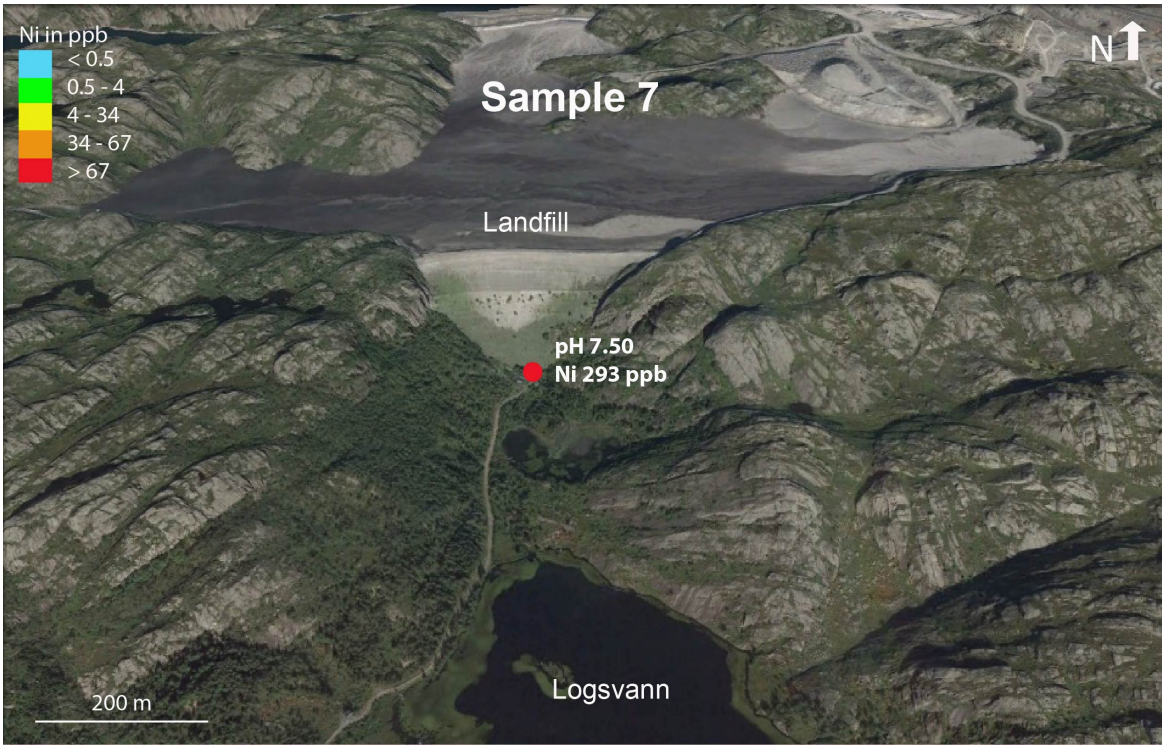


Figure 31 - Illustration of sample 7 below the water fill and the results of Ni and pH

Table 13 - Results of pH, trace elements and major ions of sample 7 below the landfill. N.a: not analysed, n.d: not detected.

| | Unit | Sample 7.1 | Sample 7.2 | Rain water Birkenes obs. | Drinking-water (WHO) | MAC- EQS freshwater | Acute toxic effect |
|---|---|---|---|---|---|---|---|
| **pH** | | 7.50 | 7 | 4.77 | | | |
| **Trace elements** | | | | | | | |
| Cr | ppb | 0.0536 | 1.38 | 0.12 | 50.0 | 3.4 | > 3.4 |
| Co | ppb | 9.99 | 14.4 | 0.01 | | | |
| Ni | ppb | 293 | 433 | 0.13 | 70.0 | 34 | > 67.0 |
| Cu | ppb | 0.596 | 81.5 | 0.39 | 2000 | 7.8 | > 15.6 |
| Zn | ppb | 50.4 | 0.759 | 2.9 | 100 | 11 | > 60 |
| Cd | ppb | 0.0085 | n.d. | 0.025 | 3 | 1.15 | >15 |
| Pb | ppb | 0.0143 | n.d. | 0.78 | 10.0 | 14 | > 57 |
| **Major ions** | | | | | | | |
| F | ppm | 0.755 | | | 1.5 | | |
| Cl | ppm | 9.72 | | 2.59 | 250 | | |
| SO4 | ppm | 211 | | 0.26 | 250 | | |
| Br | ppm | n.a. | | | 0.01 | | |
| NO3 | ppm | 0.656 | | 0.35 | 50.0 | | |
| PO4 | ppm | 0.749 | | | | | |
| Na | ppm | 18.7 | | 1.59 | 200 | | |
| K | ppm | 5.10 | | 0.08 | | | |
| Mg | ppm | 30.3 | | 0.20 | | | |
| Ca | ppm | 113 | | 0.13 | | | |

The Ni concentration in sample 7.1 was observed to be 293 ppb and in sample 7.2 it was 433 ppb, both corresponding to condition 5 (very poor) in freshwater by the Norwegian Environment Agency. Ni concentration of sample 7.2 is by far the highest value of all the water samples, exceeding guidelines for drinking water, MAC-EQS and over four times the limit of acute toxic effect for freshwater organisms. Ni concentration at sample 7.1 also exceeds both the drinking-water limits, MAC-EQS and with acute toxic effect. SO4 was observed to have the highest concentration within the major ions of 211 ppm.

Sample 8 was in a creek in Åna-Sira approximately 2.7 km below and south of the landfill, figure 32. The pH of sample 8.1 and 8.2 was measured to be 6.71 and 6. The Ni concentrations were 29.8 ppb and 17.3 ppb, within the MAC-EQS range. The results of trace elements and major ions are presented in table 14.

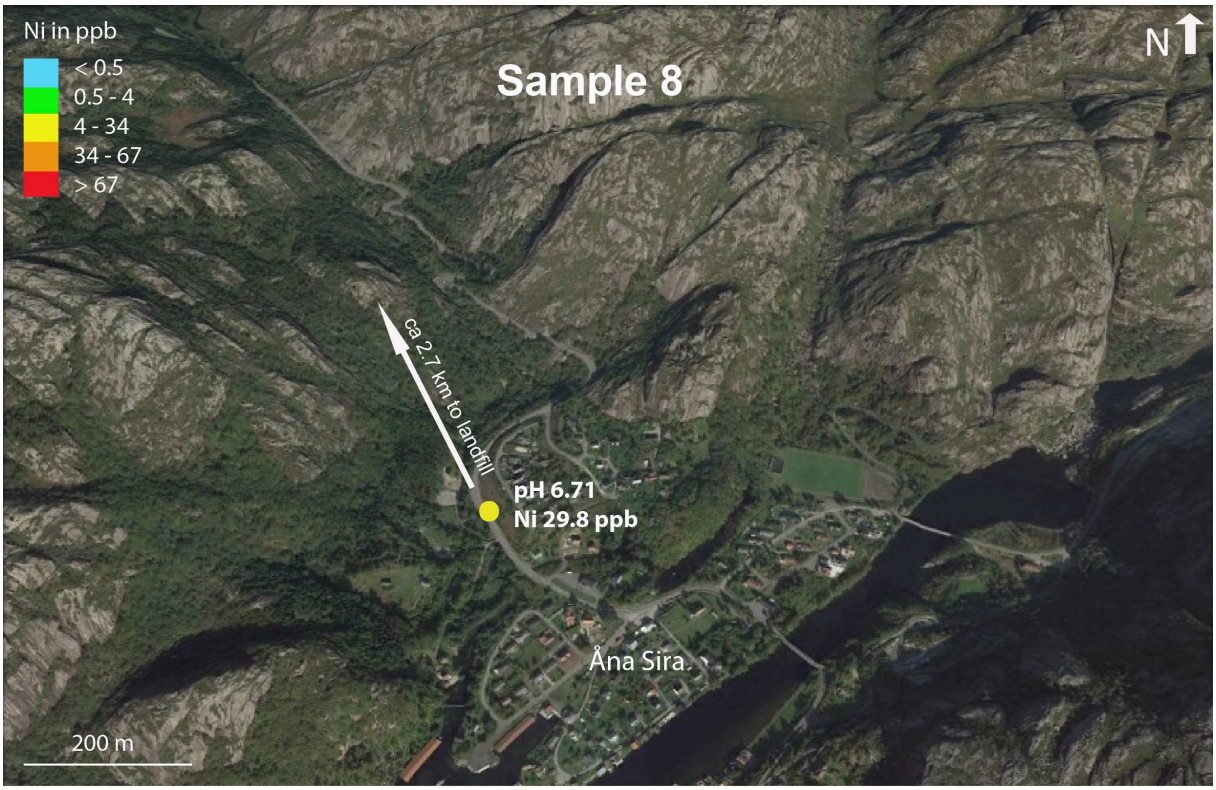


Figure 32 - Location and results of pH and Ni of sample 8 in Åna-Sira, ca 2.7 km south of the landfill

Table 14 - Results of pH, trace elements and major ions from water analysis of sample 8. N.a: not analysed.

| | Unit | Sample 8.1 | Sample 8.2 | Rain water Birkenes obs. | Drinking-water (WHO) | MAC- EQS freshwater | Acute tocix effect |
|---|---|---|---|---|---|---|---|
| **pH** | | 6.71 | 6 | 4.77 | | | |
| **Trace elements** | | | | | | | |
| Cr | ppb | 0.0336 | 0.035 | 0.12 | 50.0 | 3.4 | > 3.4 |
| Co | ppb | 0.246 | 0.0642 | 0.01 | | | |
| Ni | ppb | 29.8 | 17.3 | 0.13 | 70.0 | 34 | > 67.0 |
| Cu | ppb | 0.587 | 0.205 | 0.39 | 2000 | 7.8 | > 15.6 |
| Zn | ppb | 53.7 | 0.9287 | 2.9 | 100 | 11 | > 60 |
| Cd | ppb | 0.0199 | 0.0107 | 0.025 | 3 | 1.15 | >15 |
| Pb | ppb | 0.0469 | 0.0571 | 0.78 | 10.0 | 14 | > 57 |
| **Major ions** | | | | | | | |
| F | ppm | 0.170 | | | 1.5 | | |
| Cl | ppm | 11.2 | | 2.59 | 250 | | |
| SO4 | ppm | 57.8 | | 0.26 | 250 | | |
| Br | ppm | n.a. | | | 0.01 | | |
| NO3 | ppm | 1.06 | | 0.35 | 50.0 | | |
| PO4 | ppm | n.a. | | | | | |
| Na | ppm | 8.10 | | 1.59 | 200 | | |
| K | ppm | 2.29 | | 0.08 | | | |
| Mg | ppm | 6.70 | | 0.20 | | | |
| Ca | ppm | 21.8 | | 0.13 | | | |

Sample 8.1 and 8.2 had all concentrations below guidelines for drinking water by WHO. The highest concentration of major ions in sample 8.1 was SO4 (57.8 ppm), well below the drinking water limits of WHO.

Sample 9 (figure 33) was in a creek beside a football court in Åna-Sira. The pH was 5.64 (sample 9.1) and 5 (sample 9.2) and the Ni concentration was 0.65 ppb and 0.38 ppb, within good condition. The results from trace elements and major ions are presented in table 15 below.

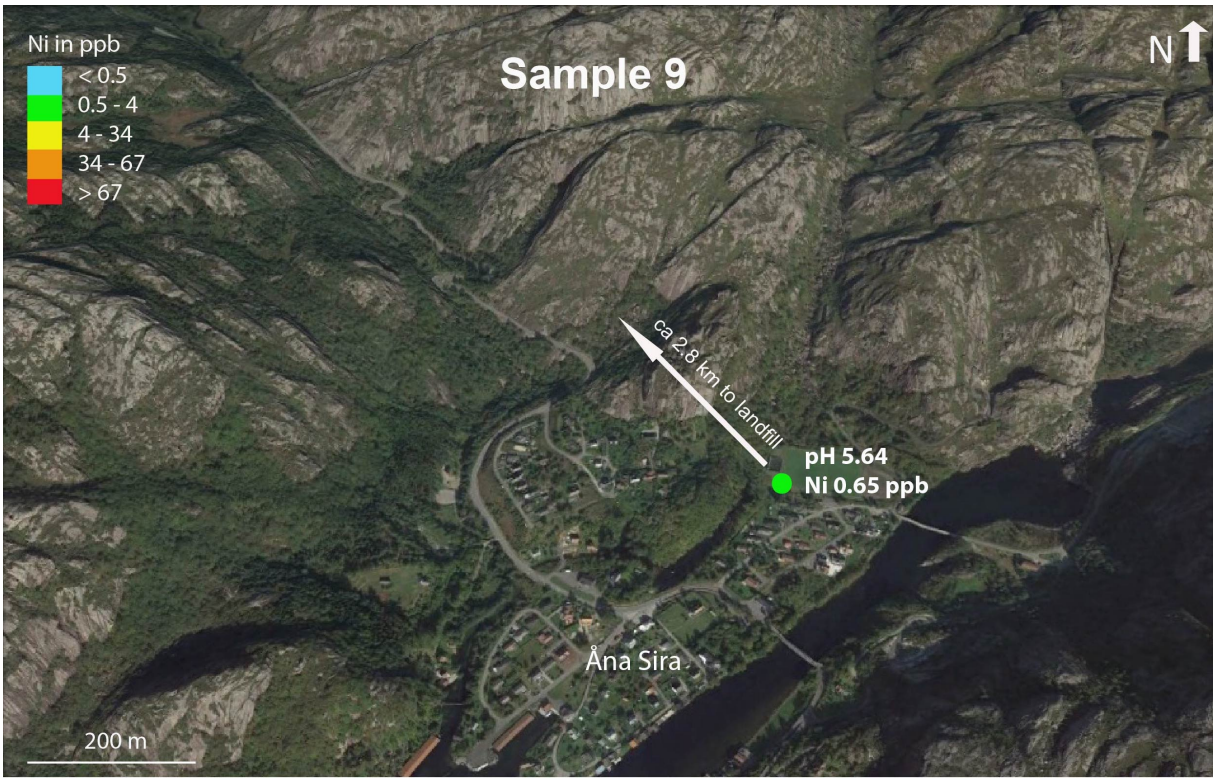


Figure 33 - Location of sample 9 in a creek by a football court in Åna-Sira, ca 2.8 km below and south of the landfill.

Table 15 - Results of pH, trace elements and major ions after water analysis of sample 9 in Åna-Sira. N.a: not analysed.

| | Unit | Sample 9.2 | Sample 9.2 | Rain water Birkenes obs. | Drinking-water (WHO) | MAC- EQS freshwater | Acute toxic effect |
|---|---|---|---|---|---|---|---|
| **pH** | | 5.64 | 5 | 4.77 | | | |
| **Trace elements** | | | | | | | |
| Cr | ppb | 0.0911 | 0,0581 | 0.12 | 50.0 | 3.4 | > 3.4 |
| Co | ppb | 0.398 | 0,0629 | 0.01 | | | |
| Ni | ppb | 0.650 | 0.379 | 0.13 | 70.0 | 34 | > 67.0 |
| Cu | ppb | 0.307 | 0,2216 | 0.39 | 2000 | 7.8 | > 15.6 |
| Zn | ppb | 94.5 | 9,861 | 2.9 | 100 | 11 | > 60 |
| Cd | ppb | 0.0609 | 0,0331 | 0.025 | 0.005 | 1.15 | >15 |
| Pb | ppb | 0.351 | 0,1685 | 0.78 | 10.0 | 14 | > 57 |
| **Major ions** | | | | | | | |
| F | ppm | 0.136 | | | 1.5 | | |
| Cl | ppm | 9.91 | | 2.59 | 250 | | |
| SO4 | ppm | 2.05 | | 0.26 | 250 | | |
| Br | ppm | n.a. | | | 0.01 | | |
| NO3 | ppm | 1.56 | | 0.35 | 50.0 | | |
| PO4 | ppm | n.a. | | | | | |
| Na | ppm | 4.81 | | 1.59 | 200 | | |
| K | ppm | 1.80 | | 0.08 | | | |
| Mg | ppm | 0.594 | | 0.20 | | | |
| Ca | ppm | 0.596 | | 0.13 | | | |

Sample 9.1 in Åna-Sira had the lowest Ni concentrations (0.65 ppb) of all water samples from campaign 1 and sample 9.2 had a Ni concentration of 0.379, both corresponding to good condition in freshwater by the Norwegian Environment Agency (Miljødirektoratet, 2016).

The pH values and nickel concentrations from campaign 1 varied considerably in the study area and are presented below (figure 34). The pH of sample 1.1 and sample 7.1 was observed to have the highest values, both with values of 7.5, followed by a pH of 7.26 in sample 2.1 below the open pit mine. The pH values of sample 1.3, 1.4 and 1.5 west of the landfill ranged from 5.54-6.5. The pH values in Åna-Sira from sample 8.1 and 9.1; approximately 2.8 km below the landfill was measured to be 5.64 and 6.71.

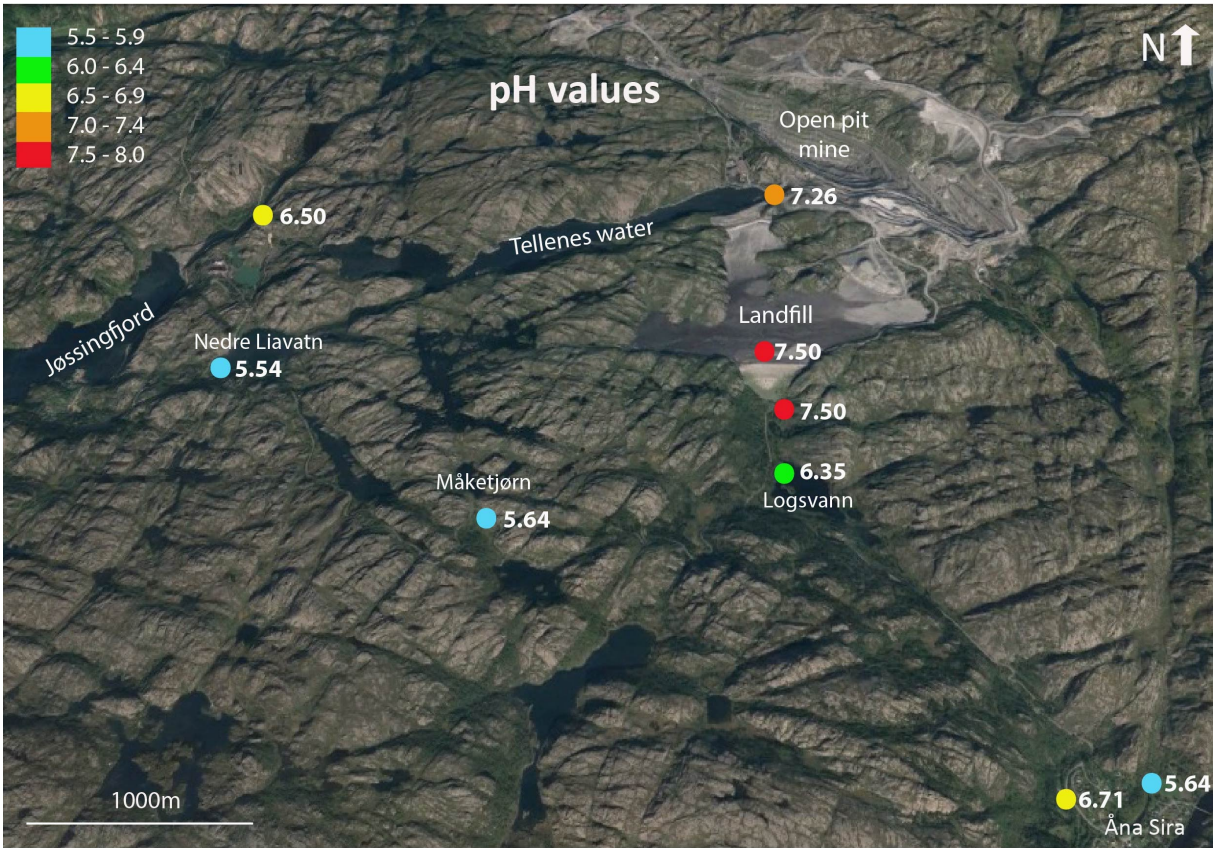


Figure 34 - pH values of the water samples in the study area at Tellenes around the Titania landfill.

The nickel concentration of the samples from campaign 1 (figure 35) in the study area also varied ranging from the lowest value of 0.65 in sample 9.1 in Åna-Sira to the highest of 293 ppb in sample 7.1 downstream of the landfill. Both the sample at the landfill and the sample below the landfill had nickel concentrations exceeding both drinking-water limits (WHO, 2017) MAC-EQS, in addition to having an acute toxic effect (Miljødirektoratet, 2016). The sample located at the landfill measured a nickel value almost a sixth of the sample below the landfill and still within poor conditions, which is further discussed in chapter 6.1.2. By comparing sample 1.1 at the landfill to sample 7.1 below the landfill, an increase was observed in Co as well, increasing from 0.589 ppb to 9.99 ppb. A small increase in Na, Mg and Ca was also observed. The sulphate content was highest in sample 1.1 at the landfill (234 ppm) and lower in sample 7.1 below the landfill (211 ppm), followed by still elevated values in sample 3.1 close to the drying plant (89.9 ppm) and sample 2.1 in Tellenes water (43.4 ppm).

Sample 1.1 on top of the landfill and sample 3.1 north of Jøssingfjord and the intake dam were both in freshwater condition 4, exceeding the maximum annual concentration by the Norwegian Environment Agency (MAC-EQS) of 34 ppb. Sample 2.1 below the open mine (30.9 ppb), sample 6.1 downstream the landfill in Logsvann (20.8 ppb) and sample 8.1 in Åna-Sira (29.8 ppb) were within freshwater condition 3 (4-34 ppb). Sample 4.1 below the intake dam, sample 5.1 southeast of the landfill and sample 9.1 in Åna-Sira were all below 4 ppb.

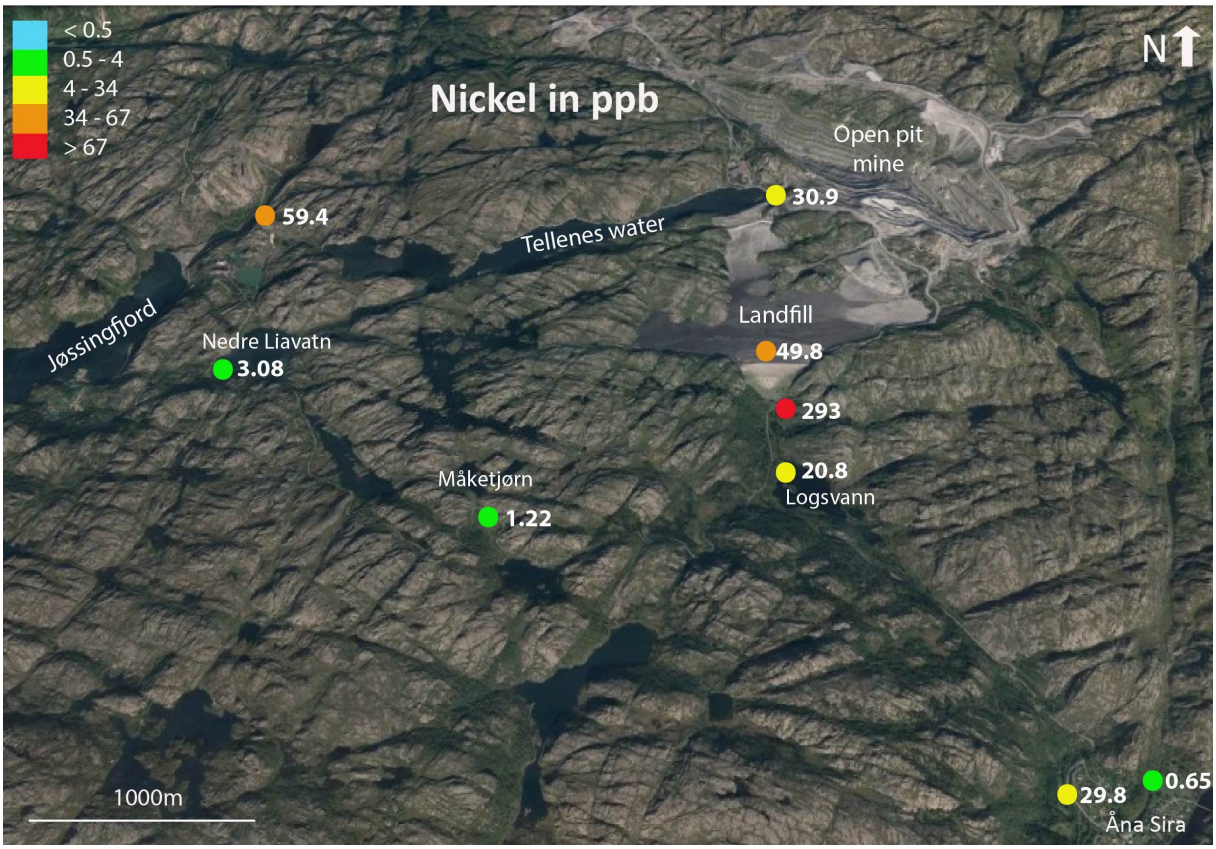

Figure 35 - Nickel concentration of the water samples in the study area. Coloured by the nickel concentration condition scale used by the Norwegian Environment Agency.

The nickel concentrations in ppb of the water samples are presented in the graph below (figure 36). The blue stippled line represents the guidelines for drinking-water quality by the world health organization (WHO, 2017) of 70 ppb whereas the yellow stippled line represents the MAC-EQS limit of 34 ppb set by the Norwegian Environment Agency (Miljødirektoratet, 2016). All the water samples, with exception of sample 7.1 (293 ppb) downstream the landfill, are below the guidelines of WHO, sample 1.1, sample 1.3 and sample and sample 4.1 (3.08 ppb), sample 5.1 (1.22 ppb) and sample 9.1 (0.65 ppb) are below both the WHO and the MAC-EQS limit for freshwater.

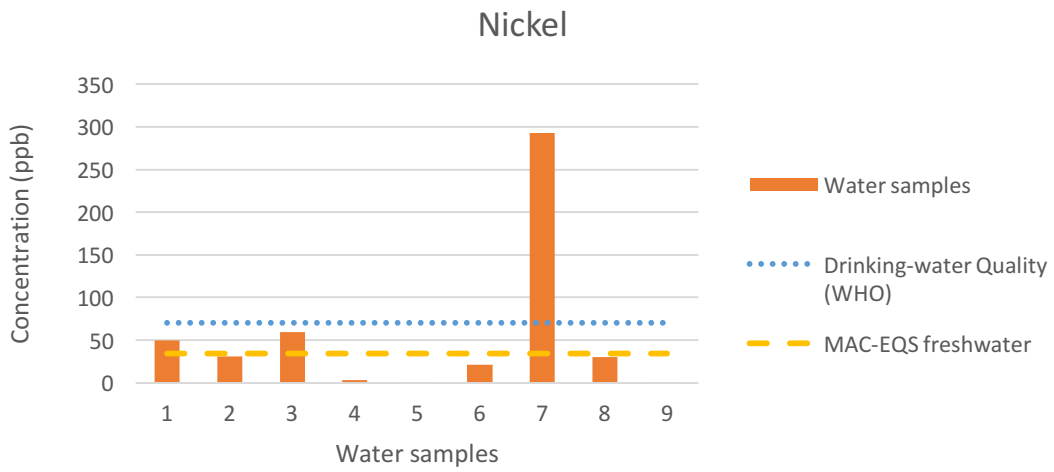


Figure 36 - Graph of nickel concentration (in ppb) of the water samples from 1 to 9 and compared with the guidelines for drinking water quality by WHO(WHO, 2017) and the MAC-EQS for freshwater by (Miljødirektoratet, 2016).

## 5.2 Tailing disposal in sea at Solbergstrand

The liners with fjord bottom sediments collected from outside of Drøbak are intended to indicate a normal marine fjord environment, which pH, Eh and a few benthic organisms also indicate. Three liners were added tailings from Titania, whereas three control liners are still representing a normal marine environment and were used for comparison when studying the effect of the tailings. The average pH of seawater is normally about 8 but can range from 7.5-8.4 (Krumbein and Garrels, 1952). The pH in the control liners were in the range 7.52-7.96. Eh in marine environments is typically in the range between -200 mV and +500 mV (Kristensen, 2000), where an oxidizing environment is above zero, and a reduced environment is below. Eh in the control liners were in the range between -93 mV and +262 mV. One sea urchin (Echinoida) was observed under the sampling with the box corer on the field boat, but no benthic animals were yet visible at the sediment-water interface. The day after sampling before the tailings was distributed over the marine sediments at least one sea anemone (Cnidaria) and a little shrimp was observed. Three days after the tailings were added

both sea urchins, sea anemones (picture 37), rag worms (Polychaeta) were observed in addition to burrows and small piles. As sea urchins normally move about below the sediment surface, the sea urchins in figure 37 on the sediments surface may be an indication of some kind of environmental stress (comment by Morten Schaanning, NIVA).

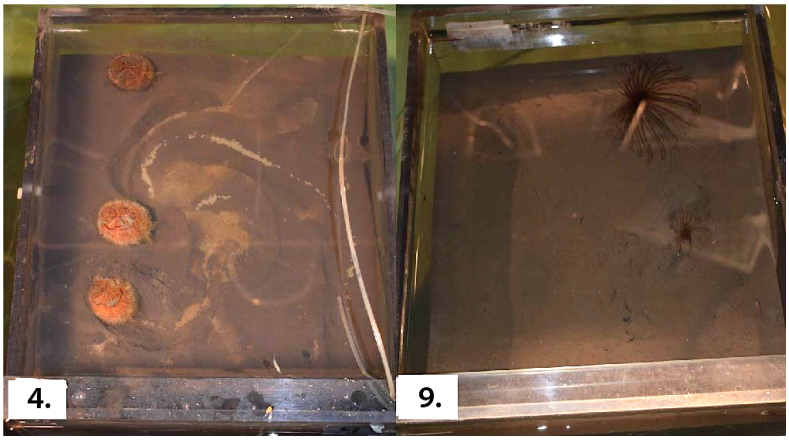


Figure 37 - Liner 4 with tailings from Titania and three sea urchins on top of the sediments. Liner 9 with no added tailings to the left with two sea anemones.

### 5.2.1 Flux measurements in sea

The measured fluxes from the sediments to the water column in the Titania liners were observed to be significantly higher than in the control liners. The fluxes of Ni were the highest, followed by Co, Zn, Cu and Cd (Appendix B, table 22). For instance was the average Ni flux in control 1.1 μg/m$^2$/day compared to the average flux in the Titania liners of 2201 μg/m$^2$/day. The values within the liners of Titania revealed also expressively differences, where liner 20 had more than two times higher fluxes than liner 14. Co fluxes ranged from 0.4-0-8 μg/m$^2$/day in the control liners, whereas from 2.3-100 μg/m$^2$/day in the Titania liners.

The average Ni flux, measuring the Ni leaching from the sediments to the water column above the sediments, was calculated to be 2201 μg/m$^2$/day. The Jøssingfjord has an area of 0.27 m$^2$ corresponding to a total Ni flux from Jøssingfjord to be 217 kg/year. This indicates that if Jøssingfjord or another site of 0.27m$^2$ where to be covered by 2cm of tailings the leaching of nickel would be approximate 217 kg/year. Total flux from 2 cm tailings in both Dyngadjupet (0.68 km$^2$) and Jøssingfjord (0.27 km$^2$) was calculated to be 876 kg/year (Appendix B, table 23).

### 5.2.2 Metal uptake in pore water

The upper 20mm in the Titania liners consist of tailings and the transition has been marked with a stippled line in both the control liners and the Titania liners to make it easier to compare, even though the control liners are not added tailings. The profiles of metal uptake in pore water by DGT-probes are presented in figure 38, in addition to pH and Eh measurements. The probes were deployed for 24 hours, thus representing fluxes (quantity/area/time), but here given in ng/cm$^2$ (all data in Appendix B, table 24 and 25).

Both Titania and control were observed to have a small increase in pH within normal values for seawater and a decrease in Eh. High Eh values/redox potential corresponds to an oxidizing environment with the absence of sulphide and sulphate reduction. Negative Eh values correspond to a reduced environment. In the control liners the pH was in the range 7.52-7.96, and the average pH gradient gradually increased from 7.63 to 7.85 whereas the Eh measurements were more vertically distributed down to a rapid decrease at 65mm depth changing from 187 mV to 32 mV and liner 10 decreasing to -92 mV. The pH in the Titania liners were in the interval 7.63-8.12 and the average gradient increased from 7.72 to 7.94. The Eh measurements had an opposite trend decreasing gradually from 195-50.67 mV and liner 4 decreasing to -38 mV.

Uptake of Mn and Fe were also an indication of the redox conditions in the liners. As illustrated in figure 8 (Chapter 3.6) the Mn concentrations increase at a certain level followed by increase of Fe. With access to oxygen, Mn4+ and Fe3+ will precipitate as oxides, whereas the concentration of $Fe^{2+}$ and $Mn^{2+}$ will increase with the absence of oxygen. This was reflected for Mn in both control and Titania liners (figure 38) where Mn increased and stabilized at a depth of 50 mm in the control liners and at a depth of 30 mm in the Titania liners. This was applied to iron as well, where a clear increase was observed at a depth of 75 mm for both. However, the curve was not stabilized for iron as for manganese, but according to the theory iron stabilizes deeper than manganese and will probably stabilize deeper down.

The average Fe flux in the control liners was observed to be under 13 ng/cm$^2$ until a significant increase to 298 ng/cm$^2$ at 70 mm depth. Mn had fluxes under the detection limit (<41 ng/cm$^2$) down to 30 mm and above the detection limit (>1600 ng/cm$^2$) deeper than 50 mm but the average values showed a trend of decrease at the first 20 mm and a rise at 50 mm to above the detection limits of 1600 ng/cm$^2$. Average Fe fluxes for Titania were observed to be under 20 ng/cm$^2$ with a sudden increase at 90-130 mm depth to 298 ng/cm$^2$. Mn values at 5 mm depth increased from 244-832 ng/cm$^2$ and exceeded the detection limits (>1600 ng/cm$^2$) from 30 mm depth and downwards.

The Cu concentrations in all of the control liners were observed to be very low at all depths. Cu was evenly vertically distributed with barely any change in values ranging between 0.57-1.17ng/cm$^2$. The Ni concentration in the control liners was below detection limits down to 50 mm where it increased a bit but yet low with an average maximum of 4.18 ng/cm$^2$ at 70 mm depth.

All the Titania liners had peaks of concentration at a depth of 20-30 mm, about where the transition between marine sediments and tailings is. The trend was similar for Ni in the Titania liners with elevated nickel concentrations at a depth of 20-30 mm. The average Ni in the Titania liners was observed to have relatively high flux increasing from 245-369 ng/cm2 the first 20mm before a gradually decrease down to 5.5 ng/cm$^2$ at depth 130 mm. In particular liner 20 differed significantly from the others with a maximum flux of 671 ng/cm$^2$ at 30 mm depth, about the double as the other liners of Titania. The Cu fluxes had a similar trend increasing from 1.10 ng/cm$^2$ to a peak of 9.4 ng/cm$^2$ at 30 mm depth before a decrease down to 0.8 ng/cm$^2$ at 130 mm depth. The concentrations of both Ni and Cu decreased further down in the sediments until almost zero concentrations at 130 mm. The low Ni and Cu concentrations at deeper depth could be because Ni and Cu have not been transported and spread as deep as 130 mm. The levels of Cu from deeper than 70 mm are more or less similar to the control liners, whereas the levels of Ni are still a bit elevated at 130 mm compared to control. Another reason for the decrease could be due to sorption by secondary minerals or due to precipitation of metal sulphides considering the reducing environment observed downwards in Eh, Fe and Mn.

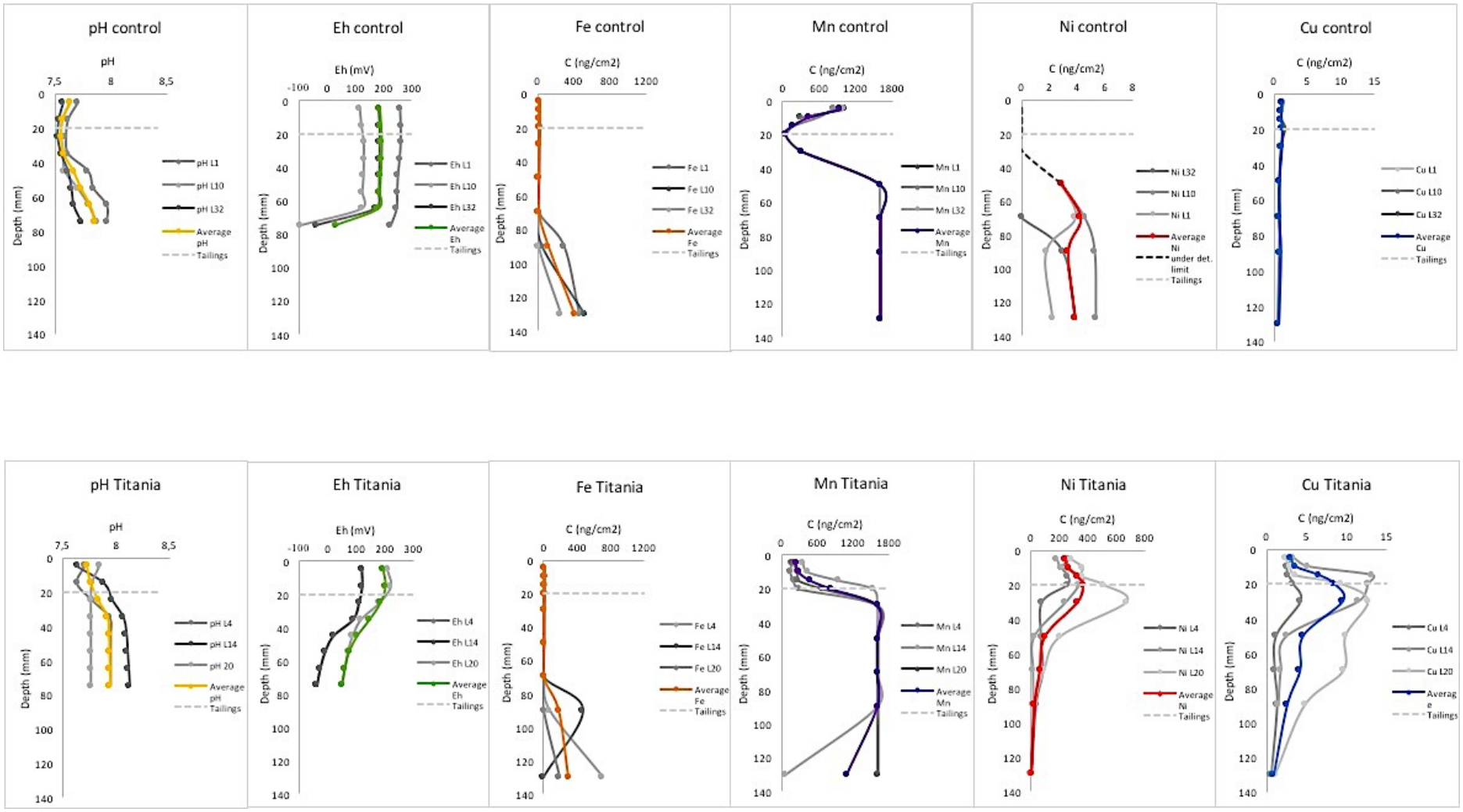


Figure 38 - Profiles of metal uptake (ng/cm2) by DGT-probes (type LSPM Loaded DGT device for metals, 0.8 mm) from both Titania and control liners deployed 24 h in mesocosm laboratory at Solbergstrand. Note that the pH and Eh electrode only reached a depth of 75 mm whereas the DGT-probes measured down to 130 mm

### 5.2.3 Relationship between fluxes and metal uptake by DGT-probes

The relationship between the measured fluxes from sediment to the water column and the uptake from pore water by DGT-probes in all the liners at Solbergstrand is presented in figure 39. The line indicates perfect correspondence between metal uptake from pore water by DGT and fluxes from sediment to water column. The correlation was obtained by plotting the log transforming the flux against the transformed metal uptake by DGT-probes before calculated and fit to the line by linear regression. Data from 29 data pairs were used (Appendix B, table 26), including another mine which will be kept anonymous. The values are observed to be spread well both above and below the slope with some points on the line. The distribution of the metals varied, Zn having all values on or above the line, whereas Co had all values on or below the regression line. The fit of the line had a correlation coefficient of 0.6463, a slope of 0.6995 and an intercept with the y-axis at 0.6283.

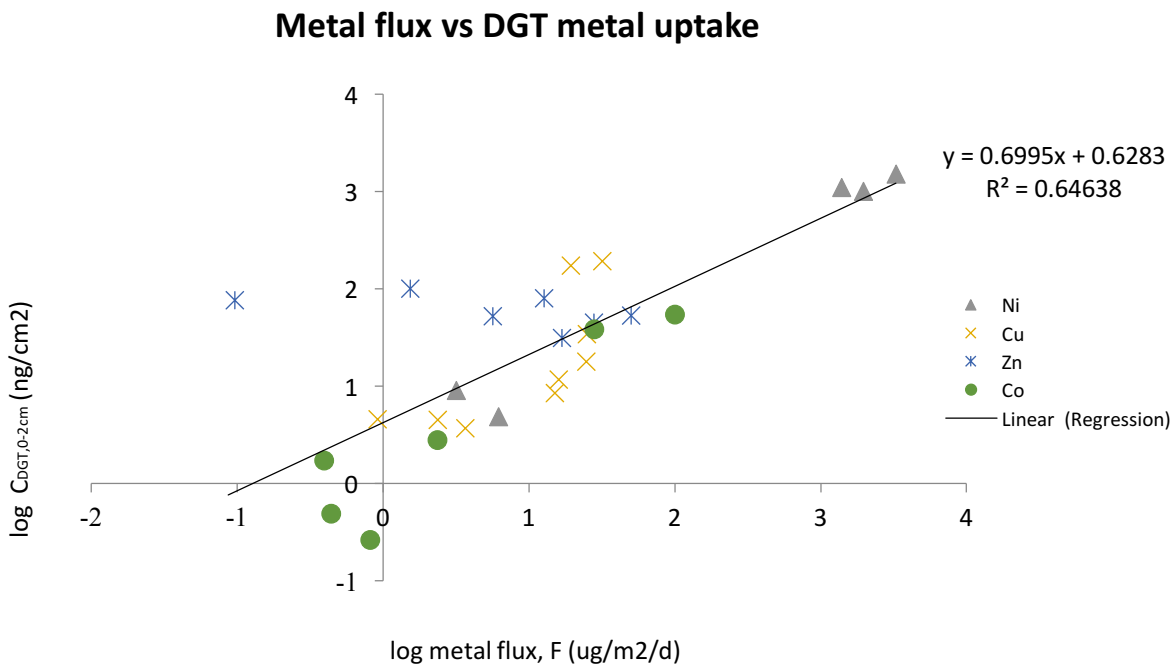


Figure 39 - The correlation between the log transformed measured metal leaching (x-axis) from the sediments to the water column, and the log transformed metal uptake of the 0-2cm interval by the DGT-probes(ng/cm2) (type LSPM Loaded DGT device for metals, 0.8 mm) in all the liners at Solbergstrand, including an anonymous mine. The curve and correlation coefficient was calculated by linear regression based on 29 data pairs.

The regression of each metal is shown in table 16 below. The correlation for Ni ($R^2$=0.975) was observed to have the highest correlation coefficient followed by Co ($R^2$=0.835), Cu ($R^2$=0.543) and Zn ($R^2$=0.314).

Table 16 - Standard error and correlation coefficient obtained from linear regression between the log transformed measured metal leaching (F) from the sediments to the water column and the log transformed metal uptake of the 0-2 cm interval by the DGT-probes). C (DGT, 0-2 cm) = k3F + b. R is the correlation coefficient, k3 is the slope, n is the number of observations and b is the intercept with the y-axis.

| Metal | $K_3$ | Std. error | b | n | $R^2$ |
|---|---|---|---|---|---|
| Ni | 0.8324 | 0.084 | 0.30 | 5 | 0.975 |
| Cu | 0.8861 | 0.511 | 0.37 | 9 | 0.543 |
| Zn | -0.104 | 0.159 | 1.85 | 7 | 0.314 |
| Co | 0.8812 | 0.159 | 0.07 | 6 | 0.835 |

The relationship between the measured flux and the uptake by DGT-probes in the liners of Titania is presented in figure 40 (Appendix B, table 27). The correlation was obtained by plotting the flux against metal uptake before fitting to the line and calculated by linear regression. The correlation coefficient was calculated to be 0.95. In total three data pair of each metal was done. Ni and Zn were observed both to have two data pairs on the line and one off, while the rest were below.

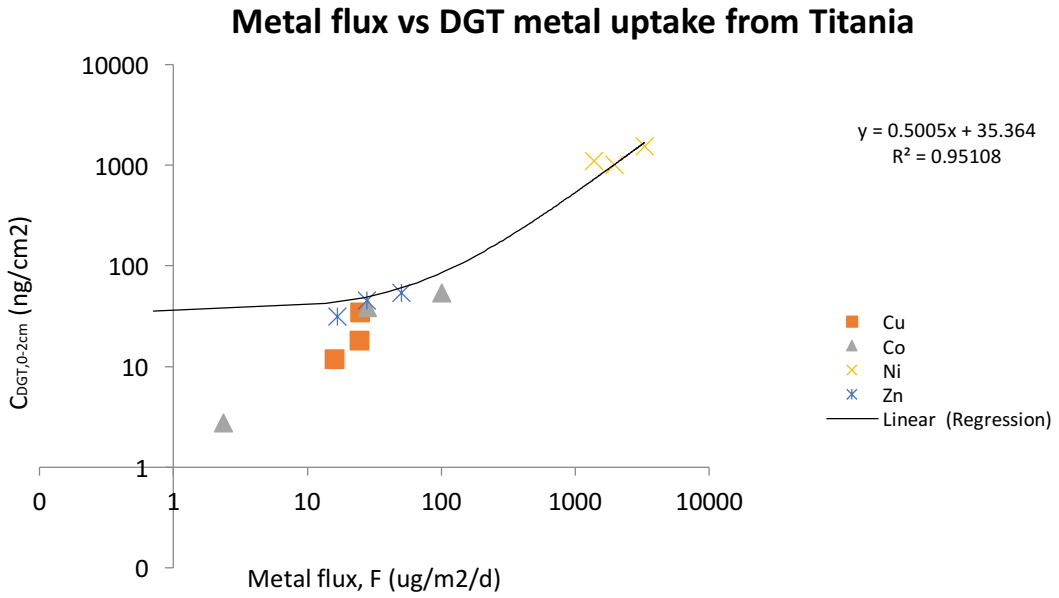


Figure 40 – The correlation between the measured metal leaching (x-axis) from the sediments to the water column and the metal uptake of the 0-2cm interval by the DGT-probes(ng/cm2) (type LSPM Loaded DGT device for metals, 0.8 mm) in the Titania liners. Both axes have logarithmic scales, and the curve and correlation coefficient was calculated by linear regression based on 12 data pairs.

# 6 Discussion

In this chapter, the effect the mine has on the environment is discussed, both on land and in sea. The results from land and sea are first discussed separately with an objective to provide an overview of dust mobilization and aqueous Ni mobilization on land, followed by Ni and Cu mobilization and the impact of bioturbation in sea. Finally, an attempt to compare fluxes from land and sea has been made.

## 6.1 Tailings disposal on land

Challenges with the current disposal site at Tellenes are elevated concentrations of Ni in the drainage downstream the landfill and airborne material from the landfill. Windblown material from the mine can be harmful to the environment mainly due to its size, but also shape. Heavy metals and dust can be spread in the environment, and the smallest particle sizes can easily be inhaled into the lungs and thus be harmful to the health of animals and humans. Aqueous transported material from the mine can be harmful to the environment by elevated values of heavy metals in waters and creeks around the mine, which can have a toxic effect on organisms, plants, animals and in worst case also humans.

### 6.1.1 Dust mobilization

Atmospheric mineral dust is typically associated to mine tailings and may be of potential risk to human health (Csavina et al., 2012). Particulate matter with a diameter smaller than 10 μm (PM10) is among the substances in the pollution regulations by the Norwegian Environment Agency, with a maximum limit of 50 $\mu m/m^3$ a day (24 h) (Bratland et al., 2015). In the report by Tønnesen (2008) mentioned in chapter 2.9, none of the values from Åna-Sira exceeded this limit. Besides, the dust emission flux measured from the dust filters in this study was measured to be significantly lower, of $2.61*10^{-7}$ $\mu m/m^3$. Besides, grains over a diameter of 10 μm were also included, indicating an even lower flux.

The dust filters showed that the sample in the lower part of Åna-Sira, located approximately 3 km from the landfill, was enriched in smaller particles compared to the sample in the upper part of Åna-Sira located approximately 2.7 km from the landfill. About 350 m separates the dust filters, and upper sample is about 300 m closer to the landfill than the lower sample. The result may, therefore, be realistic considering the mine as the main source, as smaller grains are transported further than larger grains. However, since only 300 m separates them after already have been transported 2.7 km, it may be possible that the differences are random. The shape of the larger grains was overall angular with sharp edges, whereas the smaller grains were subangular and subrounded. Crushed rocks from the open pit, which has to a small extent been processed, would assumedly have sharp edges and the angular grains could, therefore, originate from the mine. However, the point counting method used is subjective, and uncertainties must be taken into account. Grains might have been overseen when counting

and grains between two sizes may have been placed wrong. Besides, the elements chosen for point analysis were often chosen based on highest density, being both most interesting and easiest to find.

By comparing the two elemental maps, one from each sample (figure 23 and 24), it is also indicated that sample 4a from upper Åna-Sira should consist of larger grains than sample 3a from lower Åna-Sira. Grains likely to be plagioclase were in general larger in both dust filters compared to the ilmenite grains, which is reasonable due to higher density of ilmenite compared to plagioclase. A plagioclase grain would be transported further than an ilmenite grain of the same size.

Both plagioclase and ilmenite were among the minerals of highest percentage in the XRD analysis, linking them to the mine. Especially the ilmenite grains are likely to originate from the landfill, whereas the plagioclase can have been transported from the landfill, side rocks or industry nearby.

The Rogaland anorthosite province consists of three large anorthosite plutons, and the Tellenes ilmenite deposit belongs to the Åna-Sira anorthosite (the light pink areas in figure 41), which is enriched in plagioclase. The grey area at Tellenes is the ilmenite ore and everything within 4 km radius is anorthosite except Kalveknuden of norite, pyroxene and noritic pegmatite. Anorthosite also dominates the area around Åna-Sira. Schanche (2008, referenced within (SARB, 2014)) reported a very high content of plagioclase in the side rock of Tellenes deposit.

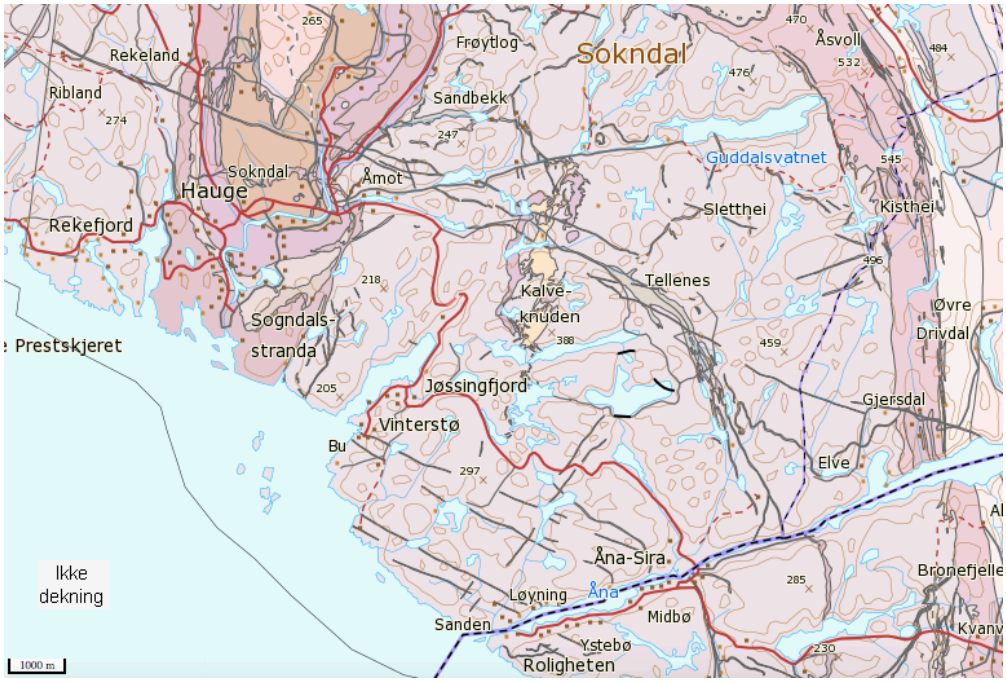


Figure 41 – Bedrock geology map of Sokndal from NGU. The grey area at consist of ilmenite and the light pink area around is anorthosite.

Plagioclase can possibly originate from all over Sokndal when encroachments and operations are done for road works or tunnels in the bedrock. In Rekefjord (at the coast to the left in figure 42) there is a quite large quarry operating on norite in east and anorthosite in the west. The production in the east is about 900 000 tonnes a year. The quarry is about 10 km from Åna-Sira, and the blasting and production of bedrock will probably also contribute to both ilmenite and plagioclase grains and at least some suspended material (Meland, 2016). Besides, there is an airport in Farsund at Lista, about 23 km southeast from Åna-Sira, which could also be a contributing source to the suspended material. Right next to the airport and southwards there are several beaches as well, that could also possibly cause aeolian dust emissions.

The dust filters are highly influenced by wind direction, wind force and precipitation. Titania measures precipitation each month themselves, and a factor for determining if the dust filters from August are representative, is the amount of precipitation in August and compared to other months. Through the year 2016, data from Titania has shown that September was the month with most rainfall, followed by November, July and August. August is the fourth most rainy month, however, still relatively normal compared to the other months with small differences that distinguish them. August 2016 is also less rainy compared to August the four previous years (Appendix A, table 19).

The closest weather stations to Åna-Sira are Lista in Farsund ca. 21.7 km from Åna-Sira and Eik in Lund 24.1 km north of Åna-Sira. Eik is closer to the landfill. However, the wind in Eik seems to be north-south dominated, and due to the surrounded mountains, the weather in Eik could be relatively local controlled. The following weather measurements are from Lista in Farsund. According to the Norwegian weather service yr.no, average wind force was about moderate breeze and average precipitation was 3.03 mm during the twenty-eight days of deployment of the dust filters. The days with the wind from north and west had, in general, the strongest wind force up to moderate gale (Appendix A, table 20) suggesting it is highly likely that the mine is the primary source of the suspended particles in the dust filters and in particular the ilmenite grains. However, since the wind only came from northern directions seven of the twenty-eight deployment days, it is not likely that the mine is responsible for all of the particles. Besides, several other sources as mentioned above can also have a small contributing role. On the other hand, it is not certain that the wind direction and force from a weather station 22 km from Åna Sira is representative enough, and in particular not for the locals in Åna-Sira which are most affected.

### 6.1.2 Aqueous Ni mobilization

The Lundetjern landfill and parts of the area around were observed to be affected by Ni. Three of the nine water samples in the area from campaign 1 were in good condition, according to the environmental quality standards set by the Norwegian Environment Agency (figure 35). Two of them were located approximately 1.6- 2.5 km west and southwest from the landfill and one in Åna-Sira. The remaining six samples were moderately or more affected by nickel.

The samples that were taken from below the landfill, were in very poor condition, according to the environmental quality standards. In spite of that, the samples in Logsvann downstream the landfill were significantly diluted compared to the samples below the landfill, although only about two hundred meters separate them. Logsvann is definitely vulnerable due to the leachate from the landfill, and the samples were in moderate condition according to the environmental quality standard regarding nickel. However, if there were no pump downstream the landfill, the concession limit of 1.5 kg Ni/day to Logsvann would probably have been exceeded, and Logsvann would have even higher values of nickel. According to Sweco (2017) the average concentration of Ni in the leachate below the landfill, after the pumping, is 0.6mg/l, about the double of what was measured in the sample below the landfill (sample 7.1). The sample from campaign 2 is also slightly higher than from campaign 1. More samples should have been taken to see a trend, as only two measurements are not enough to conclude the cause of the large variations in Ni concentrations. However, it is likely that the Ni concentrations change with the production rate, which varies from 1.5-2.5 million tonnes a year, by amount precipitation and discharge water determined by the water supply. Periods of heavy precipitation would probably dilute the Ni concentrations, whereas high production rate in combination with low precipitation would probably increase the Ni concentrations.

The large variation in drainage for Logsvann is apparent in figure 42. The diagram represents drainage from the landfill to Logsvann (Ettner and Sanne, 2017). The week during campaign 1 (week 47) is circled and is about 50 $m^3$/hour compared to over 200 $m^3$/hour during the weeks in late summer and autumn.

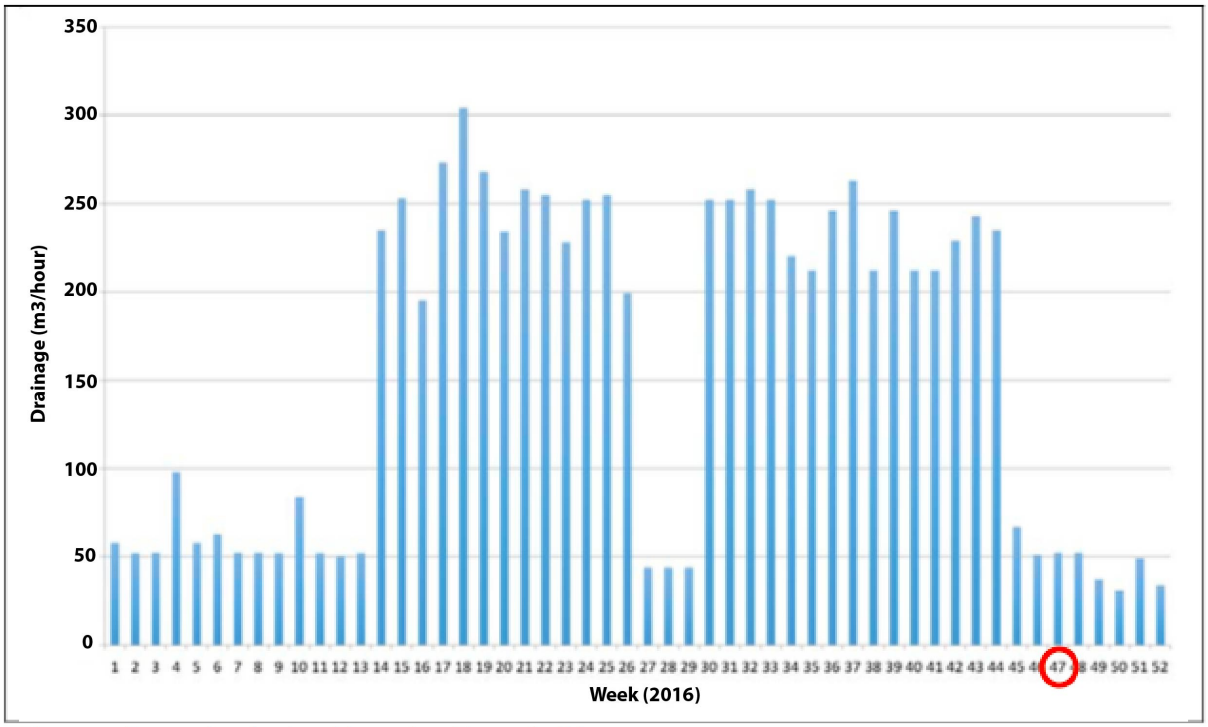

Figure 42 - Drainage from the landfill to Logsvann. The figure is copied from a report by Geode Consult AS (Ettner and Sanne, 2017) and modified with a red circle around week 47 during the period in which campaign 1 took place.

Previous studies by Ettner, found in (Mellgren, 2002), stated that it was no connection between nickel concentrations, precipitation or pH at the landfill of Titania. Nevertheless, Mellgren (2002) suggests that nickel is very likely to precipitate with salts as nickel sulphate at the top of the landfill in the unsaturated zone. Subsequently may large amounts of water, in the form of precipitation, contribute to wash out the easily soluble salt crystals and furthermore elevate the Ni concentrations in the drainage downstream.

The graph in figure 43 is made with data from Titania in 2016 and shows total discharge measurements through the landfill of Titania and Ni concentrations over a period of 44 weeks in 2016, where week 1 is the first week in a calendar year. The graph does not include drainage to Logsvann (as figure 42), as the return pumping has not been included in the calculation.

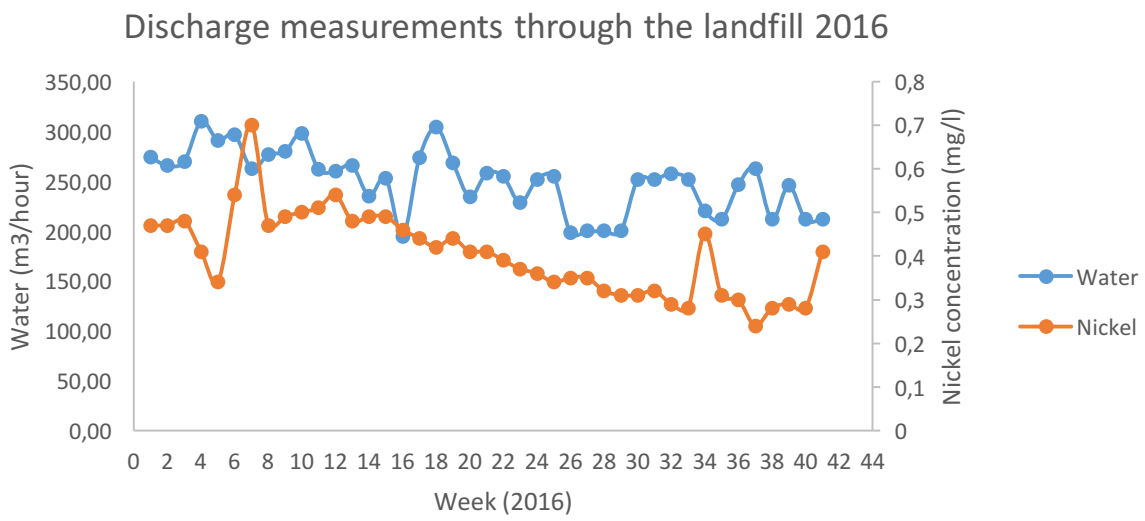


Figure 43 - Discharge measurements and Ni concentrations over 44 weeks through the landfill of Titania in 2016. The return pumping below the landfill has not been included.

Both water supply and Ni concentrations show significant changes. However, when plotted against each other in figure 44, there are no correlation, with a correlation coefficient of $R^2$=0.152, suggesting no connection between amounts of water and nickel concentrations.

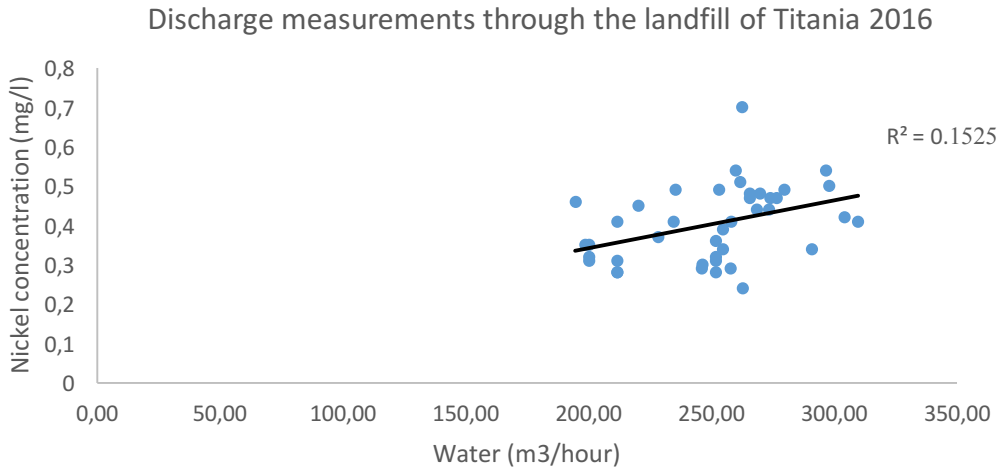


Figure 44 – Ni concentrations and was supply through the landfill of Titania during 44 weeks in 2016. Y-axis representing nickel concentrations (mg/l) and x-axis representing the water supply (m3/hour). Correlation coefficient calculated to be 0.1525. The return pumping below the landfill has not been included.

Water from mines with problems of AMD is commonly characterized by exceptionally high $SO_4^{2-}$, Fe, Al of over 1000mg/L, and elevated concentrations of Co, Cr, Ni, Pb and Zn of over 10mg/L. Elevated concentration of Ca, Mg, Na and K may also occur (Lottermoser, 2007). This does not in any way characterize any of the water samples analysed in this study. However, it gives an overview of what elements that can be expected to be elevated by the influence of the mine. When comparing the sample at the landfill to the sample below the

sample from campaign 1, an increase was observed in both Co, Na, Mg and Ca below the landfill. On the contrary, a decrease was observed in $SO_4^{2-}$. Elevated concentrations of sulphate may be expected to be a result of sulphide oxidation (Dold, 2014a), where the first step of the sulphide oxidation results in sulphate. Both the nickel sulphides millerite and pentlandite have been analysed in this study, and it is probably these minerals that nickel originated from. However, since the increase of $SO_4^{2-}$does not follow the increase of Ni, it is not possible to conclude that the increase of Ni concentration is a result of sulphide oxidation. One explanation for the high $SO_4^{2-}$could be the adding of sulphuric acid, as both the drying plant and the flotation plant uses sulphuric acid in the processes. This may also be the reason for why both the samples in Lonebekken, close to the drying plant, and the sample at Tellenes water from campaign 1 were measured to be in moderate and poor condition, respectively, according to the environmental quality standards set by the Norwegian Environment Agency (Miljødirektoratet, 2016). Drainage water from below the landfill is pumped to the top of the landfill and further to Tellenes water, and as illustrated in figure 5 (chapter 2.6), a tailings pipeline transports tailings from the drying plant to the flotation plant and further to the landfill. The acid will lower the pH and mobilize nickel ions (Lottermoser, 2007). This can be related to the measured pH of 5.5-6.5, corresponding to the range in which Ni may be mobilized (Dold, 2010), compared to the samples at the landfill and below the landfill of both 7.5.

The two samples in Åna-Sira revealed quite different Ni concentrations, with elevated Ni, $SO_4^{2-}$ and Ca concentrations in sample 9.1 compared to sample 8.1. As shown in the map over rivers and creeks in Åna-Sira (figure 45) it is likely that sample 8 drains from the landfill whereas sample 9 has its origin from Eigeland, southeast from the landfill.

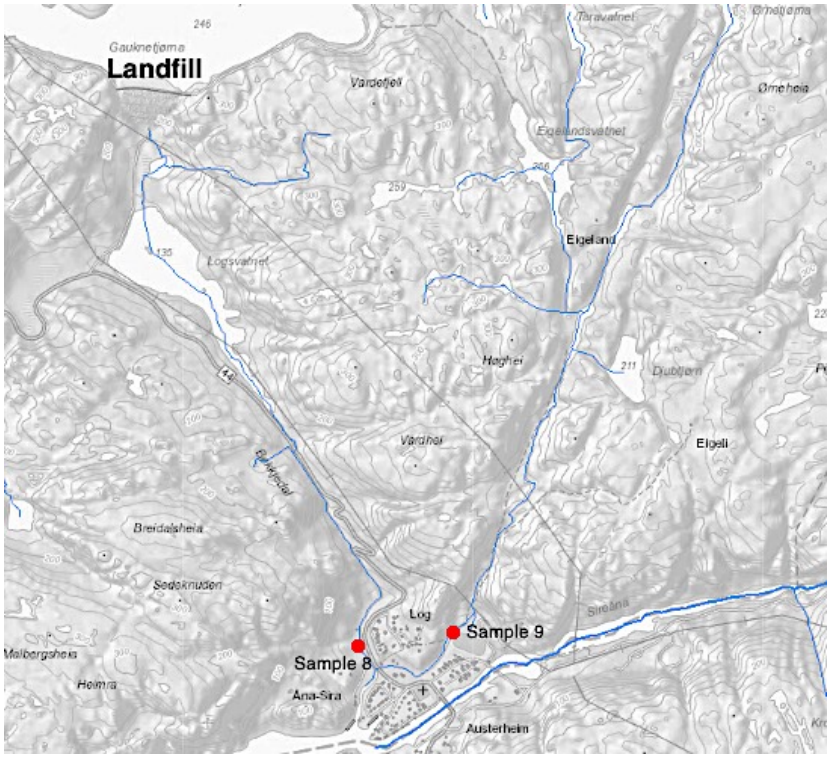


Figure 45 - Map of the rivers and creeks in Åna-Sira, modified from NVE.

Considering the low Ni values in sample 4, 5 and 9, all of which being within good condition, they are not likely to be particularly affected by the mine. Besides, the pH of all three samples corresponds to a pH of meteoric water, between 5.5 and 6 (Lottermoser, 2007).

The pH values of the other samples were partly connected to the Ni values, with the exceptions of sample 3.1 close to the drying plant. The highest Ni values were observed to have the highest pH (as shown in figure 34 and 35) although mobilization of Ni is usually associated with low pH (chapter 3.4). However, a low pH from mine waste is not a universal characteristic, and significant concentrations of nickel and other heavy metals have been documented in neutral to alkaline mine drainage (Lottermoser, 2007).

The processes in the landfill are complex, and there might be several reasons for high pH. First of all, the tailings originate from an ilmenite rich norite, a basic intrusive rock composed principally of calcic plagioclase (Bowes, 1989). Basic rock with relatively high content of calcic plagioclase can contribute with a buffering effect. Secondly, burnt chalk (calcium oxide CaO) is added to two basin thickeners close to the ore dressing plant with the purpose to make the fine particles settle at the bottom of the basin. The surface water is transported to Tellenes water whereas the bottom sediments are transported to the landfill. The chalk is not added to increase the pH (Opsal, 2017). However, it may still be an influencing factor regarding the

high pH. All samples with elevated Ni concentrations were accompanied by elevated Ca values and apply to sample 1, 2, 3, 6, 7 and 8 with concentrations of 106, 15, 28, 9.50, 113, 21.8 ppm, respectively. The elevated Ca values can appear due to the calcium oxide added, or the buffer capacity of the norite in the tailings.

Reasons for the high nickel concentrations despite the high pH, however, may be explained by sorption. The sulphide minerals in the landfill with access to oxygen will oxidize and result in $Fe^{2+}$, which may further oxidize to $Fe^{3+}$. $Fe^{3+}$ have low solubility at pH above 4 and can in the presence of oxygen precipitate as iron (oxy)hydroxides (Appelo and Postma, 2005, Dold, 2014a). These are secondary minerals and natural sorbents, and can due to their large surface area immobilize heavy metals. Their sorption capacity is highly influenced by the pH and metals behave differently at varying pH as shown in figure 7 (chapter 3.3). On a surface of a ferrihydrite, Cu and Zn are sorbed at pH 4-6, whereas Ni is sorbed between pH 6-8 (Dold, 2010). In other words, nickel can, in fact, be relatively mobile at neutral to weak basic water conditions. At pH 7,5 as measured at the landfill, there will still be nickel mobilized if iron (oxy)hydroxides were to be considered as main sorbents. Besides, Cr, Cu, Cd or Zn, all of which are sorbed at lower pH than Ni, may occupy sorption sites, leaving Ni in solution.

In the report by SARB (2014) Consulting Norge AS several potential sources of Ni have been investigated. Despite the high nickel concentrations, acid drainage from the landfill has not been observed. Column tests of tailings with drainage from the process water done by Forfang in 2005 showed significantly leaching of nickel, and the mine water from the drying plant measured even higher concentrations. Besides, a column test study by Walder (2012, reference within (SARB, 2014)) showed that leaching was more or less independent of pH. The test showed that even by adding clean water with pH 7-8 to the tailings it resulted in relatively high Ni concentration. According to Walder (SARB, 2014), the mine water from the drying plant is enriched in $Fe^{3+}$ and protons, being a contributing factor to the leaching of Ni. Oxygen is usually the oxidant during pyrite oxidation, however, according to Lindsay et al. (2015) and Dold (2014a), under acid conditions (pH<3) $Fe^{3+}$ can become the dominant oxidant. As previously mentioned (chapter 3.4) where the example of pyrite oxidation is used, oxidation by $Fe^{3+}$ produces 16 protons in comparison with oxygen which produces 2 protons (Dold, 2014a). Besides, the reaction produces $Fe^{2+}$ which may oxidize further to $Fe^{3+}$ increasing the overall oxidation by pyrite (Lindsay et al., 2015). At pH over 4, $Fe^{3+}$ would precipitate as iron hydroxides. However, the pH of the water from the drying plant is 1-2 and therefore also enriched in $Fe^{3+}$, contributing to oxidation. The presence of $Fe^{3+}$ will therefore undoubtedly have a major impact on the mobilization of Ni. Without knowing anything about costs or how easy it can be carried out, a suggestion could be to buffer the pH of the water from the drying plant for it to increase before it is mixed with the tailings to limit oxidation by $Fe^{3+}$.

Another reason for elevated Ni concentrations, according to Mellgren (2002) could be dissolution of nickel sulphate. Sulphate and nickel ions in the landfill may precipitate as nickel sulphate, a very soluble salt. When dissolved, the Ni concentrations are expected to increase, especially in the drainage.

NIVA (Tobiesen, 2003) measured nickel and pH in the discharge from the landfill to be 0.754 mg/l and pH 8.01. This is considerable higher nickel concentrations when compared to this study (0.293 mg/l and pH 7.5), despite a higher measured pH, which should rather contribute to a decrease in nickel. The higher pH measured by NIVA could be due to a change in processing since 2003, or small variations in sampling locations can also possibly explain the different values in these two studies. The more recent report by Geode Consult (Ettner and Sanne, 2016) measured an average Ni concentration in Logsvannet corresponding poor conditions of more than the double as measured in this study. However, as previously mentioned the Ni concentrations are quite variable. Besides, the sample of Geode was measured in the south whereas measured in the north in this study, which can possibly explain the different concentrations.

## 6.2 Tailings disposal in sea

Challenges related to tailings disposal in Jøssingfjord have been the dispersion of the fine grained particles, which is not discussed in this thesis, and concern regarding leaching of heavy metals. High concentrations of metals in the water column can have a toxic effect on benthic organisms and possibly further to humans.

The liners, which were covered with fjord sediments, were expected to show a transition to a reduced environment as in normal sea bottom sediments as shown in figure 8. However, none of the liners showed significant evidence of hydrogen sulphide and the very low concentrations have therefore not been included. An explanation of the absence of hydrogen sulphide could be the length of the electrodes of 75 mm. It is possible that measurements of sulphide would have been visible deeper down. It could also be due to low concentrations of organic matter and sulphate-reducing bacteria, as sulphate reducing bacteria reduces sulphate to produce hydrogen sulphide. In oxic environment, there are no sulphate reducing bacteria, and thereby no hydrogen sulphide (Konhauser, 2007).

### 6.2.1 Mobilization of Ni and Cu

Tailings from Jøssingfjord measured by a master thesis study by Gravdal (2013) was observed to have an overall mildly pollution according to the Climate and Pollution Agency environmental standards, and in particular, Ni and Cu were measured to be strongly polluted. Nickel has also distinguished itself in the tailings in this study and partly copper. An indication of the pollution potential of Ni and Cu in the Titania liners can be seen by comparing to the control liners in figure 38. Despite similar thickness of tailings, both Ni and Cu revealed very large differences within the Titania liners. Above the marine sediment-tailings interface, thus in the layer with tailings, all Ni fluxes were quite similar. However, at the transition to marine sediments in both liner 14 and liner 20 are significantly elevated. In fact, the maximum flux in liner 20 is more than 2.5 times higher than liner 4 of Titania, and more than hundred times higher than the maximum flux in the control liners. Both Ni and Cu decreases with depth, probably due to to sorption by secondary metals or precipitation of

metal sulphides. Fluxes from sediment to the water column also indicated pollution and significantly differences in both Cu and Ni fluxes in the Titania liners compared to fluxes in the control liners.

### 6.2.2 Bioturbation

Bioturbation introduces oxygen from the water into the sediments and may increase the permeability of the sediments (Kristensen, 2000, Meadows et al., 2012). Large flux differences within the liners are possible due to bioturbation. Bioturbation is usually more intense in the upper 10cm and fluxes are very likely to be increased by the influence of bioturbation. All of the liners contain a random selection of benthic animals, which is also the reality on the fjord bottom. Some parts at the fjord bottom have large colonies of organisms with higher activity whereas other parts have less or even no activity. The liners at Solbergstrand had both benthic organisms and activity, but the amount and diversity of organisms and the degree of activity in each of the liners is unknown, and so is the contribution of bioturbation to the flux values.

A study by Amato et al. (2016) investigated the ability of DGT probes to predict metal bioavailability in clean and contaminated sediments with varying degrees of disturbance by bioturbation. Only bivalves represented low bioturbation, whereas high bioturbation was represented by bivalves and an actively burrowing amphipod. The result was a significantly higher release of DGT-labile Cd, Ni, Pb and Zn (but lower Cu and Fe) in the pore water and the overlying waters in the sediments with high bioturbation. This could support the theory that the particularly high Ni values in liner 20 are due to bioturbation.

The relationship between fluxes out of the sediments and DGT uptake (in the control liners, Titania liners and anonymous mine) in figure 39 proved to have quite good correlation. The proportionality of Ni and Cu was quite well, followed by Cu and Zn. A majority of the values were under the regression line and could indicate that a DGT-uptake measured in situ and subsequently calculated by the linear regression equation in figure 40, could calculate slightly higher fluxes. The opposite was observed for Zn, with the poorest correlation coefficient, where the DGT uptake were all quite similar of 1.5-2 $ng/cm^2$, whereas the fluxes out of the sediments ranged from -1 to 2 $\mu g/m^2/d$, suggesting quite unreliable flux calculations. However, the precision increased with higher values, suggesting that the method is more optimal where concentrations are expected to be high. The same trend was seen in figure 41 for the Titania liners, where lower values were below the regression line and the precession increased with higher values. However, possible due to overall higher values in the Titania liners, the correlation coefficient was considerable higher. One explanation could be that bioturbation is likely to have a greater impact on the lower DGT fluxes, causing less correlation.

The experiment in this thesis had a 2 cm thick tailings layer. However, the benthic animals are capable of crawling through the tailings with access to “clean” sediments and nutrition. The tailings thickness in Jøssingfjord today is not 2 cm thick, but approximately 50 m thick. This

could lead to different behaviour of the benthic animals as nutrients may not be available to the same extent. Additionally, the fluxes would probably also be different when the thickness of tailings increases.

In May 2017, The Institute of Marine research and the University of Bergen (Lorentzen, 2017) collected sediment core samples from six stations in Jøssingfjord and Dyngadypet to study to what extent the fjord bottom has recovered after the last tailings were deposited in 1984 (Jøssingfjord) and 1994 (Dyngadjupet). The first results from the research were fishes and crabs at the sediment-water interface and only brittle stars (echinoderms) in the sediment cores. This contradicts the report of NIVA from 2015 (chapter 2.9) where four out of five stations were in "very good" condition and one was in "good" condition, corresponding to high species diversity. However, if the case today is only one specie, and with the assumption that bioturbation will in a higher degree influence lower DGT values, it is possible that the DGT-probes would fit this environment better considering lower activity and bioturbation.

## 6.3 Fluxes from land and sea

The bedrock in Norway has considerable mineral resources, and it is an ongoing discussion whether we should have mining at all or if it is too harmful to nature. The social demand for mineral resources is increasing, either Norway is a part of it or not. Norway has one of the world's strictest environmental requirements when it comes to the mineral industry, which may be an argument for why precisely Norway should be an example for other countries to follow. However, both land and marine disposal are accompanied by environmental challenges and management of the waste is, without doubt, the most difficult and important one. This thesis has only investigated a fraction of all the considerations that should be taken into account in advance of a decision of a future deposit for Titania. Due to their very different challenges, land and sea disposal are very difficult to compare.

However, a form of leaching or spreading of dust or heavy metals is common for both, and an attempt of simple flux calculations has therefore been made. The fluxes are not entirely representative but can give an indication of spreading/leaching. The total dust emissions on land over an arbitrary area of 1 $km^2$, based on one of the filters in Åna Sira, were calculated to be 87800 kg/year. If assuming that all particles originate from tailings of Titania with 0.03% (Mellgren, 2002) nickel, the flux of Ni is 26.3 kg/year, as illustrated in figure 46. It is not taken into account that the number of particles varies with height above ground level. In sea, the Ni flux from the sediments covered by a 2 cm thick layer of tailings to the water column of an area of 1.09$km^2$ corresponding to a total of Jøssingfjord and Dyngadjupet was 876 kg/year. The Ni flux in sea is, in other words, more than thirty times larger compared to airborne Ni flux.

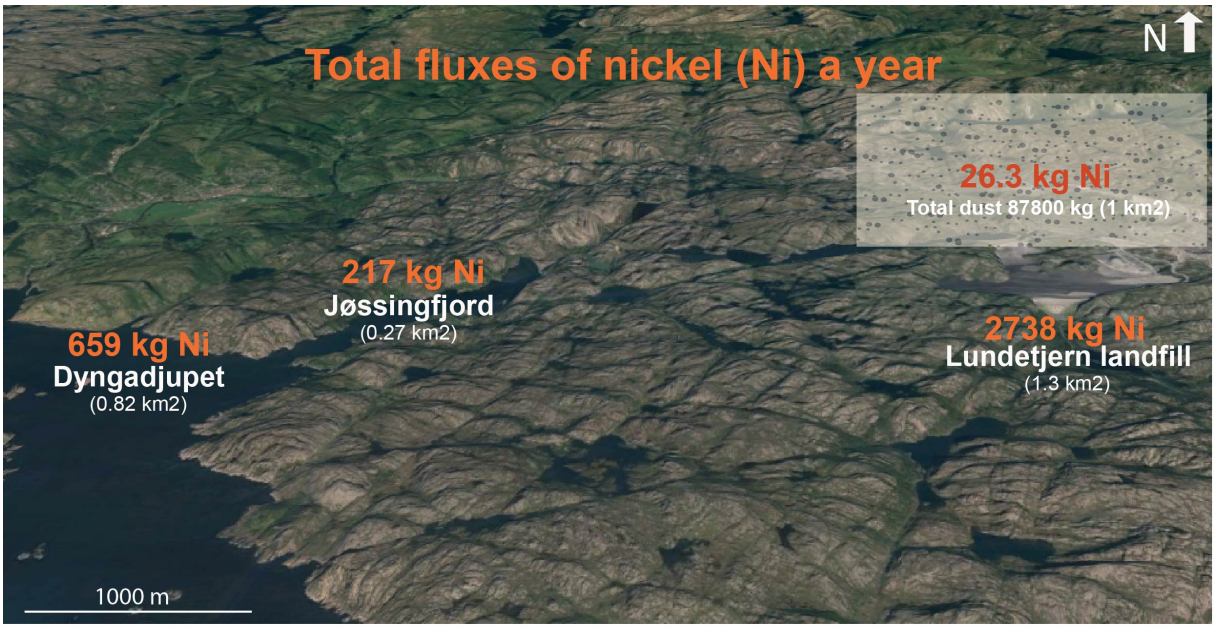


Figure 46 - Total fluxes of nickel (Ni) a year from Dyngadjupet, Jøssingfjord, Lundetjern landfill and from dust. The flux from Lundetjern is calculated from the concession limit of 7.5 kg/ day and not their actual leachate.

The discharge limits at the landfill are today, to both Logsvann and Jøssingfjord, a total of 7.5 kg Ni/day, corresponding to 2738 kg/year (figure 45). This is not their actual Ni flux a year, but their total allowance. Compared to the area of Jøssingfjord (0.27 $km^2$) with 2 cm of tailings, the aqueous flux on land is more than twelve times larger. When compared to only Dyngadjupet, the aqueous flux on land is more than ten times larger. Compared to total area of both Jøssingfjord and Dyngadjupet of 1.09 $km^2$, covered by 2 cm of tailings, the flux on land is yet more than three times larger.

In this comparison, airborne Ni fluxes on land are significantly lower than Ni fluxes in sea tailings. When including the allowed aqueous Ni flux on land, the fluxes on land are considerably higher. However, the challenge on land is not only the airborne flux of Ni, but the total dust emissions.

# 7 Conclusion

This thesis has been investigating the transport of heavy metals, in particular nickel, from both tailings in sea and on land. Based on this, the following conclusions have been made:

- The dust filters in Åna-Sira were both enriched in grains with a diameter under 10μm. However, the filter closest to the landfill had considerable more grains larger than 50μm compared to the dust filter 300m further down. Both dust filters were dominated by plagioclase and ilmenite. The ilmenite grains were likely to originate from the mine, whereas the whole Sokndal mostly consist of anorthosite being a source of plagioclase.

- The water samples collected around the landfill revealed elevated concentrations of nickel. In particular, the sample below the landfill was in very poor condition according to the environmental quality standards for freshwater; however, the concentration is far from the concession limit. The sample at the landfill and at the drying plant were both in poor condition, whereas Tellenes water, Logsvann downstream the landfill and one of the samples in Åna-Sira were in moderate condition. The last three were in good condition. Besides, all samples with exception of the one below the landfill, had acceptable nickel concentrations in accordance with the guidelines for drinking water by the world health organization. The high Ni concentrations in the leachate compared to the concentrations at the landfill could be due to oxidation of nickel sulphides. However, since the increase of Ni concentrations is not followed by an increase in SO4, but rather a decrease, the increase of Ni can not be linked sulphide oxidation.

- The large variance of metal fluxes in the liners are probably due to bioturbation. The relationship between metal fluxes from sediment to water columns and the mean metal uptake from 0-2 cm in pore water by DGT-probes corresponds quite well, indicating that the DGT-probes may be a useful till for future in situ flux measurements. However, further studies should be done as the there as still uncertainties related to the lower DGT values. The precision increases with higher concentrations, suggesting that the method is more optimal where concentrations are expected to be high or where sediments are less influenced by bioturbation.

- The total airborne Ni flux on land was calculated to be significantly lower than the Ni flux from the tailings in sea. However, in terms of dust emissions, nickel is not the main problem, but rather the total dust flux, calculated to be 87 800 kg/year. When comparing the Ni flux of 2 cm tailings in both Jøssingfjord and Dyngadjupet (total of 1.09 $km^2$) with the today's concession limit on land (7.5 kg/day), the aqueous flux on land proved to be more than three times as big as in sea.

# 8 Further Work

In terms of dust emissions and the transport of heavy metals on land and in sea, further work should be done. To better understand the spreading of dust on land, particle sizes and mineral content of dust filters as in this study should be done, but over a whole year, followed by a comparison of wind direction, wind force and precipitation. Titania measures today suspended material (SS) and precipitation. However, a suggestion would be to install a small weather station for wind direction and force, considering that the closest weather station to the mine is more than 20 km away. Wind direction and force would provide a better understanding to what degree the spreading of dust is connected to whether and to what extent the mine is responsible for dust emissions in Åna-Sira.

To better understand the mobilization of nickel in the tailings, kinetic studies of nickel sulphide should be obtained. Simulations with the geochemical modelling program PHREEQC may after that be done of kinetic dissolution of nickel sulphides, transport in the sediments and diffusion coefficients for heavy metals. The model should also consider the biosphere, as bioturbation turned out to have a major influence on the fluxes from the sediments to the water column. The effect of different thicknesses of tailings should be studied further, and parts of the experiments should be without organisms to get a measure of unaffected fluxes and for comparison with affected fluxes. The use of DGT-probes should also be further studied, considering there are still uncertainties related to the low DGT-values.

# References


AANES, K. J. 2016. Ferskvannsundersøkelser i Sira-Kvina høsten 2015. NIVA.

AAS, W., SOLBERG, S., MANØ, S. & YTTRI, K. E. 2009. Overvåkning av langtransportert forurenset luft og nedbør - Atmosfærisk tilførsel (TA-2522/2009). *In:* (SFT), S. F. (ed.). Norsk institutt for luftforskning.

AKCIL, A. & KOLDAS, S. 2006. Acid mine drainage (AMD): causes, treatment and case studies. *Journal of Cleaner Production,* 14**,** 1139-1145.

AMATO, E. D., SIMPSON, S. L., REMAILI, T. M., SPADARO, D. A., JAROLIMEK, C. V. & JOLLEY, D. F. 2016. Assessing the Effects of Bioturbation on Metal Bioavailability in Contaminated Sediments by Diffusive Gradients in Thin Films (DGT). *Environmental science & technology,* 50**,** 3055.

ANON 2007. Norwegian Standard NS-9410. Environmental monitoring of benthic impact from marine fish farms.

APPELO, C. A. J. & POSTMA, D. 2005. *Geochemistry, groundwater and pollution,* Leiden, Balkema.

BLOWES, D. W. 1997. The Environmental Effects of Mine Waste. *Mapping and Monitoring the Mine Environment,* 119.

BOWES, D. E. 1989. *Petrology,* Boston, MA, Springer US, Boston, MA.

BOZKURT, S., MORENO, L. & NERETNIEKS, I. 2000. Long-term processes in waste deposits. *The Science of the total environment,* 250**,** 101.

BRATLAND, S., BAY, B. R., LANDVIK, N. & GUTTU, S. 2015. Veileder til forurensningsforskriften kapittel 7 om lokal luftkvalitet. *M-413.* Miljødirektoratet.

BREDELI, T., NEDVOLD, F., ÅROS, S. & SMEDBERG, P. A. 1992. *Ilmenitten Titania A/S 90år 1902-1992*.

CHARLIER, B., SKÅR, Ø., KORNELIUSSEN, A., DUCHESNE, J.-C. & VANDER AUWERA, J. 2007. Ilmenite composition in the Tellnes Fe–Ti deposit, SW Norway: fractional crystallization, postcumulus evolution and ilmenite–zircon relation. *Contributions to Mineralogy and Petrology,* 154**,** 119-134.

COULTER, B. 2009. Particle Size Analyzer Brochure ISO 13320:2009. Beckman Coulter.

CSAVINA, J., FIELD, J., TAYLOR, M. P., GAO, S., LANDÁZURI, A., BETTERTON, E. A. & SÁEZ, A. E. 2012. A review on the importance of metals and metalloids in atmospheric dust and aerosol from mining operations. *The Science of the total environment,* 433**,** 58.

DELEFOSSE, M., KRISTENSEN, E., CRUNELLE, D., BRAAD, P. E., DAM, J. H., THISGAARD, H., THOMASSEN, A. & HØILUND-CARLSEN, P. F. 2015. Seeing the Unseen—Bioturbation in 4D: Tracing Bioirrigation in Marine Sediment Using Positron Emission Tomography and Computed Tomography. *PloS one,* 10**,** e0122201.

DIOT, H., BOLLE, O., LAMBERT, J.-M., LAUNEAU, P. & DUCHESNE, J.-C. 2003. The Tellnes ilmenite deposit (Rogaland, South Norway): magnetic and petrofabric evidence for emplacement of a Ti-enriched noritic crystal mush in a fracture zone. *Journal of Structural Geology,* 25**,** 481-501.

DOLD, B. 2010. *Basic concepts in environmental geochemistry of sulfidic mine-waste management*, INTECH Open Access Publisher.

DOLD, B. 2014a. Evolution of Acid Mine Drainage Formation in Sulphidic Mine Tailings. *Minerals.*

DOLD, B. 2014b. Submarine Tailings Disposal (STD)—A Review. *Minerals,* 4**,** 642-666.

DUCHESNE, J. C. 1999. Fe-Ti deposits in Rogaland anorthosites (South Norway): geochemical characteristics and problems of interpretation. *International Journal of Geology, Mineralogy and Geochemistry of Mineral Deposits,* 34**,** 182-198.
EMERSON, S. & HEDGES, J. 2003. Sediment Diagenesis and Benthic Flux. Volume 6**,** p.293-319.
ETTNER, D. C. & SANNE, E. H. 2016. Tiltaksorientert overvåking, resultater 2015 Titania AS.
ETTNER, D. C. & SANNE, E. H. 2017. Tiltaksorientert overvåking, resultater 2016.
FORCE, E. R. 1991. *Geology of titanium-mineral deposits,* Boulder, Colo.
GRAVDAL, J. K. S. 2013. *Stability of heavy metals in submarine mine tailings: A geochemical study.* Master, University of Bergen.
GULLIVER, J. S., GULLIVER, J. S. & SPRINGERLINK 2012. *Transport and Fate of Chemicals in the Environment : Selected Entries from the Encyclopedia of Sustainability Science and Technology,* Dordrecht, Springer.
HAGEDORN, B. 2007. Ion Chromatography of Fluoride, Chloride, Bromide, Nitrite, Nitrate, Sulfate and Phosphate with Supression of Eluent (Following Standard Method 4110 B).
HILLIER, S. 2000. Accurate quantitative analysis of clay and other minerals in sandstones by XRD: Comparison of a Rietveld and a reference intensity ratio (RIR) method and the importance of sample preparation.
IBREKK, H. O., BERGE, J. A., GREEN, N., GULBRANDSEN, R., IVERSEN, E., PEDERSEN, A., SKEI, J. & THAULOW, H. 1989. Miljøkonsekvensvurdering Landdeponi og sjødeponi Titania A/S. Oslo: Norwegian Institute for Water Research (NIVA).
JOHNSON, D. B. & HALLBERG, K. B. 2005. Acid mine drainage remediation options: a review. *Science of the Total Environment,* 338**,** 3-14.
KAKSONEN, A. H. & PUHAKKA, J. A. 2007. Sulfate Reduction Based Bioprocesses for the Treatment of Acid Mine Drainage and the Recovery of Metals. *Engineering in Life Sciences,* 7**,** 541-564.
KONHAUSER, K. 2007. *Introduction to geomicrobiology,* Malden, Mass, Blackwell.
KORNELIUSSEN, A., MCENROE, S. A., NILSSON, L. P., SCHIELLERUP, H., GAUTNED, H., MEYER, G. B. & STØRSETH, L. R. 2000. An overview of itanium deposits in Norway. *Norges geologiske undersøkelse,* Bulletin 436**,** 27-38.
KORRE, A., IMRIE, C. E., MAY, F., BEAUBIEN, S. E., VANDERMEIJER, V., PERSOGLIA, S., GOLMEN, L., FABRIOL, H. & DIXON, T. 2011. Quantification techniques for potential CO2 leakage from geological storage sites. *Energy Procedia,* 4**,** 3413-3420.
KOSKI, R. & KOSKI, R. 2012. Metal Dispersion Resulting from Mining Activities in Coastal Environments: A Pathways Approach. *Oceanography,* 25**,** 170-183.
KOSSOFF, D., DUBBIN, W. E., ALFREDSSON, M., EDWARDS, S. J., MACKLIN, M. G. & HUDSON-EDWARDS, K. A. 2014. Mine tailings dams: Characteristics, failure, environmental impacts, and remediation. *Applied Geochemistry,* 51**,** 229-245.
KRAUSE, H., GIERTH, E. & SCHOTT, W. 1985. Ti-Fe Deposits in the South Rogaland Igneous Complex, with Special Reference to the Åna-Sira Anorthosite Massif. Bulletin 402**,** 25-37.
KRISTENSEN, E. 2000. Organic matter diagenesis at the oxic/anoxic interface in coastal marine sediments, with emphasis on the role of burrowing animals. *The International Journal of Aquatic Sciences,* 426**,** 1-24.
KRUMBEIN, W. & GARRELS, R. 1952. Origin and classification of chemical sediments in terms of pH and oxidation-reduction potentials. *The Journal of Geology,* 60**,** 1-33.

LIBES, S. M. 1992. *An introduction to marine biogeochemistry,* New York, Wiley.
LINDSAY, M. B. J., MONCUR, M. C., BAIN, J. G., JAMBOR, J. L., PTACEK, C. J. & BLOWES, D. W. 2015. Geochemical and mineralogical aspects of sulfide mine tailings. *Applied Geochemistry,* 57**,** 157-177.
LOE, T. K. F. & AAGAARD, P. 2013. Deponering av avgangsmasser fra gruveindustrien - på land eller i vann? *Mineralproduksjon,* 4.
LORENTZEN, E. A. 2017. *Fann lite oxygen i tidligare gruvedeponi* [Online]. Havforskningsinstituttet. [Accessed].
LOTTERMOSER, B. 2007. *Mine Wastes : Characterization, Treatment and Environmental Impacts,* Dordrecht, Springer.
MEADOWS, P. S., MEADOWS, A. & MURRAY, J. M. 2012. Biological modifiers of marine benthic seascapes: Their role as ecosystem engineers. *Geomorphology,* 157**,** 31-48.
MELAND, V. 2016. Rekefjord øst. Deponi for farlig avfall. *In:* AS, W. (ed.).
MELLGREN, A. 2002. Utlutning av nikkel fra Lundetjern Landdeponi - En kartlegging av årsaker og tiltak. *In:* NTNU (ed.).
MIDDLEMAS, S., FANG, Z. Z. & FAN, P. 2015. Life cycle assessment comparison of emerging and traditional Titanium dioxide manufacturing processes. *Journal of Cleaner Production,* 89**,** 137-147.
MILJØDIREKTORATET 2016. Quality standards for water, sediment and biota M-608. *In:* AQUATEAM, N., NGI (ed.).
MYRAN, T. 2007. Rapport støvnedfall Titania, Åna Sira. Norges teknisk-naturvitenskapelige universitet: Institutt for geologi og bergteknikk.
NAGEL, A.-H. 1994. Norwegian mining in the early modern period. *An International Journal on Human Geography and Environmental Sciences,* 32**,** 137-149.
NGU 2014. Mineralressurser i Norge 2014. Publikasjon nr 1 ed. Trondheim.
NHD, N.-O. H. 2013. Strategi for mineralnæringen.
NILSEN, A. H. 2017. *RE: Personal communication (Titania AS).*
NØLAND, S.-A., GLETTE, T. & ULFSNES, A. 2008. Resipientundersøkelse Jøssingfjorden 2008.
OCEAN, C. V. I. & CONSULTING, C. E. 2013. International Assessment of Marine and Riverine Disposal of Mine Tailings. *In:* STUDY COMMISSIONED BY THE OFFICE FOR THE LONDON CONVENTION AND PROTOCOL AND OCEAN AFFAIRS, I., IN COLLABORATION WITH THE UNITED NATIONS ENVIRONMENT PROGRAMME (UNEP) GLOBAL PROGRAMME OF ACTION (ed.).
OLSGARD, F. & HASLE, J. R. 1993. Impact of waste from titanium mining on benthic fauna. *Journal of Experimental Marine Biology and Ecology,* 172**,** 185-213.
OPSAL, E. 2017. *RE: Personal communication (Titania AS).*
RAMIREZ-LLODRA, E., TRANNUM, H. C., EVENSET, A., LEVIN, L. A., ANDERSSON, M., FINNE, T. E., HILARIO, A., FLEM, B., CHRISTENSEN, G., SCHAANNING, M. & VANREUSEL, A. 2015. Submarine and deep-sea mine tailing placements: A review of current practices, environmental issues, natural analogs and knowledge gaps in Norway and internationally. *Marine Pollution Bulletin*.
REED, S. J. B. 2005. *Electron Microprobe Analysis and Scanning Electron Microscopy in Geology,* Cambridge, Cambridge : Cambridge University Press.
SÆLAND, F., DYBING, L. & DALANE, F. 2008. *Gruvedrift i Sokndal gjennom 140 år : Titania AS sitt gruveanlegg på Sandbekk : B. 1,* Kongsberg, Norsk bergverksmuseum.
SARB 2014. Mineralogisk og Geokjemisk Karakterisering av Gråberg og Avgang ved Titania AS.

SCHAANNING, M. & HANSEN, P. 2005. The suitability of electrode measurements for assessment of benthic organic impact and their use in a management system for marine fish farms. *Environmental Effects of Marine Finfish Aquaculture***,** 381-408.
SCHAANNING, M. T., TRANNUM, H. C., ØXNEVAD, S., CARROLL, J. & BAKKE, T. 2008. Effects of drill cuttings on biogeochemical fluxes and macrobenthos of marine sediments. *Journal of Experimental Marine Biology and Ecology,* 361**,** 49-57.
SCHWARTZ, F. W. Z. 2003. Fundamentals of Groundwater. New York: John Wiley & Sons.
SIMATE, G. S. & NDLOVU, S. 2014. Acid mine drainage: Challenges and opportunities. *Journal of Environmental Chemical Engineering,* 2**,** 1785-1803.
SKOOG, D. A., CROUCH, S. R. & HOLLER, F. J. 2007. *Principles of instrumental analysis,* Belmont, Calif, Thomson.
SMITH, K. S. 1999. Metal sorption on mineral surfaces: an overview with examples relating to mineral deposits. *The Environmental Geochemistry of Mineral Deposits. Part B: Case Studies and Research Topics,* 6**,** 161-182.
SØRBY, H., STORBRÅTEN, G., BRAASTAD, G., LØKELAND, M., DALEN, M., THORNHILL, M., BØE, R., RYE, H., FOSSÅ, J. H., DEKKO, T., JENSEN, T. & SKEI, J. 2010. Bergverk og avgangsdeponering. Status, miljøutfordringer og kunnskapsbehov TA-2715. Miljødirektoratet, Klima- og forurensningsdirektoratet, NIVA.
SPALLA, M. I., MAROTTA, A. M., GOSSO, G., DEFORMATION, R. & TECTONICS, C. 2010. *Advances in interpretation of geological processes : refinement of multi-scale data and integration in numerical modelling,* London, Geological Society.
SWECO 2017. Reguleringsplan med konsekvensutredning for håndtering av avgangsmasser for Titanias gruvedrift ved Tellenes Sokndal kommune. Forslag til planprogram.
TERRY, J. P. & GOFF, J. 2014. Megaclasts: Proposed Revised Nomenclature At the Coarse End of the Udden-Wentworth Grain-Size Scale for Sedimentary Particles. *Journal of Sedimentary Research,* 84**,** 192-197.
THOMAS, R. 2008. *Practical guide to ICP-MS : a tutorial for beginners,* Boca Raton, Fla, CRC Press.
TITANIA 2002. Titania. Egersund: Titania A/S.
TOBIESEN, A. 2003. Økotoksikologisk karakterisering av avløpsvann fra bedriftsområdet til Titania AS i Hauge i Dalane. NIVA.
TØNNESEN, D. 2008. Måling av svevestøv i Åna-Sira. Norsk institutt for luftforskning (NILU).
TRANNUM, H. C. 2016. Overvåkning av marin bløtbunnsfauna for Titania A/S i 2015. NIVA.
TRANNUM, H. C., NILSSON, H. C., SCHAANNING, M. T. & ØXNEVAD, S. 2010. Effects of sedimentation from water-based drill cuttings and natural sediment on benthic macrofaunal community structure and ecosystem processes. *Journal of Experimental Marine Biology and Ecology,* 383**,** 111-121.
VANNFORSKRIFTEN 2015. Forskrift om rammer for vannforvaltningen.
WHO, W. H. O. 2017. Guidelines for Drinking-water Quality: Fourth edition incorporating first addendum. Fourth edition ed.
WOLKERSDORFER, C. & BOWELL, R. 2005. Contemporary Reviews of Mine Water Studies in Europe, Part 2. *Mine Water and the Environment,* 24**,** 2-37.
ZHANG, H. & DAVISON, W. 1995. Performance characteristics of diffusion gradients in thin films for the in situ measurement of trace metals in aqueous solution. *Analytical Chemistry,* 67**,** 3391.

# Appendix

## Appendix A: Tailings disposal on land

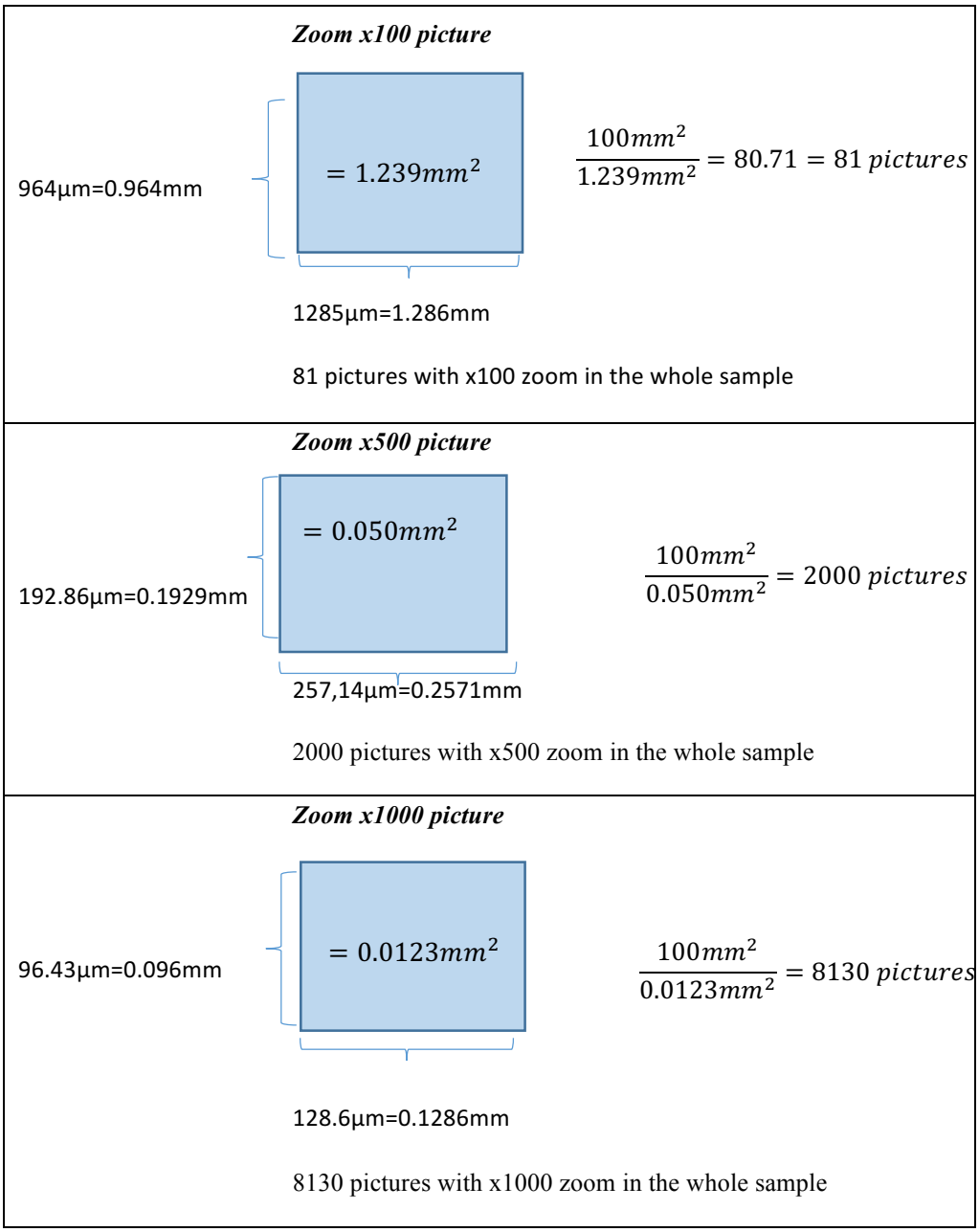

Figure 47. - How the areas for each of the zooms has been calculated

Table 17 - Points counted from sample 4a, measuring point 9354

***Sample 4a Øvre Åna-Sira (measuring point 9354)***

| Zoom | Point | <10µm | 10-50µm | 50-100µm | >100µm |
|---|---|---|---|---|---|
| x100 | Point 1 | | 39 | 1 | 1 |
| x100 | Point 2 | | 25 | 1 | 1 |
| x100 | Point 3 | | 33 | 1 | 0 |
| x100 | Point 4 | | 23 | 3 | 0 |
| x100 | Average point | | 30 | 1,5 | 0,5 |
| x100 | Whole sample | | 2430 | 121,5 | 40,5 |
| x500 | Point 1 | 109 | 2 | 1 | 0 |
| x500 | Point 2 | 64 | 1 | 0 | 0 |
| x500 | Point 3 | 59 | 1 | 0 | 0 |
| x500 | Point 4 | 82 | 1 | 0 | 0 |
| x500 | Average | 78,5 | 1,25 | 0,25 | 0 |
| x500 | Whole sample | 157000 | 2500 | 500 | 0 |
| x1000 | Point 1 | 53 | 0 | 0 | 0 |
| x1000 | Point 2 | 36 | 0 | 0 | 0 |
| x1000 | Point 3 | 24 | 1 | 0 | 0 |
| x1000 | Point 4 | 35 | 1 | 0 | 0 |
| x1000 | Average | 37 | 0,5 | 0 | 0 |
| x1000 | Whole sample | 307470 | 4155 | 0 | 0 |

Table 18 - Points counted from sample 3a, measuring point 9353

***Sample 3a Nedre Åna-Sira (measuring point 9353)***

| Zoom | Point | <10µm | 10-50µm | 50-100µm | >100µm |
|---|---|---|---|---|---|
| x100 | Point 1 | | 24 | 0 | 0 |
| x100 | Point 2 | | 32 | 1 | 1 |
| x100 | Point 3 | | 41 | 1 | 0 |
| x100 | Point 4 | | 58 | 2 | 0 |
| x100 | Average point | | 38,75 | 1 | 0,25 |
| x100 | Whole sample | | 3138,75 | 81 | 20,25 |
| x500 | Point 1 | 141 | 1 | 0 | 0 |
| x500 | Point 2 | 86 | 5 | 0 | 0 |
| x500 | Point 3 | 146 | 1 | 0 | 0 |
| x500 | Point 4 | 154 | 7 | 0 | 0 |
| x500 | Average | 131,75 | 3,5 | 0 | 0 |
| x500 | Whole sample | 265608 | 7056 | 0 | 0 |
| x1000 | Point 1 | 47 | 1 | 0 | 0 |
| x1000 | Point 2 | 39 | 0 | 0 | 0 |
| x1000 | Point 3 | 60 | 1 | 0 | 0 |
| x1000 | Point 4 | 35 | 1 | 0 | 0 |
| x1000 | Average | 45,25 | 0,75 | 0 | 0 |
| x1000 | Whole sample | 367882,5 | 6097,5 | 0 | 0 |

Table 19 - Precipitation at Titania (mm per month).

**Precipitation Titania (mm per month)**

| | 2012 | 2013 | 2014 | 2015 | 2016 | 2017 |
|---|---|---|---|---|---|---|
| January | 240,5 | 100,7 | 258,3 | 300 | 111 | 183,7 |
| February | 181,1 | 36,6 | 240 | 194 | 132,5 | 229,5 |
| March | 122,8 | 19,1 | 174,1 | 160 | 82,7 | 123,3 |
| April | 136,9 | 98,2 | 115,5 | 96,9 | 112,5 | 43,8 |
| May | 122,9 | 133 | 59,6 | 215,6 | 130,5 | 103,9 |
| June | 88,6 | 144,5 | 20,4 | 86,7 | 157 | 142,5 |
| July | 187 | 35,9 | 191,4 | 87,6 | 167,2 | 183 |
| August | 210,3 | 194,2 | 184,8 | 205,1 | 158,9 | |
| September | 255,7 | 239 | 98,7 | 341,2 | 209,5 | |
| October | 233 | 161,6 | 257,1 | 67,5 | 75,9 | |
| November | 355,4 | 162,1 | 85,8 | 187,7 | 164,7 | |
| December | 177,1 | 381,7 | 222,8 | 255,7 | 151,6 | |
| Sum | 2311,3 | 1706,6 | 1908,5 | 2198 | 1654 | 1009,7 |

Table 20 - Wind in the period of the dust filters (Lista weather station).

| Date | Wind (m/s) | Wind direction | precipitation (mm) |
|---|---|---|---|
| 04-Aug | 4,8 | southeast | 8,6 |
| 05-Aug | 11,1 | west-northwest | 18,2 |
| 06-Aug | 12,2 | northwest | 0,2 |
| 07-Aug | 6,8 | southwest | 0,1 |
| 08-Aug | 16,1 | west | 11 |
| 09-Aug | 12,6 | northwest | 4,8 |
| 10-Aug | 11 | northwest | 1,7 |
| 11-Aug | 5 | west | 0 |
| 12-Aug | 8,1 | west-southwest | 1,4 |
| 13-Aug | 7,4 | west | 14,5 |
| 14-Aug | 8,5 | northwest | 3,1 |
| 15-Aug | 4,8 | northwest | 0 |
| 16-Aug | 3 | west | 0 |
| 17-Aug | 3,3 | north-northwest | 0 |
| 18-Aug | 3 | west-southwest | 0 |
| 19-Aug | 7,2 | east-southeast | 0 |
| 20-Aug | 11,2 | east-southeast | 0 |
| 21-Aug | 9,5 | east-southeast | 4,6 |
| 22-Aug | 8,4 | south | 5,6 |
| 23-Aug | 4,7 | west-northwest | 0 |
| 24-Aug | 9,4 | east-southeast | 0 |
| 25-Aug | 2,9 | southeast | 0 |
| 26-Aug | 8,8 | west-northwest | 10,5 |
| 27-Aug | 4,3 | west | 0,2 |
| 28-Aug | 7,2 | east | 0,2 |
| 29-Aug | 11,7 | northwest | 0,1 |
| 30-Aug | 7,1 | west-northwest | 0,1 |
| 31-Aug | 8,7 | south | 0 |
| Average | 7,8 | | 3,0 |

Table 21 - Estimation of total dust emissions on land from dust filter sample 4a in Åna-Sira

## Mass calculations sample 4a

| Diameter | **<10µm** | **10-50µm** | **50-100µm** | **>100µm** |
|---|---|---|---|---|
| Average of all zooms | 232235,00 | 3028,33 | 310,75 | 40,50 |

| Radius | **5µm** | **15µm** | **30µm** | **75µm** | **SUM** |
|---|---|---|---|---|---|
| particles | 232235,00 | 3028,33 | 310,75 | 40,50 | |
| volume pr particle ($dm^3$) | 5,23E-13 | 1,41E-11 | 1,13E-10 | 1,77E-09 | |
| mass pr particle | 1,41E-09 | 3,82E-08 | 3,05E-07 | 4,77E-06 | |
| total mass (g) a month | 3,28E-04 | 1,16E-04 | 9,48E-05 | 1,93E-04 | 7,32E-04 |

| | | |
|---|---|---|
| Total mass of all particles in sample 4a is | 0,001 | g/cm2/month |
| | 7,317 | g/m2/28month |
| | 0,007 | kg/m2/28month |

| | | |
|---|---|---|
| Flux | 0,088 | kg/m2/year |

**An area of 1km^2**

| | |
|---|---|
| 87799,779 | kg/year |
| **26,340** | **kg Ni/year** |

1µm=0.00001dm

assumed density = 2700g/dm^3

area of sample =1cm^2

assumed Ni =0.03%

$$m = \rho * V$$

$$V = \frac{4}{3}\pi r^3$$

# Appendix B: Tailing disposal in sea

Table 22 - Flux measurements from the sediments to the water column in the liners. C stands for control liner, A for anonymous liner and T for Titania liners.

| Fluxes from the sediments to the water column in liners (µg m-2 d-1) | | | | | | | |
|---|---|---|---|---|---|---|---|
| **Treatment** | **Core nr** | **F-Pb** | **F-Cd** | **F-Cu** | **F-Co** | **F-Ni** | **F-Zn** |
| C | **1** | -0,2304 | 0,0960 | 2,3520 | 0,4416 | 1,5840 | 0,0960 |
| C | **10** | -0,8352 | 0,0144 | 0,9120 | 0,8160 | 0,7200 | 5,6160 |
| C | **32** | -0,8016 | 0,0816 | 3,6480 | 0,3696 | 1,0560 | -0,3360 |
| A | **16** | -0,8352 | 0,1488 | 31,7280 | 1,6800 | 6,1920 | 12,6240 |
| A | **18** | -0,8016 | 0,0912 | 15,0720 | 0,3408 | 3,1680 | -1,4400 |
| A | **21** | -0,8352 | 0,0864 | 19,3440 | 0,3936 | 1,7280 | 1,5360 |
| T | **4** | -0,4800 | 0,7104 | 15,9360 | 2,3568 | 1959,0 | 50,1120 |
| T | **14** | -0,1776 | 0,4224 | 24,8640 | 27,9360 | 1381,1 | 16,7040 |
| T | **20** | -0,7680 | 0,8736 | 24,5760 | 99,9360 | 3264,6 | 27,6960 |

Table 23 - Calculated average Ni fluxes from Jøssingfjord and Dyngadjupet.

**Nickel fluxes in sea**

| **Treatment** | **Core nr** | **F-Ni (µg m-2 d-1)** |
|---|---|---|
| T | **4** | 1959,0 |
| T | **14** | 1381,1 |
| T | **20** | 3264,6 |

| | | |
|---|---|---|
| **Average** | 2201,6 | µg m-2 d-1 |
| | 2,20E-06 | kg/m2/day |
| | 8,04E-04 | kg/m2/year |

| **Area** | **m2** |
|---|---|
| Jøssingfjord and Dyngadjupet - 1.09 km2 | 1090000 |
| Jøssingfjord - 0,27 km2 | 270000 |
| Dyngadjupet - 0,82 km2 | 820000 |

| **Average Ni** | kg/year |
|---|---|
| Jøssingfjord and Dyngadjupet | 875,90 |
| Jøssingfjord | 216,97 |
| Dyngadjupet | 658,93 |

Table 24 - DGT uptake from the Titania liners (ng/cm2). Red values are under the detection limit and have not been used.

| DGT uptake Titania (ng/cm2) | | | | | | | | | |
|---|---|---|---|---|---|---|---|---|---|
| | | | | | | | | | |
| LINER 4 | **Cr** | **Mn** | **Fe** | **Co** | **Ni** | **Cu** | **Zn** | **Cd** | **Pb** |
| **4 0-5** | 0,92 | 177,34 | 14,14 | 0,73 | 268,80 | 3,27 | 15,84 | 0,23 | 0,42 |
| **4 5-10** | 0,76 | 154,34 | 10,07 | 0,53 | 219,60 | 2,47 | 13,31 | 0,14 | 0,50 |
| **4 10-15** | 1,07 | 207,75 | 18,65 | 0,67 | 258,76 | 2,67 | 13,10 | 0,13 | 0,35 |
| **4 15-20** | 0,87 | 295,62 | 9,03 | 0,83 | 255,70 | 3,25 | 11,28 | 0,17 | 0,22 |
| **4 20-30** | 0,71 | - | 6,38 | 3,35 | 81,83 | 4,19 | 12,81 | 0,11 | 1,06 |
| **4 30-50** | 0,67 | - | 6,41 | 4,04 | 73,65 | 1,12 | 9,41 | 0,24 | 0,41 |
| **4 50-70** | 0,51 | - | 6,51 | 4,05 | 86,59 | 0,94 | 7,20 | 0,14 | 0,22 |
| **4 70-90** | 0,59 | - | 74,41 | 4,12 | 39,93 | 1,24 | 8,42 | 0,15 | 0,31 |
| **4 90-130** | 0,47 | - | 703,16 | 2,10 | 8,11 | 0,52 | 7,67 | 0,03 | 0,23 |
| | | | | | | | | | |
| LINER 14 | **Cr** | **Mn** | **Fe** | **Co** | **Ni** | **Cu** | **Zn** | **Cd** | **Pb** |
| **14 0-5** | 0,43 | 355,75 | 13,52 | 3,64 | 180,95 | 3,31 | 5,74 | 0,06 | 0,00 |
| **14 5-10** | 0,54 | 435,20 | 7,83 | 4,97 | 214,14 | 5,14 | 6,88 | 0,10 | 0,00 |
| **14 10-15** | 0,67 | 949,95 | 7,47 | 15,47 | 362,14 | 13,17 | 9,05 | 0,14 | 0,00 |
| **14 15-20** | 0,71 | 1519,76 | 7,05 | 14,20 | 339,26 | 12,60 | 9,72 | 0,14 | 0,00 |
| **14 20-30** | 0,42 | - | 6,79 | 10,48 | 244,13 | 11,45 | 10,10 | 0,15 | 0,00 |
| **14 30-50** | 0,32 | - | 7,05 | 2,52 | 21,89 | 2,47 | 8,43 | 0,08 | 0,00 |
| **14 50-70** | 0,36 | - | 5,59 | 2,77 | 13,49 | 1,70 | 7,94 | 0,08 | 0,01 |
| **14 70-90** | 0,53 | - | 467,70 | 5,44 | 13,38 | 1,41 | 15,17 | 0,05 | 0,00 |
| **14 90-130** | -0,01 | 78,07 | 1,14 | 0,03 | 0,43 | -0,01 | 0,01 | 0,00 | 0,00 |
| | | | | | | | | | |
| LINER 20 | **Cr** | **Mn** | **Fe** | **Co** | **Ni** | **Cu** | **Zn** | **Cd** | **Pb** |
| **20 0-5** | 0,46 | 199,77 | 11,77 | 9,18 | 283,83 | 2,29 | 11,37 | 0,12 | 0,00 |
| **20 5-10** | 0,54 | 265,33 | 16,25 | 11,66 | 366,55 | 2,94 | 11,06 | 0,15 | 0,00 |
| **20 10-15** | 0,66 | 278,86 | 11,59 | 11,94 | 359,51 | 3,48 | 10,35 | 0,13 | 0,00 |
| **20 15-20** | 1,25 | 678,27 | 18,97 | 21,15 | 512,36 | 9,22 | 12,50 | 0,18 | 0,00 |
| **20 20-30** | 0,57 | - | 10,80 | 33,46 | 670,73 | 12,64 | 11,19 | 0,32 | 0,00 |
| **20 30-50** | 0,40 | - | 6,58 | 13,41 | 209,85 | 9,86 | 10,01 | 0,21 | 0,00 |
| **20 50-70** | 0,35 | - | 5,32 | 7,98 | 95,32 | 9,61 | 13,84 | 0,12 | 0,00 |
| **20 70-90** | 0,33 | - | 6,42 | 4,32 | 32,21 | 4,78 | 56,58 | 0,07 | 0,00 |
| **20 90-130** | 0,30 | - | 189,89 | 2,49 | 8,00 | 1,08 | 12,78 | 0,01 | 0,00 |

Table 25 - DGT uptake from the Control liners (ng/cm2). Red values are under the detection limit and have not been used.

| DGT uptake Control (ng/cm2) | | | | | | | | | |
|---|---|---|---|---|---|---|---|---|---|
| | | | | | | | | | |
| **LINER 32** | **Cr** | **Mn** | **Fe** | **Co** | **Ni** | **Cu** | **Zn** | **Cd** | **Pb** |
| **32 0-5** | 0,82 | 991,88 | 8,90 | 0,16 | 0,55 | 0,91 | 7,71 | 0,08 | 0,30 |
| **32 5-10** | 0,98 | 538,67 | 10,36 | 0,16 | 7,14 | 0,94 | 7,68 | 0,11 | 0,21 |
| **32 10-15** | 0,75 | 41,39 | 8,06 | 0,04 | 0,44 | 0,98 | 7,10 | 0,04 | 0,37 |
| **32 15-20** | 0,64 | 9,66 | 4,98 | 0,05 | 0,36 | 0,87 | 5,95 | 0,05 | 0,15 |
| **32 20-30** | 0,84 | 15,53 | 8,03 | 0,07 | 0,87 | 1,10 | 7,28 | 0,07 | 0,20 |
| **32 30-50** | 0,74 | - | 5,31 | 0,28 | 1,43 | 0,66 | 6,72 | 0,08 | 0,19 |
| **32 50-70** | 0,59 | - | 4,85 | 1,28 | 2,00 | 0,70 | 7,12 | 0,08 | 0,09 |
| **32 70-90** | 0,41 | - | 4,91 | 2,34 | 2,93 | 0,71 | 7,54 | 0,06 | 0,14 |
| **32 90-130** | 0,40 | - | 246,41 | 2,83 | 3,84 | 0,56 | 9,02 | 0,02 | 0,14 |
| | | | | | | | | | |
| **LINER 10** | | | | | | | | | |
| **10 0-5** | 0,74 | 833,54 | 15,27 | 0,26 | 4,56 | 1,34 | 18,94 | 0,06 | 0,29 |
| **10 5-10** | 0,73 | 561,32 | 15,85 | 0,18 | 3,73 | 1,10 | 11,42 | 0,08 | 0,31 |
| **10 10-15** | 0,80 | 165,81 | 7,64 | 0,10 | 2,56 | 1,00 | 8,90 | 0,05 | 0,26 |
| **10 15-20** | 0,84 | 52,58 | 10,13 | 0,14 | 1,79 | 1,12 | 13,19 | 0,07 | 0,43 |
| **10 20-30** | 0,76 | 13,80 | 8,64 | 0,09 | 2,14 | 1,13 | 12,38 | 0,06 | 0,23 |
| **10 30-50** | 0,68 | - | 5,79 | 0,4885 | 2,83 | 0,77 | 10,62 | 0,07 | 0,12 |
| **10 50-70** | 0,47 | - | 5,39 | 2,03 | 4,54 | 0,80 | 11,10 | 0,12 | 0,17 |
| **10 70-90** | 0,40 | - | 41,22 | 2,49 | 5,23 | 0,74 | 11,07 | 0,02 | 0,20 |
| **10 90-130** | 0,41 | - | 514,10 | 1,74 | 5,32 | 0,55 | 9,15 | 0,01 | 0,36 |
| | | | | | | | | | |
| **LINER 1** | | | | | | | | | |
| **1 0-5** | 0,53 | 1017,48 | 11,74 | 0,24 | 5,36 | 1,04 | 46,74 | 0,03 | 0,01 |
| **1 5-10** | 0,71 | 292,25 | 12,63 | 0,10 | 4,25 | 0,92 | 9,02 | 0,06 | 0,01 |
| **1 10-15** | 0,55 | 32,56 | 13,25 | 0,08 | 2,37 | 1,02 | 11,77 | 0,05 | 0,02 |
| **1 15-20** | 0,66 | 20,67 | 19,97 | 0,08 | 2,10 | 1,53 | 9,42 | 0,06 | 0,03 |
| **1 20-30** | 0,59 | 319,45 | 9,36 | 0,56 | 2,23 | 0,95 | 7,98 | 0,06 | 0,03 |
| **1 30-50** | 0,48 | - | 6,36 | 0,67 | 2,89 | 0,67 | 8,18 | 0,08 | 0,03 |
| **1 50-70** | 0,38 | - | 7,22 | 2,09 | 3,83 | 0,62 | 7,83 | 0,04 | 0,01 |
| **1 70-90** | 0,36 | - | 289,09 | 2,51 | 1,77 | 0,91 | 8,41 | 0,055 | 0,03 |
| **1 90-130** | 0,46 | - | 462,62 | 2,08 | 2,21 | 0,59 | 7,64 | 0,019625 | 0,01 |

Table 26 – The log transformed measured fluxes from the sediments to the water column (log Flux), and the log transformed metal uptake of the 0-2cm interval by the DGT-probes(ng/cm2) (Log DGT), used for the linear regression in figure 40. C stands for control liner, A for anonymous liner and T for Titania liners.

| Treatment | Core nr | Fluxes | DGT C(0-2cm) | Log Flux | Log DGT |
|---|---|---|---|---|---|
| | | F-Pb | DGT-Pb | | |
| C | 1 | -0,2304 | 1,48 | | |
| C | 10 | -0,8352 | 1,29 | | |
| C | 32 | -0,8016 | 0,88 | | |
| A | 16 | -0,8352 | 0,86 | | |
| A | 18 | -0,8016 | 0,88 | | |
| A | 21 | -0,8352 | 3,35 | | |
| T | 4 | -0,4800 | 0,04 | | |
| T | 14 | -0,1776 | | | |
| T | 20 | -0,7680 | 0,00 | | |
| Treatment | Core nr | F-Cd | DGT Cd | | |
| C | 1 | 0,7104 | | | |
| C | 10 | 0,0144 | | | |
| C | 32 | 0,0816 | | | |
| A | 16 | 0,1488 | | | |
| A | 18 | 0,0912 | | | |
| A | 21 | 0,0864 | 0,57 | | |
| T | 4 | 0,0960 | 0,23 | | |
| T | 14 | 0,4224 | | | |
| T | 20 | 0,8736 | | | |
| Treatment | Core nr | F-Cu | DGT Cu | | |
| C | 1 | 2,3520 | 4,52 | 0,371437317 | 0,654753933 |
| C | 10 | 0,9120 | 4,56 | -0,040005162 | 0,659060072 |
| C | 32 | 3,6480 | 3,70 | 0,56205483 | 0,567849451 |
| A | 16 | 31,7280 | 193,28 | 1,501442697 | 2,286193658 |
| A | 18 | 15,0720 | 8,55 | 1,178170885 | 0,931915317 |
| A | 21 | 19,3440 | 174,17 | 1,286546284 | 2,240960884 |
| T | 4 | 15,9360 | 11,66 | 1,202379321 | 1,066549539 |
| T | 14 | 24,8640 | 34,22 | 1,395570997 | 1,534229237 |
| T | 20 | 24,5760 | 17,92 | 1,390511198 | 1,253241054 |
| Treatment | Core nr | F-Ni | DGT Ni | | |
| C | 1 | 1,5840 | | | |
| C | 10 | 0,7200 | | | |
| C | 32 | 1,0560 | | | |
| A | 16 | 6,1920 | 4,87 | 0,791830948 | 0,687885525 |
| A | 18 | 3,1680 | 8,98 | 0,500785173 | 0,953082844 |
| A | 21 | 1,7280 | | | |
| T | 4 | 1959,0 | 1002,86 | 3,292039757 | 3,00123901 |
| T | 14 | 1381,1 | 1096,48 | 3,140226383 | 3,040001903 |
| T | 20 | 3264,6 | 1522,26 | 3,513833169 | 3,182489121 |

| Treatment | Core nr | F-Zn | DGT Zn | | |
|---|---|---|---|---|---|
| C | **1** | 0,0960 | 76,96 | -1,017728767 | 1,886248129 |
| C | **10** | 5,6160 | 52,46 | 0,749427099 | 1,719786891 |
| C | **32** | -0,3360 | 28,44 | | |
| A | **16** | 12,6240 | 80,19 | 1,101196986 | 1,904136461 |
| A | **18** | -1,4400 | 61,12 | | |
| A | **21** | 1,5360 | 100,71 | 0,186391216 | 2,003059659 |
| T | **4** | 50,1120 | 53,52 | 1,699941736 | 1,728532334 |
| T | **14** | 16,7040 | 31,39 | 1,222820481 | 1,49673597 |
| T | **20** | 27,6960 | 45,28 | 1,442417051 | 1,655887235 |
| **Treatment** | **Core nr** | **F-Co** | **DGT Co** | | |
| C | **1** | 0,4416 | 0,49 | -0,354970935 | -0,311580178 |
| C | **10** | 0,8160 | 0,26 | -0,088309841 | -0,585026652 |
| C | **32** | 0,3696 | | | |
| A | **16** | 1,6800 | | | |
| A | **18** | 0,3408 | | | |
| N | **21** | 0,3936 | 1,70 | -0,40494491 | 0,230704314 |
| T | **4** | 2,3568 | 2,76 | 0,372322729 | 0,440279213 |
| T | **14** | 27,9360 | 38,28 | 1,446164222 | 1,582960584 |
| T | **20** | 99,9360 | 53,93 | 1,999721963 | 1,731838473 |

Negative flux

Below detection limit

Table 27 - Data used for the correlation between the measured fluxes from the sediments to the water column and the metal uptake of the 0-2cm interval by the DGT-probes(ng/cm2) in the Titania liners.

| Treatment | Core nr | Fluxes | DGT C(0-2cm) |
|---|---|---|---|
| | | F-Pb | DGT Pb |
| T | 4 | -0,4800 | |
| T | 14 | -0,1776 | |
| T | 20 | -0,7680 | |
| Treatment | Core nr | F-Cd | DGT Cd |
| T | 4 | 0,7104 | |
| T | 14 | 0,4224 | |
| T | 20 | 0,8736 | |
| Treatment | Core nr | F-Cu | DGT Cu |
| T | 4 | 15,9360 | 11,66 |
| T | 14 | 24,8640 | 34,22 |
| T | 20 | 24,5760 | 17,92 |
| Treatment | Core nr | F-Co | DGT Co |
| T | 4 | 2,3568 | 2,76 |
| T | 14 | 27,9360 | 38,28 |
| T | 20 | 99,9360 | 53,93 |
| Treatment | Core nr | F-Ni | DGT Ni |
| T | 4 | 1959,0 | 1002,86 |
| T | 14 | 1381,1 | 1096,48 |
| T | 20 | 3264,6 | 1522,26 |
| Treatment | Core nr | F-Zn | DGT Zn |
| T | 4 | 50,1120 | 53,52 |
| T | 14 | 16,7040 | 31,39 |
| T | 20 | 27,6960 | 45,28 |